UNCLASSIFIED

AD NUMBER

AD203393

NEW LIMITATION CHANGE

TO

Approved for public release, distribution unlimited

FROM

Distribution authorized to U.S. Gov't. agencies and their contractors; Administrative/Operational Use; JAN 1959. Other requests shall be referred to Wright Air Development Center, Wright-Patterson AFB, OH 45433.

AUTHORITY

ASD/USAF ltr dtd 8 Aug 1974

THIS PAGE IS UNCLASSIFIED

AD-203393

D-20

WADC TECHNICAL REPORT 57-744
ASTIA DOCUMENT NO. 203393

A JET ENGINE THERMOCOUPLE SYSTEM FOR MEASURING TEMPERATURES UP TO 2300°F

MICHAEL E. IHNAT
THE GENERAL ELECTRIC COMPANY

JANUARY 1959

Materials

20070924070

WRIGHT AIR DEVELOPMENT CENTER

NOTICES

When Government drawings, specifications, or other data are used for any purpose other than in connection with a definitely related Government procurement operation, the United States Government thereby incurs no responsibility nor any obligation whatsoever; and the fact that the Government may have formulated, furnished, or in any way supplied the said drawings, specifications, or other data, is not to be regarded by implication or otherwise as in any manner licensing the holder or any other person or corporation, or conveying any rights or permission to manufacture, use, or sell any patented invention that may in any way be related thereto.

- - - - -

Qualified requesters may obtain copies of this report from the Armed Services Technical Information Agency, (ASTIA), Arlington Hall Station, Arlington 12, Virginia.

- - - - -

Copies of WADC Technical Reports and Technical Notes should not be returned to the Wright Air Development Center unless return is required by security considerations, contractual obligations, or notice on a specific document.

WADC TECHNICAL REPORT 57-744
ASTIA DOCUMENT NO. 203393

A JET ENGINE THERMOCOUPLE SYSTEM FOR MEASURING TEMPERATURES UP TO 2300°F

MICHAEL E. IHNAT
THE GENERAL ELECTRIC COMPANY

JANUARY 1959

PROPULSION LABORATORY
CONTRACT NO. AF 33(600)-32302
PROJECT NO. 3073-30245

WRIGHT AIR DEVELOPMENT CENTER
AIR RESEARCH AND DEVELOPMENT COMMAND
UNITED STATES AIR FORCE
WRIGHT-PATTERSON AIR FORCE BASE, OHIO

McGregor & Werner Midwest Corp., Dayton, O.
21-453-200-3-5-59

FORWARD

This report has been prepared by the General Electric Company, Instrument Department under USAF Contract No. AF33(600)-32302. The present report is the final technical report on the development. The contract was administered under the direction of the Propulsion Laboratory of Wright Air Development Center. Project engineers during the period covered by this report were Mr. F. Miller and Mr. J. Fulton. This development was administered by Mr. R. C. Lever, Manager - Materials and Processes Unit representing the laboratory while Mr. R. B. Clark, Manager of Aircraft Temperature Devices, Design and Production Unit represented the engineering component.

Fulton 23193 -

Included among those who cooperated in the development and preparation of the report were the following development engineers: Mr. J. Freedman, Mrs. M. C. Hallinan, Mr. T. P. Haselton, Mr. M. E. Ihnat, Mr. D. Jaffe, Mr. P. Kissinger, Mr. G. Marshall, Mr. P. Oldow, Mr. P. Richardson, Mr. P. Ricupero, Mr. G. Samstead, Mr. B. D. Trott, Mr. C. S. Smith, and the following assistants: Mr. L. Stiles, Mr. G. Robinson, and Mr. R. Curran.

ACKNOWLEDGMENTS

The author wishes to express his sincere appreciation to the following individuals and organizations who were very helpful during this development.

Mr. Frank Caldwell	National Bureau of Standards
Mr. Paul Freeze	National Bureau of Standards
Mr. Ken Flodin	Kennametal Inc., Latrobe, Pa.
Mr. John Redmond	Kennametal Inc., Latrobe, Pa.
Mr. W. Sterling	Firth Sterling Inc., Pittsburgh, Pa.
Mr. G. L. Merritt	Driver Harris Co., Harrison, N. J.
Mr. F. Dickinson	Haynes Stellite Co., New York, N.Y.
Mr. J. Keady	Climax Molybdenum Co., New York, N.Y.
Mr. W. Dettwhiler	Baker Co., Inc., Newark, N.J.
Mr. W. Person	Norton Refractories, Worcester, Mass.
Mr. H. P. Tucker	International Nickel Co., Boston, Mass.
Mr. R. Cohn	Sigmund Cohn Co., Mt. Vernon, N.Y.
Dr. B. Brenner	Sigmund Cohn Co., Mt. Vernon, N.Y.
Mr. D. Lundy	J. Bishop Co., Malvern, Pa.
Mr. P. Fly	Tube Methods Co., Norristown, Pa.
K. C. Sherrer	H. K. Portor Co., Inc., Philadelphia, Pa.
Mr. R. T. Merriman	McDanel Refractory Co., Beaver Falls, Pa.
Mr. J. Jakielski	Western Gold & Platinum Co., Belmont, California
Mr. H. Moseby	Linde Air Products, Speedway, Indiana
Dr. L. Navias	G. E. Research Laboratory
Dr. A. Gratti	G. E. Research Laboratory
Mr. A. I. Dahl	G. E. General Engineering Laboratory
Mr. W. Zimmerman	G. E. Flight Propulsion Laboratory
Mr. M. Pohlman	G. E. Flight Propulsion Laboratory
Mr. W. Moran	G. E. Small Aircraft Engine Department
Mr. D. Rubinstein	G. E. General Engineering Laboratory

ABSTRACT

A reliable thermocouple temperature sensing system for aircraft jet engines having an operating temperature range of 1800°F (982°C) to 2300°F (1260°C) has been developed. The purpose of this system is for pre-turbine installation to allow potential increases in engine thrust.

The system is unique in that it uses a thermoelement combination of palladium and platinum 15% iridium. Provisions are also made for matching lead wires up to ambient temperatures in the 1300 to 1500°F (704° to 816°C) temperature range.

The system has been shown to be reliable over the specified temperature range for a 400 hour period.

PUBLICATION REVIEW

The publication of this report does not constitute approval by the Air Force of the findings or conclusions contained herein. It is published only for the exchange and stimulation of ideas.

FOR THE COMMANDER:

Charles M. Michaels

CHARLES M. MICHAELS
Chief, Air Breathing Propulsion Division
Propulsion Laboratory

TABLE OF CONTENTS

Section		Page
I	Introduction	1
II	Thermoelements	6
	Addendum	13
	System Calibration Results	13
	Conclusions	21
III	Lead Wires	22
	Platinum-Platinum 13% Rhodium System	23
	The Palladium Systems	24
	Nickel-Silicon Alloys	26
	Nickel-Manganese Alloys	26
	Nickel-Aluminum Alloys	26
	Nickel-Manganese-Silicon Alloys	26
	Palladium-Platinum 10% Iridium Thermocouple	28
	Palladium-Platinum 15% Iridium Thermocouple	30
	Lead Wire Stability	30
	Lead Wire Conclusions	33
IV	Insulation	34
	Factors Affecting Choice of Insulation	37
	Resistivity	37
	Mechanical Strength	42
	Resistance to Thermal Shock	42
	Vibrational Stress	42
	Expansion	42
	Chemical Compatability	42
	Fabrication	42
	Testing of Refractories	44
	Refractories	44
	Magnesium Oxide	44
	Periclase	48
	Aluminum Oxide	48
	Beryllium Oxide	48
	Conclusions	49
V	Sheath Materials	50
	Cermets and Alloys	61
	Conclusions	61
VI	System Design	72
	Fast Response System	72
	Test Results	76
	Conclusions	76
	High Recovery System	81
	Design Conclusions	84
VII	Connectors	86
	Evaluation	87
	Conclusions	90

TABLE OF CONTENTS
(continued)

Section		Page
IX	Conclusions	96
	Fast Response System	96
	High Recovery System	96
	National Bureau of Standards Informal Report	96
X	General Bibliography	99

APPENDICES

Appendix I	Thermoelectric Properties of Materials Compiled for Study	104
Appendix II	Thermoelectric Characteristics of Base Metal Alloys Used in Lead Wire Development	110
Appendix III	Statistical Analysis of Lead Wire Experiment	114

LIST OF TABLES

		Page
Table 1.	Present Thermocouple Systems	2
Table 2.	Melting Point of the Elements	3
Table 3.	General Characteristics of Palladium and Platinum	9
Table 4.	Experimental Test Results of Development Systems	17
Table 5.	Maximum Percentage E.M.F. Deviation During Life Cycle	17
Table 6.	Calibration of Palladium/Platinum 15% Iridium Thermocouple	20
Table 7.	Refractory Data Notes	38
Table 8.	Oxidation Resistance of Iron, Nickel, and Cobalt Base Alloys	51
Table 9.	Intergranular Oxidation of Iron, Nickel, and Cobalt Base Alloys	53
Table 10.	Comparative Results as Calculated from High Temperature Sheath Tests	63
Table 11.	Material Characteristics for Time Response Estimates	74
Table 12.	Time Response Results	78

LIST OF ILLUSTRATIONS

		Page
Figure 1.	Approximate Melting Point Limits of Material Types	3
Figure 2.	Thermal E.M.F. between Rhodium-Platinum and Pure Platinum	7
Figure 3.	Thermal E.M.F. of Platinum Alloys vs. Platinum at 1200°C	7
Figure 4.	Thermal E.M.F. of Noble Metals vs. Platinum at Temperature	7
Figure 5.	Combustion Test Facility	10
Figure 6.	Structural Variation of Palladium in an Oxidizing atmosphere at 1316°C	11
Figure 7.	Life Test Data for Determination of Palladium Thermo-electric Stability	13
Figure 8.	a. Palladium Junction Failure During Combustion Testing	14
	b. Effects of Welding in Air or Inert Atmosphere	14
Figure 9.	Comparative Output of Chromel/Alumel and Development Systems	15
Figure 10.	Experimental Concentric Thermocouple Assembly	16
Figure 11.	Thermocouple Calibration Test	19
Figure 12.	National Bureau of Standards System Dimensions	20
Figure 13.	Lead Wire Output Comparison for Alloy Development Purposes	25
Figure 14.	Effect on E.M.F. Output of Silicon and Manganese in a Nickel Alloy	25
Figure 15.	Effect on Output of Increasing Silicon in a Nickel-Silicon Alloy	27
Figure 16.	Effect on Output of Increasing Aluminum Content of a Nickel-Aluminum Alloy	27
Figure 17.	Triangular Data Plot for Ternary Lead Wire Development	29
Figure 18.	The Effect of Cold Working a Nickel Base Lead Wire	29
Figure 19.	The Effect of Annealing Time on a Nickel Base Lead Wire	29
Figure 20.	Effect of Replacing Nichrome by Nichrome V or 242T	31
Figure 21.	Insulation Configurations	35
Figure 22.	Resistivity Values Obtained from Literature and from Test	38
Figure 23.	Resistance vs. Dimensions at Various Resistivity Values	39
Figure 24.	Resistivity vs. Dimensions at Various Thermoelement Diameters	40
Figure 25.	Resistivity vs. Outer Insulation Dimensions for Various Systems	41
Figure 26.	Error in Thermocouple Output as Measured by Simulated Resistance Decrease	43
Figure 27.	Resistance as a Function of Temperature for Various Dimensions and Materials.	45
Figure 28.	Resistance as a Function of Temperature for Various Magnesium Oxide Samples	46
Figure 29.	Resistivity vs. Temperature for Aluminum Oxide Samples	47
Figure 30.	Temperature and Velocity Contour at the Segmental Entry to a Turbine	51
Figure 31.	Oxidation of Inconel 702 and Inconel	55
Figure 32.	Oxidation of Inconel X	56
Figure 33.	Intergranular Oxidation of Inconel 702 at 2450°F	57
Figure 34.	Probe Force as a Function of Temperature and Pressure	59
Figure 35.	Comparative Mechanical Properties of Inconel 702, Inconel, and Stainless Steel 321.	60
Figure 36.	High Temperature Axial Load Test	62
Figure 37.	Results of Combustion Testing Sheath Materials at 2500°F	64
Figure 38.	Kennametal Cermets - As Received	65
Figure 39.	Kennametal Cermets after 25 Hours Combustion Test and One Thermal Shock Cycle	65

LIST OF ILLUSTRATIONS
(continued)

		Page
Figure 40	Haynes Stellite Cermet LT-1 Test Results	66
Figure 41	Haynes Stellite Cermet LT-1-B Test Results	67
Figure 42	Haynes Stellite Cermet LT-2 Test Results	68
Figure 43	Inconel 702 Protected by LA-1 - As Received	70
Figure 44	Inconel 702 Protected by LA-1 - After Test	70
Figure 45	Inconel 702 Protected by LA-3 - As Received	71
Figure 46	Inconel 702 Protected by LA-3 - After Test	71
Figure 47	Experimental Time Response	74
Figure 48	Speed of Response Test	77
Figure 49	Concentric Sub-miniature Thermocouple Junctions	77
Figure 50	Junction Types Used for Time Response Tests	80
Figure 51	Total Temperature Probe	83
Figure 52	General Electric High Recovery Probe	85
Figure 53	Williamsgrip Connector	88
Figure 54	General Electric Type 705 Connector	89
Figure 55	Canadair Connector	89
Figure 56	Five Basic Harness Designs	92
Figure 57	High Temperature Flexible Thermocouple Cable Assembly	94
Figure 58	Probable Lead Wires for Pt-Pt 10% Rh Thermocouple	111
Figure 59	Probable Lead Wires for Pt-Pt 13% Rh Thermocouple	112
Figure 60	Probable Lead Wires for Pt 6% Rh/Pt 30% Rh Thermocouple	113

SECTION I - INTRODUCTION

A reliable thermocouple temperature sensing system for aircraft jet engines having an operating temperature range of 1800°F (982°C) to 2300°F (1260°C) has been developed. The purpose of this system is for pre-turbine installation to allow potential increases in engine thrust. Thrust gains of 29 to 45 percent are possible by increasing the turbine inlet temperature from 1500°F (816°C) to 1900°F (1038°C).

Although numerous combinations of thermocouple materials exist, few have become popular. The types of Table 1 account for well over 98% of the thermocouples in use today.

Selection of suitable thermoelements for any application, and this application in particular, represents a compromise of accuracy, life, ruggedness, response time as influenced by conduction, radiation losses, partial adiabatic recovery, errosion, size, convective heat transfer, etc.

Extensive investigations in the past have been conducted on thermocouple systems other than those listed in Table 1, and it became apparent early in this project that a consolidation of scattered high temperature thermocouple information was necessary. In consolidating this information, it was found systems reported as suitable for high temperatures were done so without proper clarification of atmosphere, life and stability. For this reason, the conclusions that can be drawn from such a compilation are necessarily very general ones.

Very few materials are capable of withstanding a specified steady-state operating temperature of 2300°F (1260°C) with short-time transients to 2500°F (1371°C). Listed in Table 2 are elements, having melting points in excess of 2500°F (1371°C) in ascending order. Because of the exceptional reliability required of the materials for pre-turbine installation, determination of proper materials presented the major problem.

A tabulation of all types of materials would be prohibitive, however their approximate range of melting points are shown in Figure 1. In addition to limitations imposed by the melting point, sufficient reliability make it necessary that the additional factors listed below be considered.

1. Good oxidation resistance
2. Good impact properties
3. Good thermal shock characteristics
4. Adequate strength
5. Good fatigue properties
6. Resistance to excessive scaling
7. Adequate creep properties

Revised manuscript released by the author October 1958 for publication as a WADC Technical Report.

TABLE 1. PRESENT THERMOCOUPLE SYSTEMS

Thermocouple	Max. Temperature Cont. Use	Max. Temperature Spot Readings	Output mv/100°C
Chromel-Constantan	1000°C (1832°F)		7.65 @ 1000°C
Iron-Constantan	800°C (1472°F)	1100°C (2012°F)	5.69 @ 800°C
Copper-Constantan	400°C (752°F)	500°C (932°F)	5.22 @ 400°C
Nickel 18% Molybdenum-Nickel	1300°C (2372°F)		5.17 @ 1300°C
Chromel-Alumel	1100°C (2012°F)	1300°C (2372°F)	4.04 @ 1300°C
Platinum-Platinum 13% Rhodium	1600°C (2912°F)	1750°C (3182°F)	1.17 @ 1600°C
Platinum 1% Rhodium - Platinum 13% Rhodium	1600°C (2912°F)	1750°C (3182°F)	1.17 @ 1600°C
Platinum-Platinum 10% Rhodium	1600°C (2912°F)	1750°C (3182°F)	1.05 @ 1600°C
Platinum 5% Rhodium-Platinum 20% Rhodium	1600°C (2912°F)	1750°C (3182°F)	0.672 @ 1600°C
Platinum 6% Rhodium - Platinum 30% Rhodium	1600°C (2912°F)	1750°C (3182°F)	0.704 @ 1600°C
Platinum 20% Rhodium - Platinum 40% Rhodium	1800°C (3272°F)	1800°C (3272°F)	0.6 @ 1800°C
Iridium-Iridium 60% Rhodium	2000°C (3632°F)		0.5 @ 1650°C & 2000°C

TABLE 2. MELTING POINT OF THE ELEMENTS

ELEMENT	MELTING POINT °C	MELTING POINT °F	ELEMENT	MELTING POINT °C	MELTING POINT °F
Silicon	1410	2570	*Rhodium	1966	3571
Yttrium	1452	2646	Boron	2100	3812
Nickel	1455	2651	Hafnium	2130	3866
Cobalt	1493	2719	Ruthenium	2500	4352
Iron	1540	2804	Columbium	2415	4379
Chromium	1550	2822	*Iridium	2454	4449
*Palladium	1554	2829	Molybdenum	2622	4752
Titanium	1690	3074	Osmium	2700	4892
*Platinum	1773	3223	Tantalum	2996	5425
Zirconium	1830	3326	*Rhenium	3167	5732
Thorium	1842	3348	Tungsten	3400	6152
Vanadium	1900	3452			

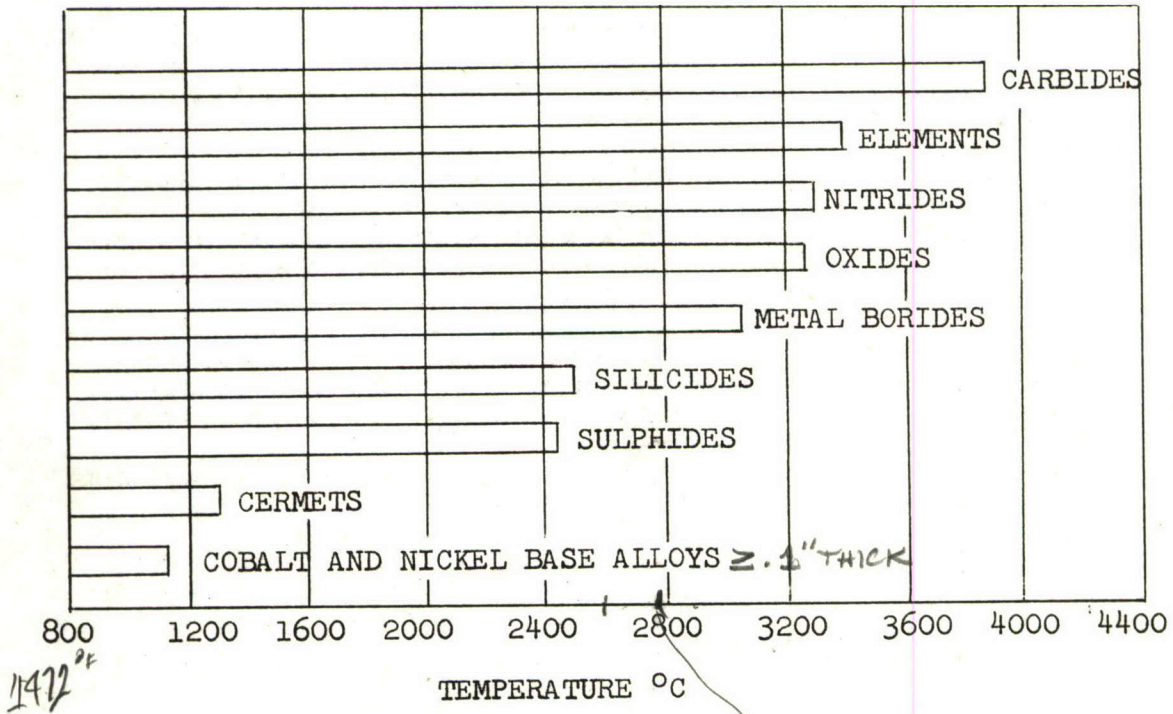


FIGURE 1. APPROXIMATE MELTING POINT LIMITS OF MATERIAL TYPES

With these additional requirements demanded, it was found, for example, that carbides, nitrides, oxides, metal borides, silicides and cermets fulfilling melting point requirements, did not satisfy all the properties as listed above. The only category of material likely to have a future, although many have been tested with only fair success, appeared to be the cermets consisting of hard carbides such as titanium and chromium carbide bonded with cobalt and nickel. These materials received some consideration during this development and are discussed in a later section.

It was apparent that the elements listed in Table 2 provide a starting point in a search for suitable material. These materials were considered with respect to the requirements listed above. The requirement of good oxidation resistance dictated that materials having good characteristics without protection be considered first and then those which require protection. The elements possible to employ unprotected were the noble metals rhenium, iridium, rhodium, platinum, and palladium. Of these five, only the latter four were commercially available in practical quantities and the volatilization of these materials at the higher temperature became a major consideration.

Crooks (30) reports that the loss of rhodium at 2372°F (1300°C) in air is only one-half that of platinum, one-sixth that of palladium, and one-sixtieth that of iridium. This also represents the order of choice of material for this application other things being equal.

For clarification, the component parts of systems in the discussion following are identified as follows:

1. Thermoelements - Two different metals joined together at two common junctions. When one of the junctions is maintained at some temperature other than the temperature of the second junction, an emf is generated. The generated electromotive force, provided it is small, is proportional to the temperature difference.

2. Lead wires - Consist of two different metals, having thermoelectric characteristics similar to those of the thermoelements. Any difference of output from thermoelements will introduce error in the system when the lead wire - thermoelement junction is at a temperature other than that of the cold junction.

3. Insulation - This is the thermocouple system insulating medium which provides high resistance leakage paths between the system components. Low resistance leakage paths are a source of inaccuracies in output.

4. Sheath - The sheath serves as the system supporting member containing insulation and thermoelements.

5. Connectors - Provide a means of system interconnection.

6. Harness - Usually used for structure mounting and providing interconnection of several thermocouple probes to obtain average temperature reading over a large area.

The specific requirements of these individual components as required by this contract are given prior to their discussion which follows.

II. THERMOELEMENT

The requirements of the thermoelements are as follows:

1. Steady state temperature range. 0-2300°F (1260°C)

2. Maximum transient temperature range. Up to 2500°F (1371°C)

3. Accuracy - The thermocouples shall conform to NBS standardization within plus or minus 0.5%; the overall accuracy of the system shall be within plus or minus 0.75%.

4. Output - The highest possible signal output (about 22 millivolts at 2000°F) is desirable, however, it is probable a compromise may be made between output, structural strength, and mechanical workability.

5. Constancy of Calibration - Subsequent to all tests of this contract, the calibration of the thermocouples and the complete system shall not deviate from the requirements of Paragraph 3.

6. Gas Flow Rate - The thermocouple system shall be capable of measuring the temperature of gases with velocities from 0 to 0.8 Mach.

7. Engine Test - The complete thermocouple system as required, shall be capable of satisfactory operation in a turbojet or turboprop engine selected by WADC. The operating temperatures and temperatures to be measured will be 1800-2300°F. The ambient temperature of the harness shall not exceed 1500°F. The test shall be for a 400-hour period and will be conducted on engine test stands at WADC according to the test procedures outlined in military specification MIL-E-5009B. After completion of tests, the thermocouple system shall be tested for conformance to Paragraphs 3 and 4.

An extension of the thermoelement materials presented in the introduction appears in Appendix I. This listing also includes alloys, rhodium, platinum and their alloys. However, taking into account the output requirements of Section 5 and Figure 2, it was found that these materials would not satisfy the above specification.

In considering other combinations, it was noted from Fig. 3 that a material could be made to provide an adequate signal when placed in combination with palladium. Figure 4 indicated that a platinum-iridium alloy would be adequate with the palladium vs. platinum-iridium combination yielding the larger output. On this basis, the materials palladium and platinum-iridium were chosen for detailed investigation.

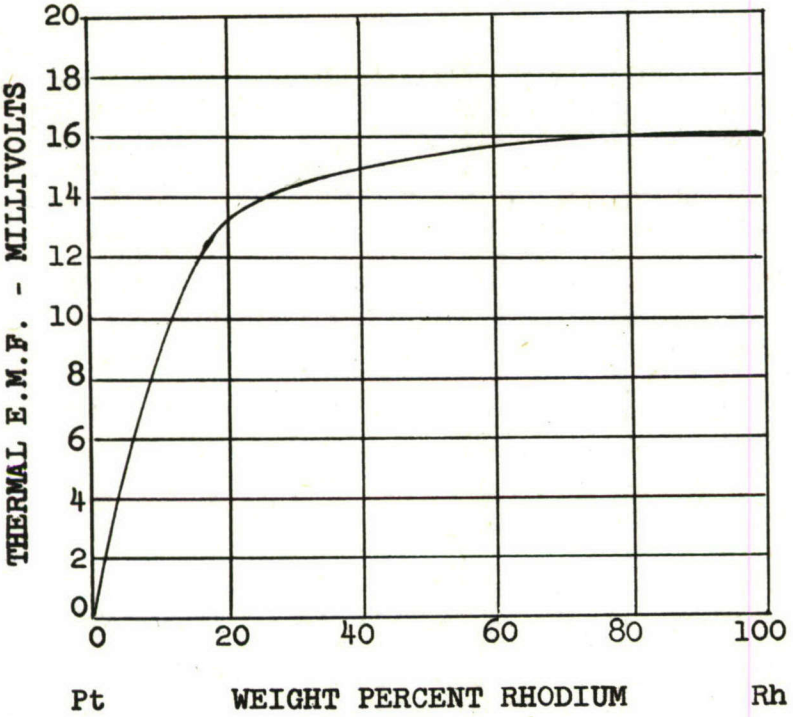


FIGURE 2. THERMAL E.M.F. BETWEEN RHODIUM-PLATINUM AND PURE PLATINUM REFERENCE AT 1100°C

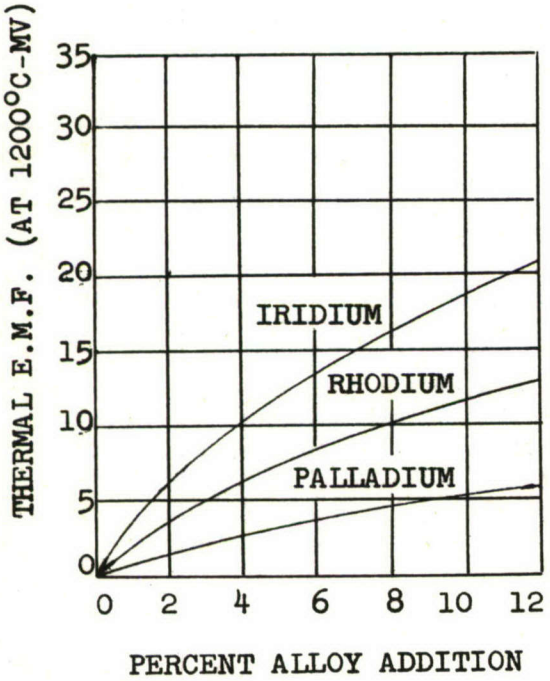


FIGURE 3. THERMAL E.M.F. OF PLATINUM ALLOYS VS. PLATINUM AT 1200°C

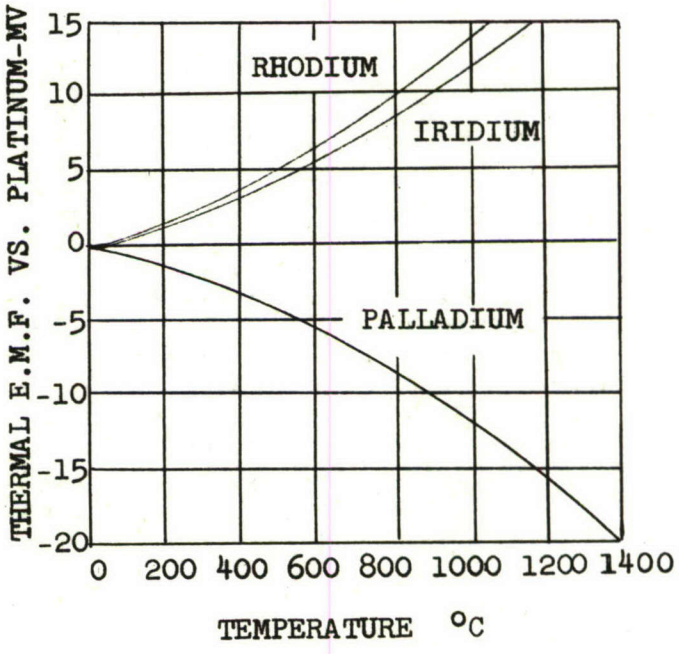


FIGURE 4. THERMAL E.M.F. OF NOBLE METALS VS. PLATINUM (AS A FUNCTION OF TEMPERATURE)

Palladium was the only noble material negative to platinum capable of providing an increased output, it was interesting to examine why this material has not found more general thermocouple use. Table 3 presents a comparison of properties of platinum and palladium, and it was noted that little variation in general exist between the two materials. There were, however, some characteristics distinct to palladium as noted below:

1. Palladium is superficially oxidized if heated to a temperature of 700°C (1292°F). The oxide (PdO) formed decomposes above 875°C (1607°F) and a bright metal remains.

2. Palladium will absorb as much as 800 to 900 times its own volume of hydrogen over a range of temperature.

3. Subjected to alternate oxidizing and reducing atmospheres surface blistering is apt to result.

Little prior information existed on the thermoelectric stability and capability of palladium to operate at elevated temperatures. An extensive literature survey produced only one reference (81) which indicated excellent stability in the 392 to 1112°F (200 to 600°C) range when usedin combination with silver, therefore, the present work assumed an extensive study to determine the characteristics of palladium at high temperatures.

The program to determine these characteristics can be detailed as follows: Figure 5 illustrates the combustion chamber designed for simulation of service atmospheres. The chamber was operated on number two fuel oil and maintained test hold tamperatures to approximately ± 25°F in the 2000 to 2500°F (1093 to 1371°C) range and ± 50°F in the 2500 to 2700°F (1371 to 1482°C) range.

Chemically pure palladium was suppled by Baker and Co., Inc., Newark, New Jersey and subjected to environmental testing in the combustion chamber at 2400°F (1316°C). Figure 6 illustrates the photomicrographs of structural changes with time. Other than grain-growth, there was no evidence of internal or surface damage in the simulated atmosphere for 175 hours.

Thermoelectric stability tests were performed by calibrating against assumed stable materials. The materials chosen for these test were rhodium, platinum, and platinum 20% rhodium. Figure 7 shows observed percentage emf changes after operation at temperature for the indicated time. These deviations were obtained by noting the change from initial calibration at 1093°C (2000°F). From these figures the variability of palladium/platinum was more random than that of palladium/rhodium or palladium/platinum 20% rhodium. On the basis of these tests, it was concluded that palladium was thermoelectrically stable in the temperature range concerned in this development.

TABLE 3. GENERAL CHARACTERISTICS OF PALLADIUM AND PLATINUM

		PALLADIUM	PLATINUM	
Density @ 20°C, g/cc.		12.02	21.45	
Crystal Lattice		F.C.C.	F.C.C.	
Lattice Cell, A		3.8825	3.9158	
Melting Point		1554 (2829°F)	1773.5 (3224.3°F)	
Thermal Conductivity @ 20°C		0.168	0.166	
Cal/sec/cm^2/°C @ 100°C		0.177	0.172	
Specific heat @ 0°C		0.058	0.031	
cal/gm/°C @ 20°C		0.058	0.032	
100°C		0.059	0.032	
500°C		0.064	0.035	
1000°C		0.071	0.038	
1500°C		--	0.042	
Resistivity 0°C		10.0	9.83	
Micro-ohm-cm 20°C		10.8	10.6	
100		14.3	13.6	
500		27.5	27.9	
1000		40.0	43.1	
1500		--	55.4	
Coef. of Expansion @ 100°C		11.1	9.1	
X 10^6	500	12.4	9.6	
	1000	13.6	10.2	
Tensile Strength	200°C	27.0*	19.5*	18.0**
psi x 10^{-3}	400	19.0	17.0	15.0
	600	13.0	15.0	11.0
	800	8.0	12.0	7.7
	1100	3.0	4.0	3.5
Elasticity Modulus psi x 10^{-6}		13.8	21.4	
Brinell Hardness		46	42	
Machinability		Poor	Poor	

* GRADE 1
**C.P. (Chemically Pure)

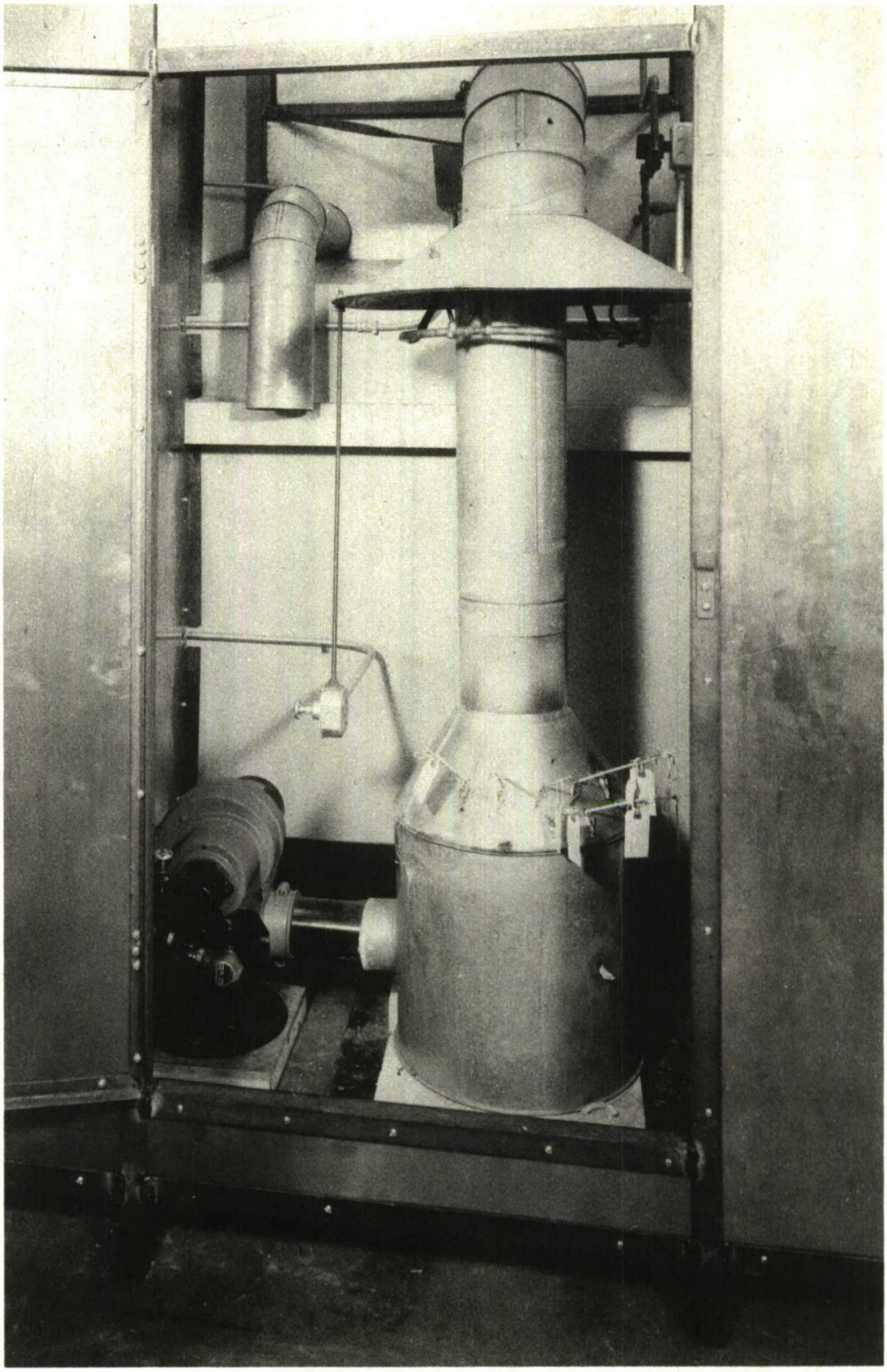
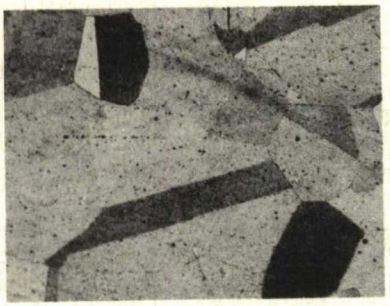
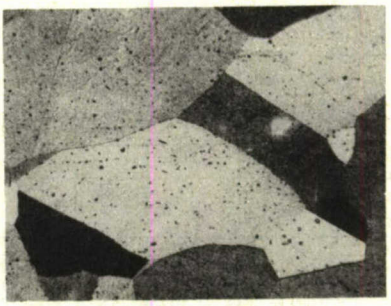


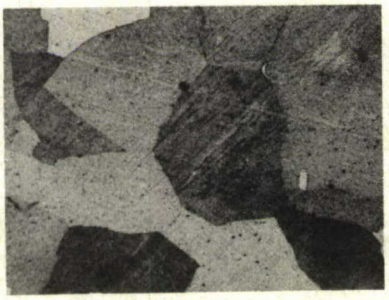
FIGURE 5. COMBUSTION TEST FACILITY. AIRCRAFT HIGH-TEMPERATURE THERMOCOUPLE



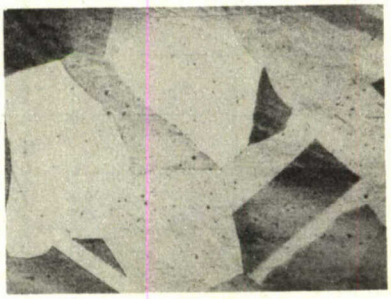
25 HOURS



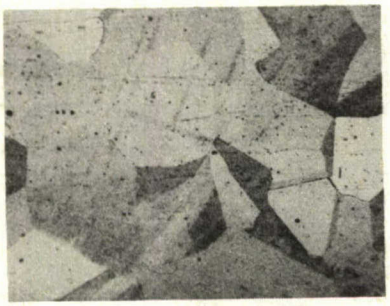
100 HOURS



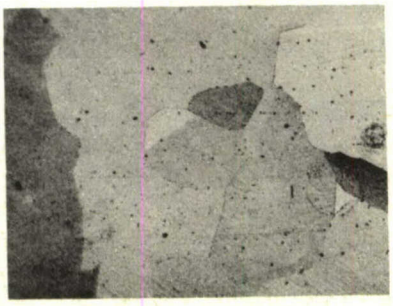
50 HOURS



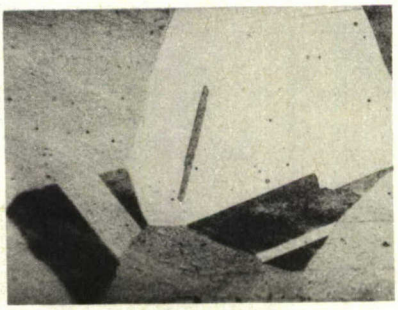
125 HOURS



75 HOURS

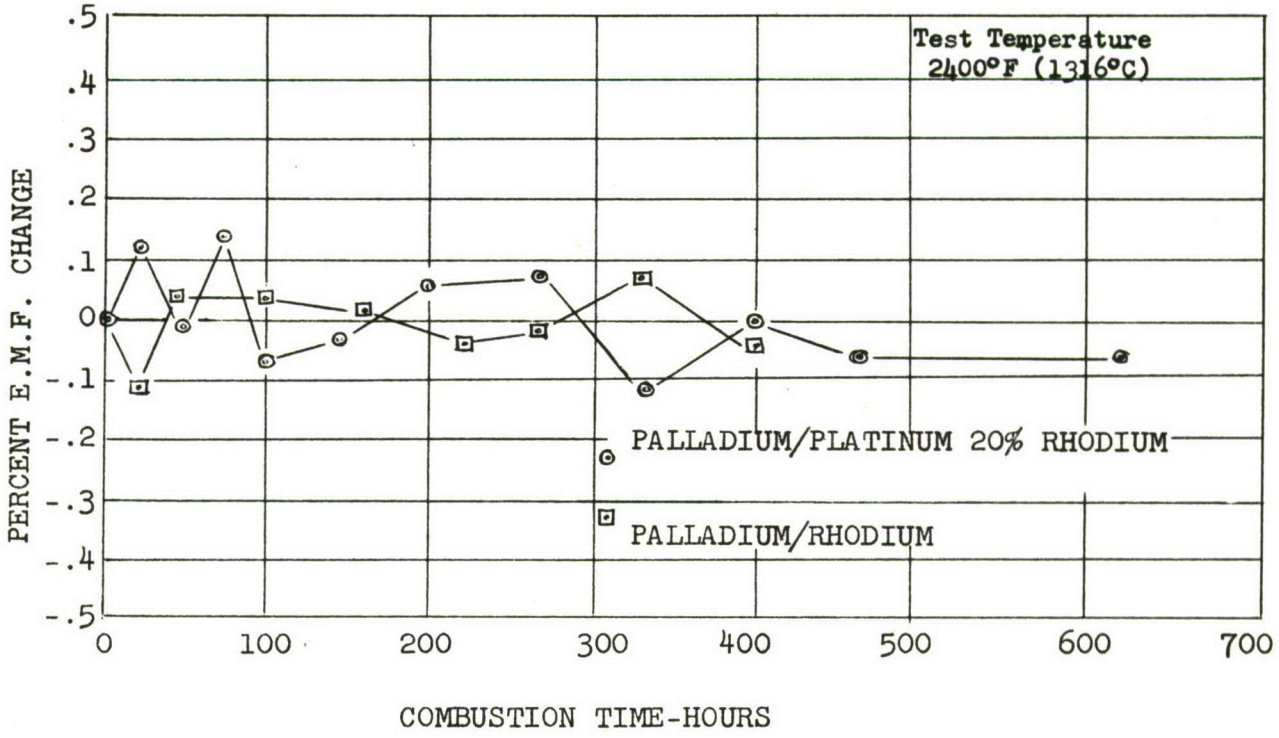


150 HOURS



175 HOURS

FIGURE 6. STRUCTURAL VARIATION OF PALLADIUM IN AN OXIDIZING ATMOSPHERE AT 2400°F (1316°C)



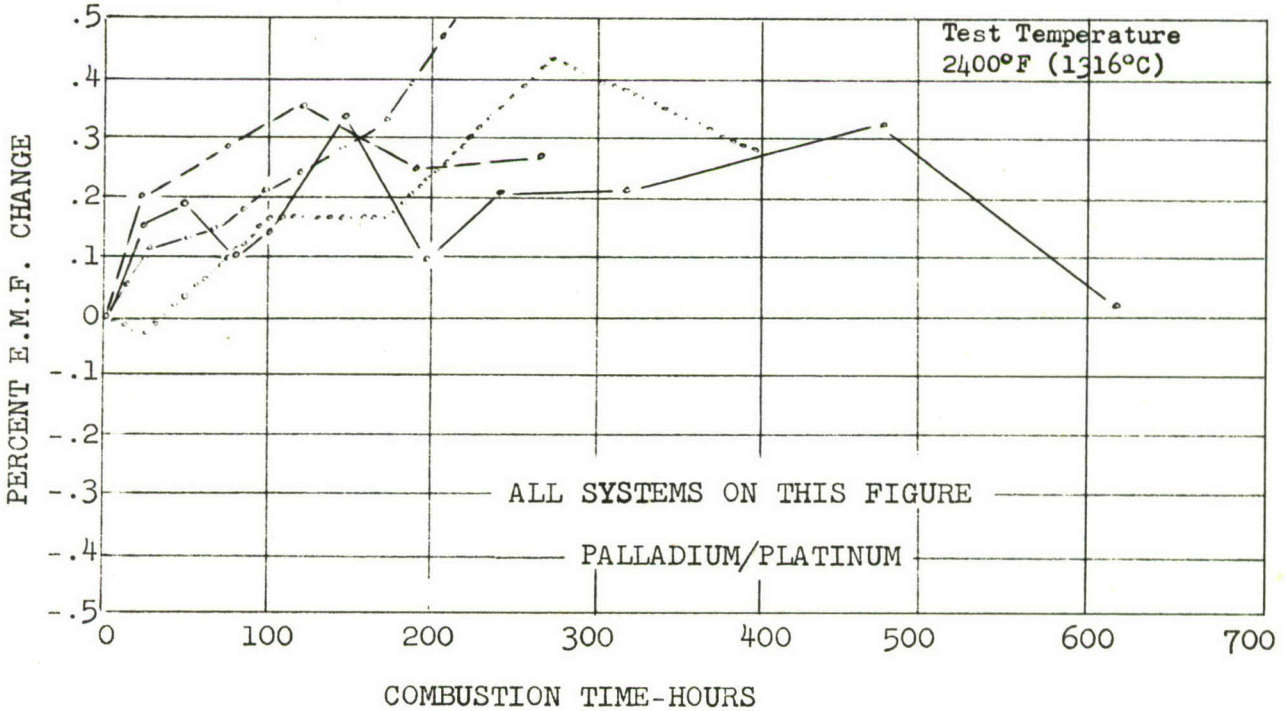


FIGURE 7. LIFE TEST DATA FOR DETERMINATION OF PALLADIUM THERMOELECTRIC STABILITY

During the initial testing of the thermoelements indicated above, several failures were observed as illustrated in Figure 8a. These failures were of concern since the prior tests of palladium did not indicate this effect. As a result, a study was made to determine the reasons for the voids appearing throughout the palladium. Since it was more or less confirmed that combustion (See Figure 6) was not the source of this damage, junction welding techniques were suspected. These suspicions were confirmed by the fact that the inclusions occured in close proximity to the junction. Figure 8b shows the results of electric arc-welding as compared to inert-arc welding. When inert-arc welding was used on additional test units, the failures disappeared.

Since one of the objectives of this work was to obtain a high output system, several other materials (Appendix I) were also tested. The output of the additional systems chosen for testing are shown in Figure 9 as compared to the characteristics of chromel/alumel. Since some of the materials of these experimental units were oxidizable they were assembled in the concentric construction of Figure 10. The results of testing these units are shown in Table 4. Although only those combinations which had probability of success earlier, completed the test, the significance was that palladium did afford some protection to materials such as tungsten and titanium.

As a result of the latter tests, either palladium/platinum 10% iridium or palladium/platinum 15% iridium were found to be suitable thermoelements for use in this project.

Addendum

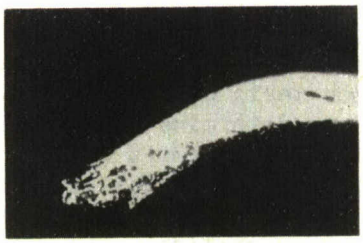
During the extensive testing of thermoelements, several combinations in the platinum series were tested for possible application to temperatures as high as 2700°F (1482°C). These were tested prior to modification of objectives under this contract. The results of these tests are shown in Table 5. It will be noted that all of the platinum/platinum-rhodium series prove adequate for the proposed application excepting the output requirement. The one system consisting of iridium/iridium 60% rhodium included in Table 5 served to prove that even at 2400°F (1316°C) the volatility of iridium was sufficient to prevent operation beyond 300 hours.

Calibration Results

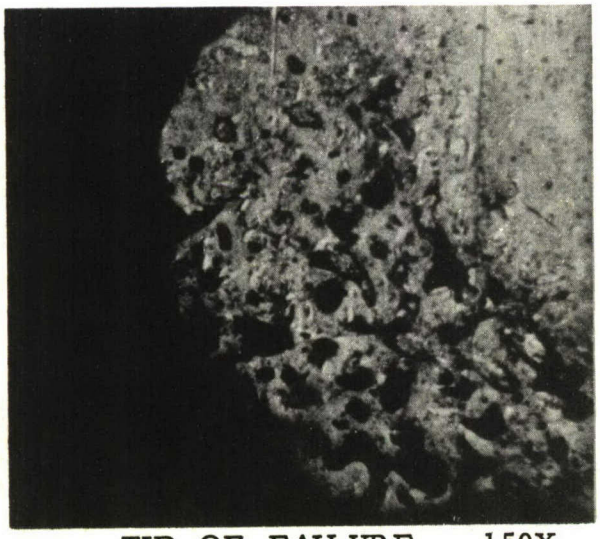
Calibration involves the problem of variability of thermoelement materials. In all cases, developmental thermoelement materials were specified to be as follows:

Palladium - Chemically pure, special pure or specially refined (Grade two in platinum grading system). Supplied by Baker & Co. Newark, New Jersey.

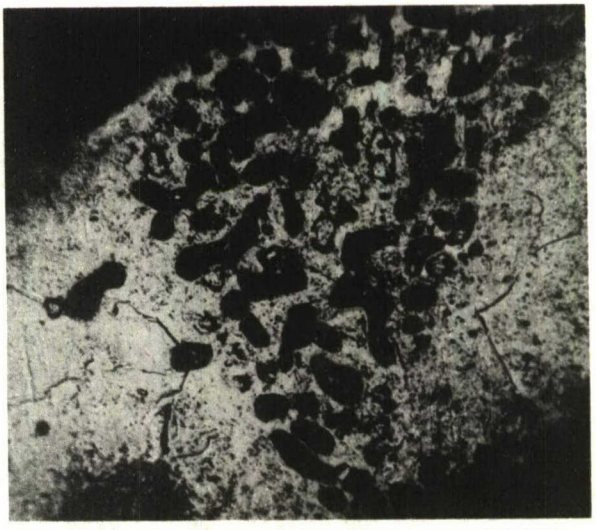
Platinum 15% Iridium - I.S.A. standard. Supplied by Sigmund Cohn Corp., Mt. Vernon, New York.



JUNCTION FAILURE 40X

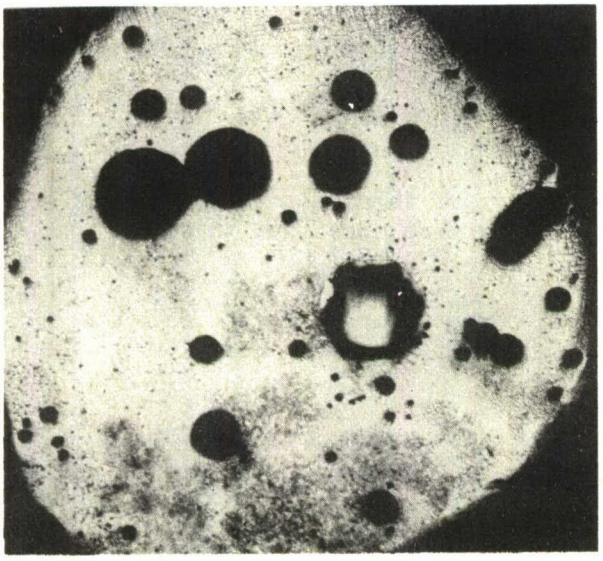


TIP OF FAILURE 150X

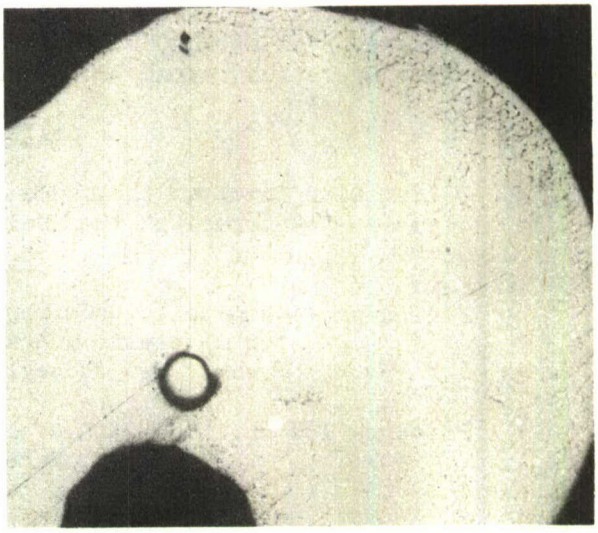


AREA NEXT TO TIP 150X

FIGURE 8a. PALLADIUM JUNCTION FAILURE DURING COMBUSTION TESTING



AIR WELD 60X



INERT WELD 60X

FIGURE 8b. EFFECTS OF WELDING IN AIR OR INERT ATMOSPHERE

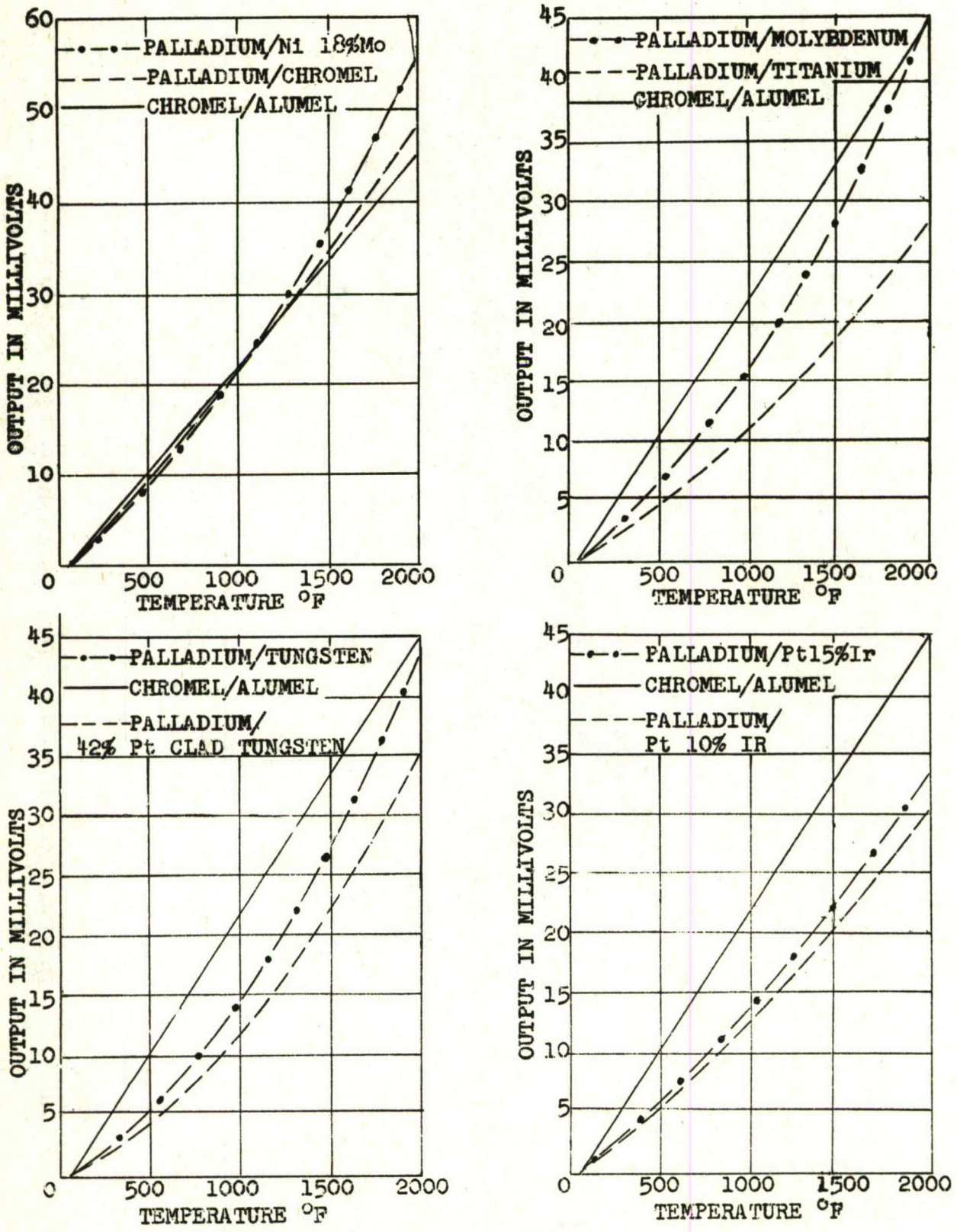


FIGURE 9. COMPARATIVE OUTPUT OF CHROMEL-ALUMEL AND DEVELOPMENT SYSTEMS

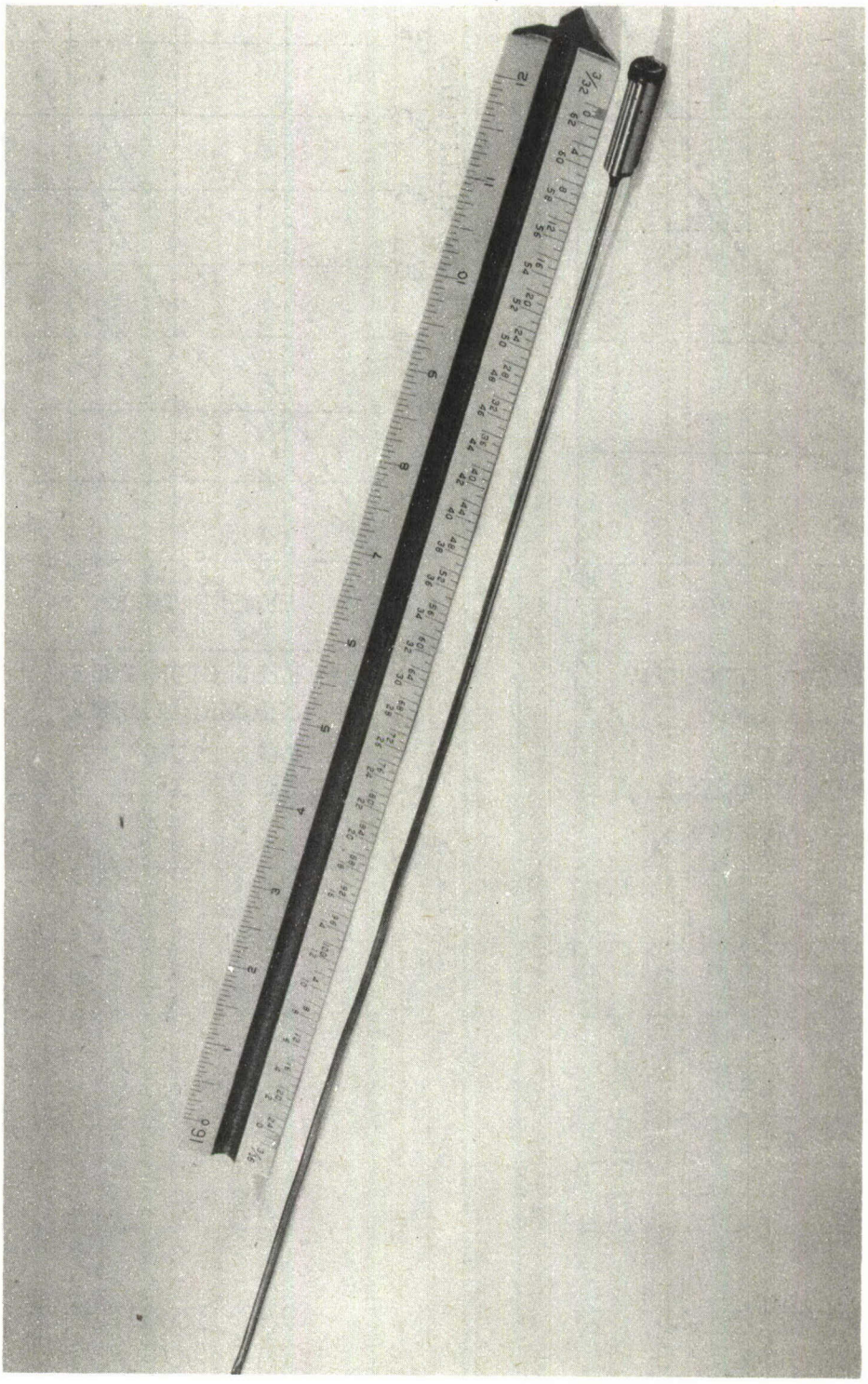


FIGURE 10. EXPERIMENTAL CONCENTRIC THERMOCOUPLE ASSEMBLY

TABLE 4. EXPERIMENTAL TEST RESULTS OF DEVELOPMENT SYSTEMS

SYSTEM	MAXIMUM COMBUSTION TIME - HOURS	MAXIMUM COMBUSTION TEMP.- °F
Palladium/Nickel 18% Molybdenum	50	2300
Palladium/Chromel	50	2200
Palladium/Tungsten	18	2400
Palladium/42% Platinum Clad Tungsten	50	2400
Palladium/Platinum 15% Iridium	400+	2300
Palladium/Rhodium *	600+	2400
Palladium/Titanium	25	2200
Palladium/Platinum 10% Iridium*	400+	2300
Platinum/Platinum 13% Rhodium	800+	2700

*Standard construction, butt-welded junction-all others of concentric construction.

TABLE 5. MAXIMUM PERCENT E.M.F. DEVIATION DURING LIFE TEST CYCLE

SYSTEM	WIRE DIAMETER INCHES	**MAXIMUM PERCENT CHANGE 400 HRS.	800 HRS.
Platinum/Platinum 10% rhodium	.020	-0.30	
" " "	.040	0.10	0.22
" " "	.020		0.22
Platinum/Platinum 13% rhodium	.020	0.02	
" " "	.020*	-0.21	0.13
" " "	.020		0.13
Platinum 6% rhodium/Platinum 30% Rhodium	.040	-0.09	0.15
" " "	0.20	0.06	
Plat. 5% Rhodium/Plat. 20% Rh.	.020	0.27	
" " "	.020	--	.048
Ir/Ir 60% Rh	.035	Ir completely volatilized @ 300 hrs. in combustion.	

* Coated with Rokide "A" as supplied by Norton Company, Worcester, Mass.

**First 600 hours operated at 1316°C (2400°F) and the last 200 hours at 1482°C (2700°F).

It was found that these specifications still allowed a variability of ±0.35% in the thermoelement thermoelectric characteristics. Acknowledging that this variability would exist until the materials were qualified as standard thermocouple materials, the following calibration was established using the equipment of Figure 11.

(Reference Junction at 32°F)

Temp. (°F)	Output (MV)	Temp. (°F)	Output (MV)	Temp. (°F)	Output (MV)
200	1.72	850	10.49	1500	22.25
250	2.29	900	11.29	1550	23.27
300	2.87	950	12.11	1600	24.29
350	3.47	1000	12.94	1650	25.36
400	4.09	1050	13.80	1700	26.42
450	4.73	1100	14.67	1750	27.50
500	5.38	1150	15.56	1800	28.60
550	6.06	1200	16.45	1850	29.71
600	6.75	1250	17.39	1900	30.83
650	7.46	1300	18.33	1950	31.96
700	8.19	1350	19.28	2000	33.12
750	8.94	1400	20.27	2050	34.27
800	9.70	1450	21.25	2100	35.48

System Calibration Results

Although system calibration concerns the individual calibration of thermoelements and lead wires, discussion of lead wires is deferred to a latter section of the report. System calibration can be discussed now because of the strong interdependence between system calibration and thermoelements.

Ten complete systems of the open junction, butt welded type construction were fabricated, using 16 gauge (0.051 inch) diameter wires. A system consisted of C. P. palladium, platinum 15% iridium, an alloy of 4.31% silicon-balance nickel, and standard Nichrome.* Eight of the indicated systems were shipped to the National Bureau of Standards in partial fulfillment of this contract while two identical systems were kept for calibration. The approximate system dimensions were as shown in Figure 12. The system calibration results of the Instrument Department, West Lynn, are shown in Table 6.

*Trademark - Driver-Harris Company

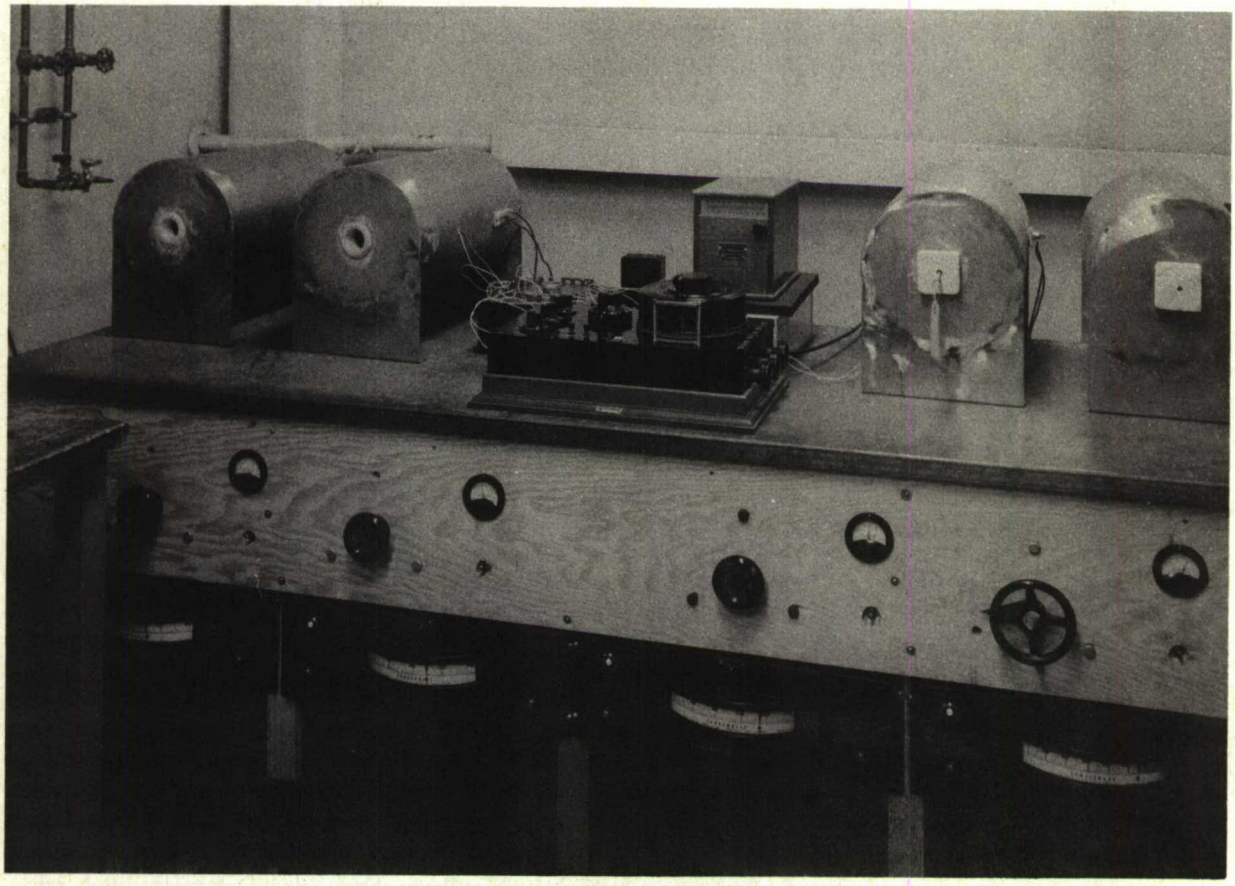


FIGURE 11. SECONDARY THERMOCOUPLE CALIBRATION TEST

TABLE 6. G. E. CALIBRATION OF PALLADIUM-PLATINUM 15% IRIDIUM THERMOCOUPLE (INCLUDING LEAD WIRES)

TEMPERATURE °F	°C	OUTPUT IN MILLIVOLTS
-82.7	-63.7	-1.04
-38.7	-39.3	-0.66
+ 1.0	-17.2	-0.31
83.5	28.6	0.52
120.7	51.3	0.93
158.4	70.3	1.29
250	121	2.32
500	260	5.46
750	399	9.06
1000	538	13.04
1250	677	17.46
1500	816	27.27
2000	1093	32.65

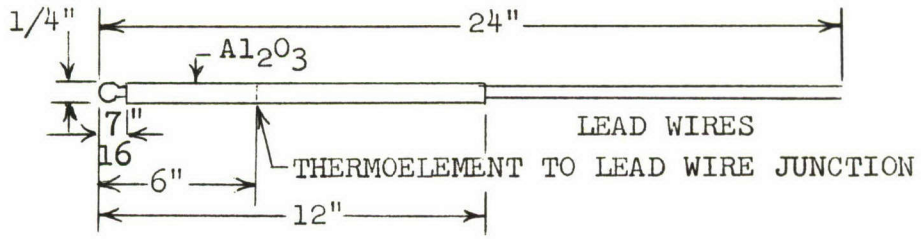


FIGURE 12. N.B.S. CALIBRATION SYSTEM DIMENSIONS

CONCLUSIONS

A system of thermoelements consisting of palladium/platinum 15% iridium was found not to deviate more than ±0.5% when subjected to an oxidizing atmosphere for more than 400 hours in the 1800 to 2300°F (982 to 1260°C) temperature range. The output of this material combination was found to be approximately three-fourths that of chromel/alumel.

The general characteristics of these materials are similar to a platinum/platinum 13% rhodium system, (strength, etc.) however, the cost of palladium is as low as one-fifth that of platinum.

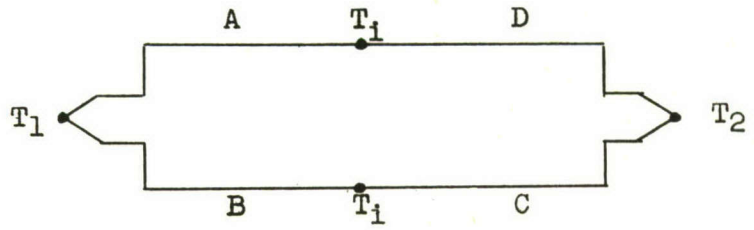
The fabrication of junctions using palladium must be done under an inert atmosphere.

The operation of this system is not recommended for a hydrogen atmospheres since a hydrogen saturated metal when checked against pure metal can give a signal of as much as 27 microvolts per degree centigrade. A system subjected to hydrogen saturation is also susceptible to the damage discussed in this section previously.

Section III - Lead Wires

Lead wires, particularly for noble metal thermoelements, have received comparitively little attention in the past. This section of the report deals with the development of lead wires having specific output characteristics for the noble metals under consideration. Although lead wires are now available that have practically the same temperature emf relation as some noble metals, they do so over a very limited range. In most cases, accuracies of from 1% to 3% in the range from 32 to 392°F (0 to 200°C) are common.

The figure below represents a schematic of a thermocouple (A & B) with interconnecting lead wires (C & D).



Letting

E_{ABCD} = Emf of the system

T_1 = Hot temperature

T_i = Intermediate temperature $T_1 > T_i > T_2$

T_2 = Cold junction temperature

e_{AB} = Thermoelectric power due to Metals A and B

e_{CD} = Thermoelectric power due to Metals C and D

The system consists essentially of two thermocouples. The first, metal A in combination with metal B with a hot junction at T_1 and effectively a cold junction at T_i The second, metal C in combination with metal D with a hot junction effectively at T_i and a cold junction at T_2.

Using normal thermometry procedure,

$$E_{AB} = e_{AB}(T_1 - T_i)$$

and

$$E_{CD} = e_{CD}(T_i - T_2)$$

These are additive so,

$$E_{ABCD} = E_{AB} + E_{CD} + e_{AB} (T_1 - T_i) + e_{CD} (T_i - T_2)$$

which can be modified to

$$E_{ABCD} = e_{AB} (T_1 - T_2) - (e_{AB} - e_{CD}) (T_i - T_2)$$

From this relation if $e_{AB} = e_{CD}$ the output emf of the system is -

$$E_{ABCD} = e_{AB} (T_1 - T_2)$$

and in effect, the system appears to contain only metals A & B.

The contract specifications which governed the study in this area were as follows:

1. Accuracy - The overall accuracy of the system shall be within plus or minus 0.75%.

2. Constancy of Calibration - Subsequent to all tests of this contract, the calibration of the thermocouples and the complete system shall not deviate from the requirements of paragraph one, above.

3. Ambient Temperature - Varying the thermocouple system ambient temperature from 250°F to 1300°F* shall not affect the system's accuracy more than an additional 0.25%.

4. Spurious emf - Each connector of the thermocouple system shall be tested for spurious junction effect. The amount of emf generated when a temperature gradient of 100°F is imposed across any one harness connection shall not introduce an error of plus or minus 5°F. When a 1000°F gradient is imposed, the amount of emf generated by any firewall connection, if applicable, shall not exceed plus or minus 5°F.

The first step in obtaining adequate lead wires for any thermoelement was to investigate several probable base metal material combinations. Since this development was concerned earlier with a platinum series of systems and then a palladium series, a compilation of closest matches found along with the characteristics of other base metals are present in Appendix II for reference purposes.

Platinum-Platinum 13% Phodium System

At the beginning of the lead wire development program it was noted that the Platinum-Platinum 13% Rhodium thermocouple would be selected, so lead wires to match this system were investigated. The choice of base-metal alloy was a stainless steel paired with a high nickel alloy. A general survey was made by measuring the output of sixteen stainless steel wires with

*Item 3 not changed during formal objective change, however, should read 1300°F to conform with requirements of Item 4.

each of three high nickel alloys. From the results, it was found that, while no pair of leads gave a perfect match to the thermocouple, it was possible to fabricate a stainless steel alloy of such a composition that, when paired with a nickel alloy, would have characteristics close to those of the Pt-Pt 13% Rh thermocouple. The wires tested were all chemically analyzed and this information, together with the output data, formed the basis of a statistical analysis performed by the Statistical Methods Section of the General Electric, General Engineering Laboratory.

The report of this analysis is given in Appendix III. From it, the approximate effect on output of each constituent of a stainless steel alloy could be obtained at each temperature indicated. From this data, the composition of alloys giving a close match to the Pt-Pt 13% Rh was calculated.

The closest calculated match was an alloy containing 12.4% nickel, 18.7% chromium and the balance iron with traces of carbon, phosphorous, columbium, and titanium. It was paired with a high nickel alloy, (19.7% chromium, 0.5% manganese, 0.3% iron, 1.3% silicon and the balance nickel). As the calculated result could not be relied on to give a perfect fit, melts were made up to investigate the outputs of alloys whose composition surrounded that of the theoretical alloy. All the melts were of nickel, chromium and iron, and in different series of melts, the percentages of nickel and chromium, and also their ratio, were varied. For each case, a set of ingots based on the composition of the calculated alloy was obtained.

The melts were cast in sand molds, then rolled down to rods of diameter 0.289 inches. One set of rods was tested in this cold worked condition while a duplicate set was annealed at 1830°F for 1/2 hour before testing.

By the time all the rods from the first melt had been tested, it had been decided to concentrate on one of the high output palladium thermocouple systems so no further testing was done on the stainless steel alloys. None of the stainless steel rods tested had a deviation of less than ±5.0% from the Pt-Pt 13% Rh thermocouple, so that the effort in this area represents one of probable investigation for future work.

The Palladium Systems

The stainless steel alloys have too low an output to be considered as lead wires for a palladium-platinum iridium thermocouple. Several commercial high nickel alloys were tested against Nichrome* (60% nickel, 16% chromium, balance iron) and the results (Fig 13&14) indicated that by varying the percentage of silicon and manganese in these alloys a close match for the palladium systems should be obtainable.

An investigation of the effects of adding manganese, silicon, and aluminum to nickel both separately and in pairs, was made. The first tests indicated a unidirectional change in output at any temperature due to an increase in the

*Trademark - Driver Harris Co.

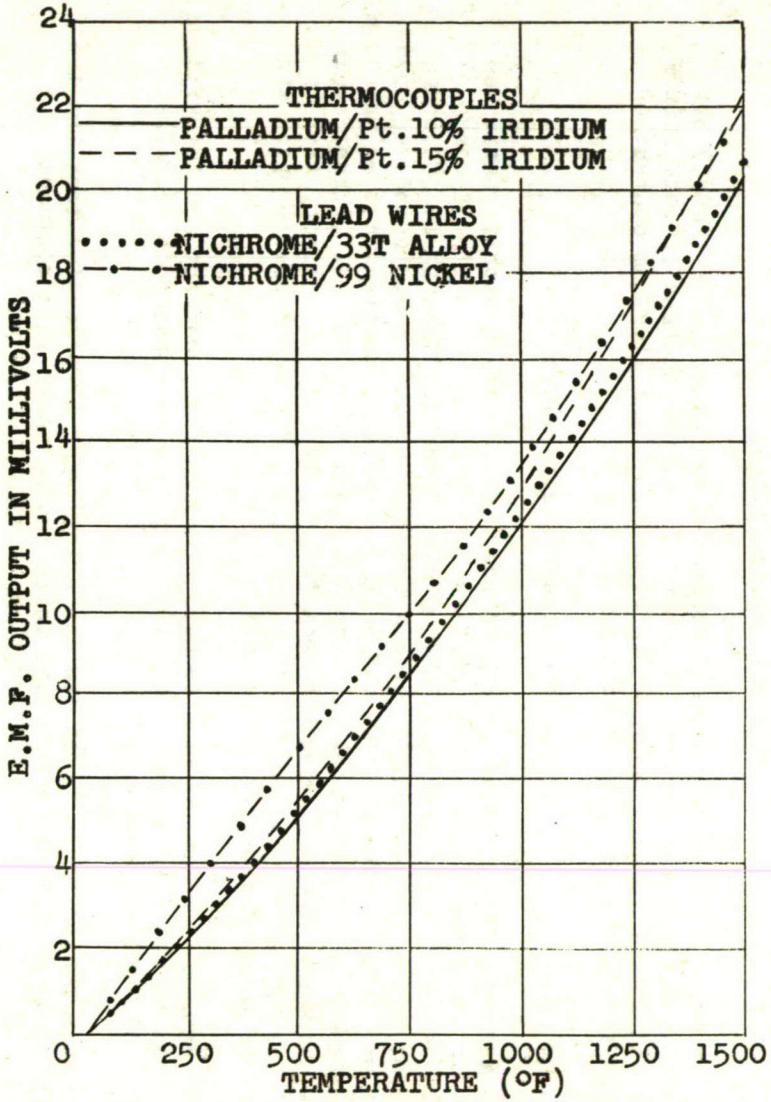


FIGURE 13. LEAD WIRE OUTPUT COMPARISON FOR ALLOY DEVELOPMENT PURPOSES

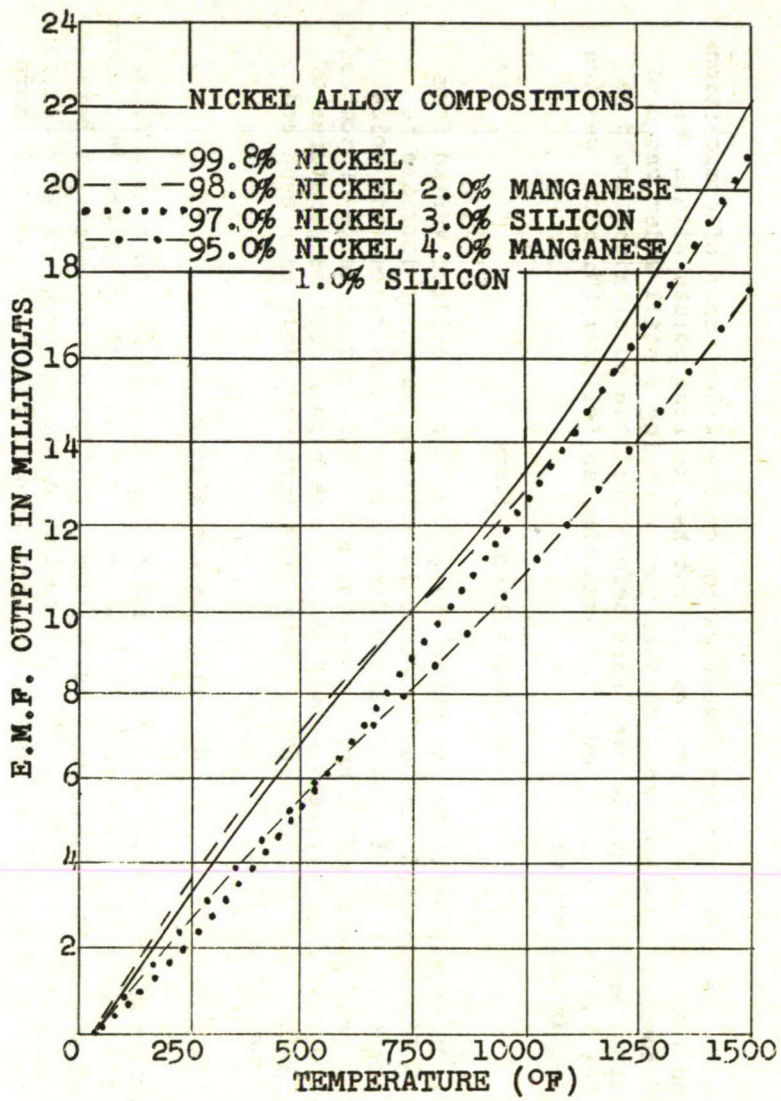


FIGURE 14. EFFECT ON E.M.F. OUTPUT OF SILICON AND MANGANESE IN A NICKEL ALLOY (ALL ALLOYS MEASURED AGAINST NICHROME)

variable, but a more detailed investigation over a wider range of compositions indicated that the trend is not regular but has turning points within the range of compositions studied. Further work covering a still wider range of compositions was found to be necessary before reliable conclusions could be drawn, but the results obtained were summarized as follows: (Nichrome was the second leg in all cases).

Nickel-Silicon Alloys

The first set of melts, in which the percentage of silicon varied from 1.86 to 3.86, indicated that an increase in silicon caused an increase in output above about 600°F (316°C) and a decrease in output below this point. However, tests performed on melts covering a slightly larger range of compositions (1.07% - 5.25% silicon) showed that at the higher test temperatures of 1000°F (538°C) and 1500°F (816°C), where were turning points near each end of the range (Fig. 15).

Nickel-Manganese Alloys

There was not enough test data available on this binary to draw a final conclusion. A preliminary test indicated that an increase in manganese content increases output at temperatures below 1100°F (593°C) and decreases it between 1100°F (593°C) and 1500°F (816°C), but further tests only confirm this for part of the range. Further test work would be necessary to investigate this more fully.

Nickel-Aluminum Alloys

An increase in aluminum content decreased output at 500°F (260°C) but once more turning points occured at about 4% aluminum content at both 1000°F (538°C) and 1500°F (816°C) as shown in Figure 16. The aluminum content of the melts varied between 0.93% and 4.12%.

Nickel-Manganese-Silicon Alloys

It was more difficult to interpret results from tests with ternaries as, under existing conditions, it was difficult to keep the quantity of one variable constant while examining the effect of varying the other. However, in one set of melts the silicon content was kept to 2.85 ° 0.05% and manganese content was varied between 2.79% and 4.84%. Results indicated that an increase in manganese content decreased the output all all temperatures. These results were supported by those from melts containing 1.72 ± 0.02% silicon, the manganese varying from 1.79% to 3.57%, as well as further melts in which the silicon had a greater degree of variation.

The manganese content was also held approximately constant and the silicon content was varied. An increase in silicon here also produced a decrease in output all all temperatures.

A large number of melts of similar alloys were prepared for test but the shortage of time did not permit them to be tested under this contract.

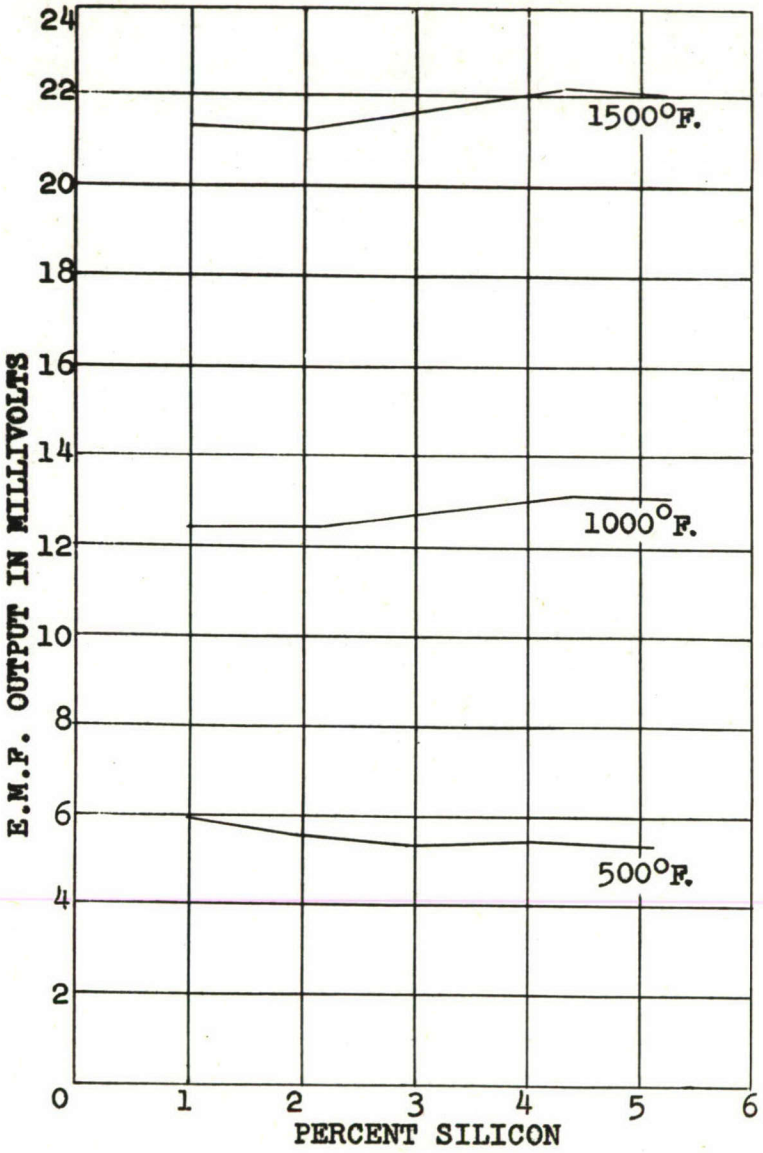


FIGURE 15. EFFECT ON OUTPUT OF INCREASING SILICON IN A NICKEL-SILICON ALLOY

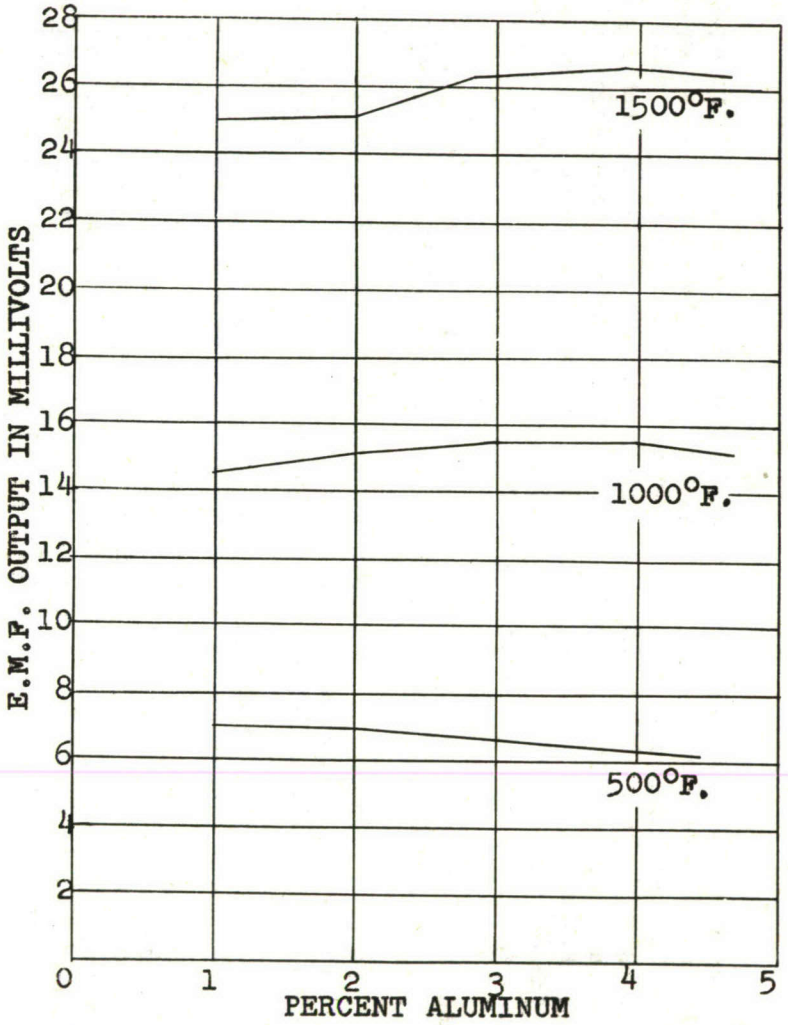


FIGURE 16. EFFECT ON OUTPUT OF INCREASING ALUMINUM CONTENT OF A NICKEL-ALUMINUM ALLOY

Data obtained from the ternaries was plotted with the aid of triangular coordinates in order to predict the composition of a ternary which would meet any feasible output specifications, supposing that such an alloy exists. However, a great deal of data must be available to be plotted if such a prediction is to be accurate. A graph of some of the initial data obtained is shown in Figure 17 and indicated that the approximate alloy composition to match the output of a Pd-Pt 10% Ir thermocouple. The latter figure has been included to illustrate the technique only.

All the preceding melts were tested in the form of swaged rods of diameter 0.162" after annealing for one hour at either 1600°F (871°C) or 1750°F (954°C).

Two nickel-silicon alloys were found that closely matched the two palladium systems that were considered and the remaining time was spent on trying to perfect these two alloys instead of continuing the more general investigation.

Palladium-Platinum 10% Iridium Thermocouple

In the preliminary survey of commercial alloys, it was noticed that fully annealed 97% nickel - 3% silicon alloy with Nichrome as the other leg provided a close match to the Pd-Pt 10% Ir thermocouple. The greatest deviation between the two was 2.5% at 500°F. By increasing the amount of cold work in the alloy, the maximum deviation was reduced to 0.5% (Fig. 18) but tests showed that this gave the wire poor stability at high temperatures (Fig. 19).

A nickel-silicon melt, containing 3.14% silicon, which had been cast in a sand mold, swaged to 0.162", then annealed for one hour at 1600°F (871°C) was a close match to the Pd-Pt 10% Ir thermocouple except at the lower end of the temperature range; the other lead wire leg was Nichrome, annealed at 1830°F(1000°C) for 1/2 hour. The rod was then drawn down to wire of diameter 0.036" and annealed as before, then retested giving the following percentage deviations from a particular Pd-Pt 10% Ir calibration.

Temperature	250°F	500°F	750°F	1000°F	1250°F	1500°F
% Deviation	+0.20	+2.2	+0.30	+0.41	+0.10	-0.55

It should be noted that the variability of the thermoelements themselves can be as much as ±0.35%. The above results were obtained by measuring the output of both lead wires and thermoelements separately, at specified temperatures. The lead wires were then welded to the thermoelements and the system as a whole was tested; the hot junction being maintained at 1692°F (922°C) and the ambient temperature varied as follows:

Temperature	259°F	478°F	755°F	947°F	1262°F	1449°F
% Deviation	+0.86	+0.33	+0.25	+0.25	+0.16	+0.04

This was repeated with the hot junction at 996°F with the following results:

Ambient Temp.	125°F	258°F	525°F	742°F
% Deviation	+2.5	+2.8	+1.7	+1.4

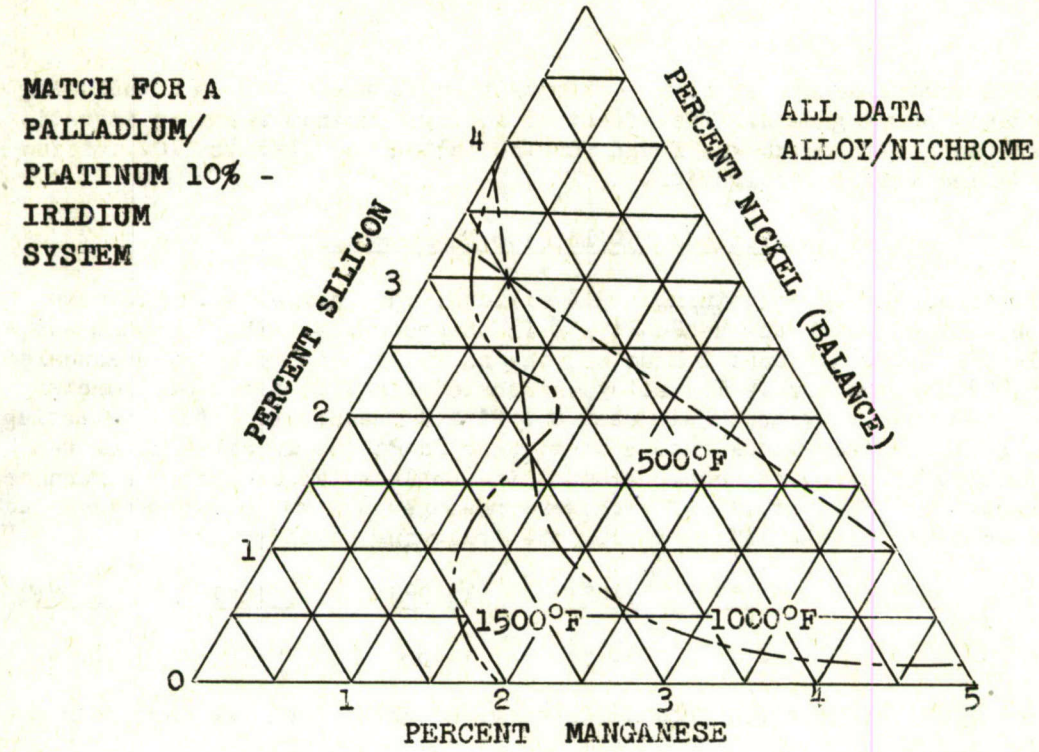


FIGURE 17. TRIANGULAR DATA PLOT FOR TERNARY LEAD WIRE DEVELOPMENT
(Each curve represents a constant output at the indicated temperature)

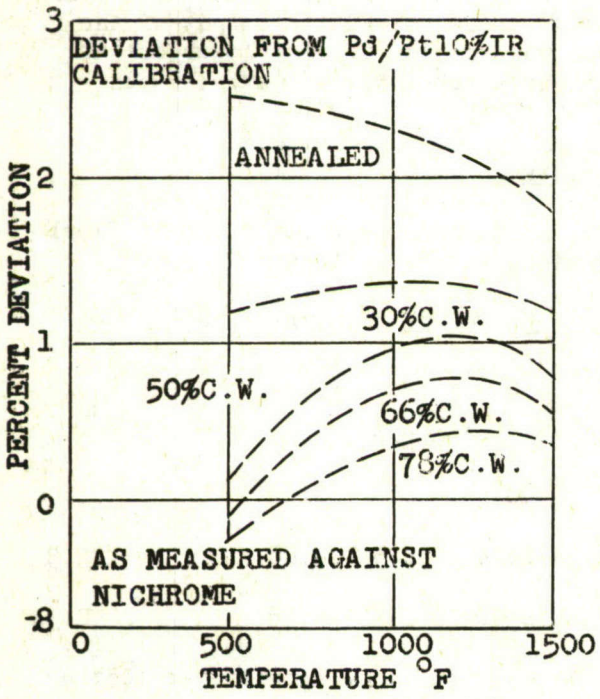


FIGURE 18. THE EFFECT OF COLD WORKING A NICKEL BASE LEAD WIRE ALLOY (Ni 3.00% Si)

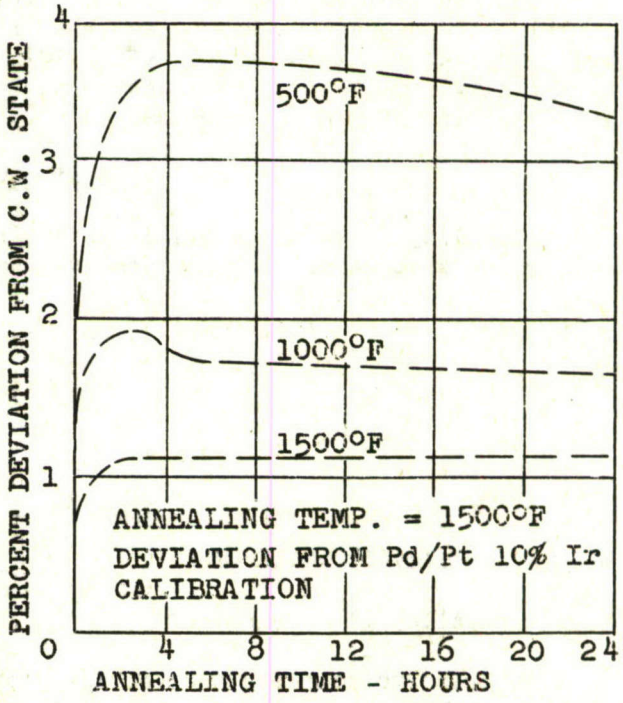


FIGURE 19. THE EFFECT OF ANNEALING TIME ON A NICKEL BASE LEAD WIRE (Ni 3.00% Si)

Other melts were made up, similar in composition to the above, but including very small amounts of manganese. The effect of adding aluminum was also investigated; however, no closer match was found for the palladium, platinum 10% iridium thermocouple during this investigation.

Palladium-Platinum 15% Iridium Thermocouple

A nickel-silicon alloy containing 4.31% silicon, when paired with Nichrome, appeared to be a close match to the Pd-Pt 15% Ir thermocouple. The Nichrome was annealed at 1830°F (1000°C) for 1/2 hour and the nickel-silicon alloy was annealed at 1750°F (954°C) for one hour. The alloy was tested first as a rod of diameter 0.162", then drawn down to wire of diameter 0.052" and reannealed before retesting. The deviation of these lead wires from a particular Pd-Pt 15% Ir calibration was measured by butting a lead wire couple against the noble metal couple in a furnace at known temperature. The outputs of each were measured by two potentiometers and the percentage deviation calculated, giving the following results.

Temperature	263°F	499°F	780°F	1010°F	1316°F	1442°F
% Deviation	-0.47	-0.71	+0.56	+0.53	-0.39	-1.40

These are average values obtained from tests on wires drawn from two ingots from the same melt.

Other melts, varying slightly in composition from the above, were made up and tested, but none was a closer fit than the 4.31% nickel-silicon alloy.

The non-variable leg of the lead wire does not have to be Nichrome. Two other nickel alloys were used to replace the Nichrome. These raised the output of the lead wires at all temperatures (Fig. 20) and so were tested against lower output nickel alloys made up in the Instrument Department Laboratory. However, no uniformly-close match was discovered.

Lead Wire Stability

Stability tests of materials having nearly identical composition of the final lead wires were made. The comparative compositions are as follows:

Lead Wire	Trade Name	C	Ni	Cr	Si	Mn	Cb	Fe
Test Alloy	33T	0.5	96.5		3		1	
Lead Wire Alloys	--		96.5		3.4			
Test Alloy	242	0.1	77.9	20	1			
Lead Wire Alloy I	Nichrome		57.6	16.4	1.5	0.08		23.3
Lead Wire Alloy II	Nichrome V		77.9	19.0	1.31	0.48		0.34

In order to complete the testing within the alloted time, accelerated testing was undertaken subjecting the materials to the following cycle:

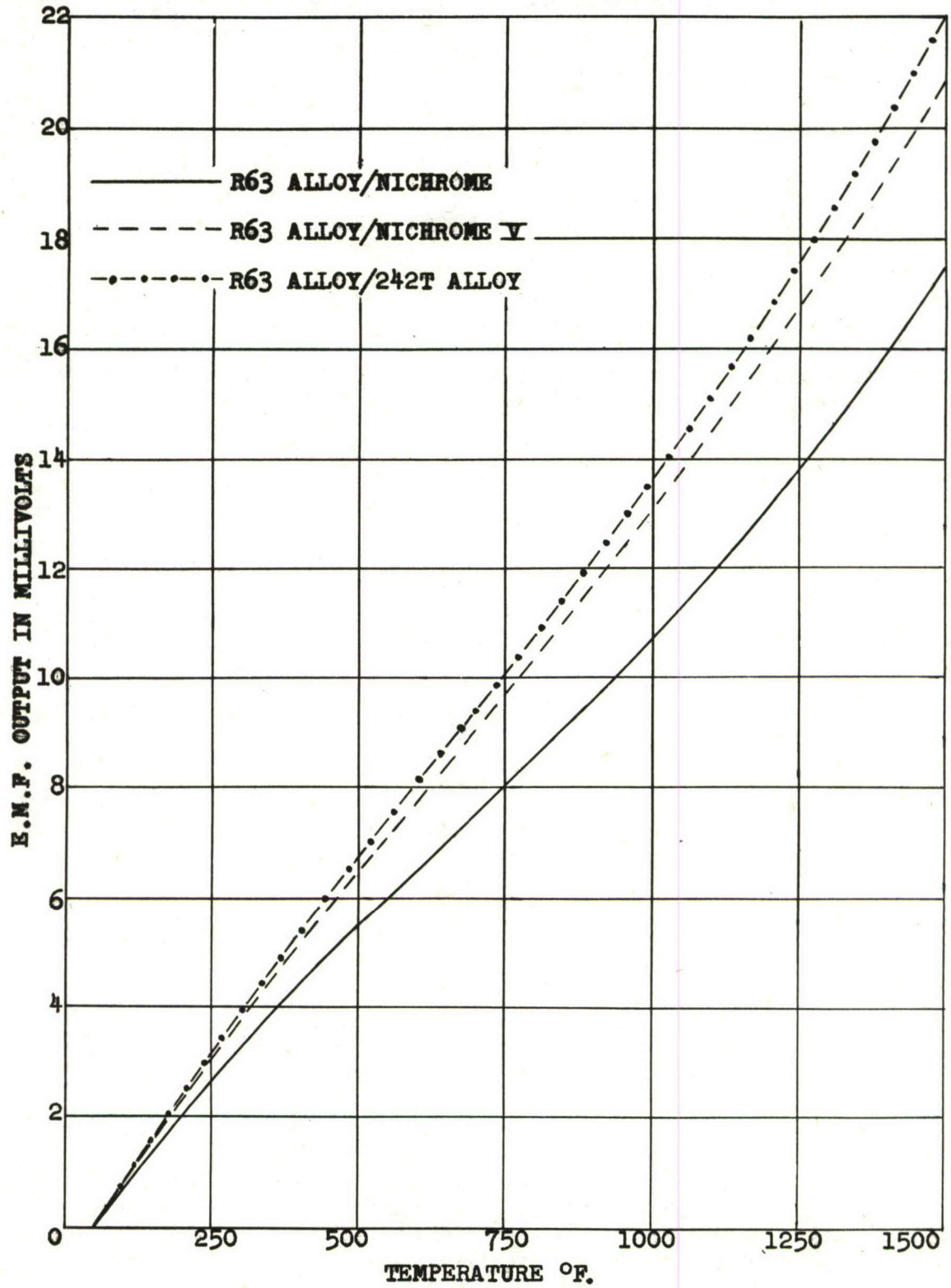


FIGURE 20. EFFECT OF REPLACING THE NICHROME LEAD WIRE BY NICHROME V OR 242T ALLOY

1. Initial stabilizing treatment. Anneal in air for 24 hours at 1832°F (1000°C).

2. Load into cold furnace.

3. Purge with hydrogen and ignite.

4. Raise temperature to 1832°F (1000°C) and hold for 24 hours.

5. Purge with nitrogen while at 1832°F (1000°C).

6. Circulate air for 24 hours.

7. Slow cool to room temperature.

After a 576 hour period, the lead wire alloys showed a marked change in output and the test was stopped with the following tabulated results.

NO. HOURS	% Change in Indicated Temp.*
0	0 (after initial stabilization)
48	-0.21
96	-0.02
144	-0.03
192	+0.12
240	+0.21
288	+0.48
336	+0.54
384	+0.60
432	+0.84
480	+0.54
528	+0.42
576	-2.5

* Average of ten units

Since the temperature to which these units were subjected are much higher than the specified ambients of this development, the recommended lead wires were concluded to be of suitable thermoelectric stability to be used with the recommended system of palladium-platinum 15% iridium.

Lead Wire Conclusions

An attempt has been made in the preceding discussion to show the steps of development to the recommended lead wire combination. It has also been pointed out that several areas appear to be fruitful areas of extended investigation not only from the standpoint of lead wires, but improved output from base metal systems. It may be worthy to also point out that all of the prior work was accomplished using standard foundry techniques.

Section IV - Insulation

Insulation is one of those areas which required a very careful analysis since it has been thoroughtly investigated by others, yet contains many conflicts as to reported results. Extensive work in this phase was not accomplished by this laboratory since another component of the General Electric Company had recently completed a thorough study of commercial insulation parameters (72). An extended study of those materials which appear applicable to this development was completed, however, and these are discussed in more detail in the following analysis.

The materials considered as insulators have a negative temperature coefficient and their resistivities vary with temperature according to the formula,

$$\rho = A(\rho)^{B/T}$$

where ρ = electrical resistivity in ohm - cm.

T = absolute temperature

A and B= constants for a given material

Two designs of thermocouples were considered. For the standard design, in an infinite conductor (Figure 21) using two parallel thermoelements, the resistance between the thermoelements (R_{AB}) and the resistance between the thermoelements and the sheath (R_{AC}) are given by the following formulae.

$$R_{AB} = \frac{\rho}{\pi l} \ln \left[\frac{2S}{D_1} \cdot \frac{D_2^2 - S^2}{D_2^2 + S^2} \right]$$

$$R_{AC} = \frac{\rho}{2\pi l} \ln \left[\frac{D_2^2 - S^2}{D_1 D_2} \right]$$

where: ρ = electrical resistivity in ohm - cm.

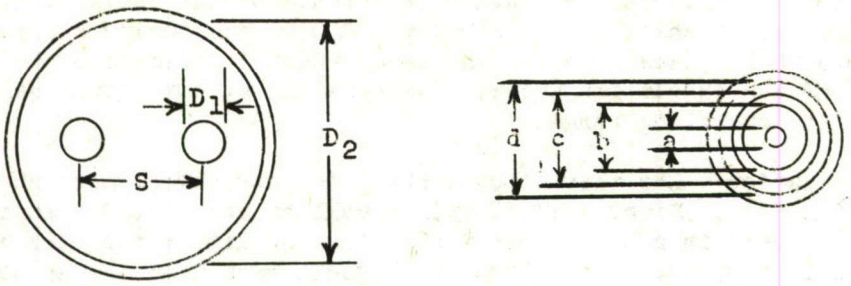
l = probe length in cm.

S = distance between thermoelements in cm.

D_2 = inner sheath diameter

D_1 = thermoelement diameter

A symmetrical configuration is assumed in this case. (Figure 21)



Standard Concentric

FIGURE 21 - THERMOCOUPLE INSULATION CONFIGURATIONS

It can also be shown that for conditions of maximum interconductor resistance, for any given values of D_1 and D_2.

Therefore:

$$\frac{\partial R_{AB}}{\partial S} = 0$$

$$S = 0.486\ D_2$$

With this condition and practicable dimensions for the variables,

$$R_{AB} : R_{AC} = 5:3$$

All future reported calculations are for resistance between thermoelements, R_{AB}.

For the concentric design thermocouple, see figure (21), the governing relations are given by:

$$R_{AB} = \frac{\rho}{2\pi l} \ln \left(\frac{b}{a} \right)$$

$$R_{AC} = \frac{\rho}{2\pi l} \ln \left(\frac{d}{c} \right)$$

where: a = diameter of inner thermoelement in cm.

b = inner diameter of outer thermoelement in cm.

c = outer diameter of outer thermoelement in cm.

d = inner sheath diameter in cm.

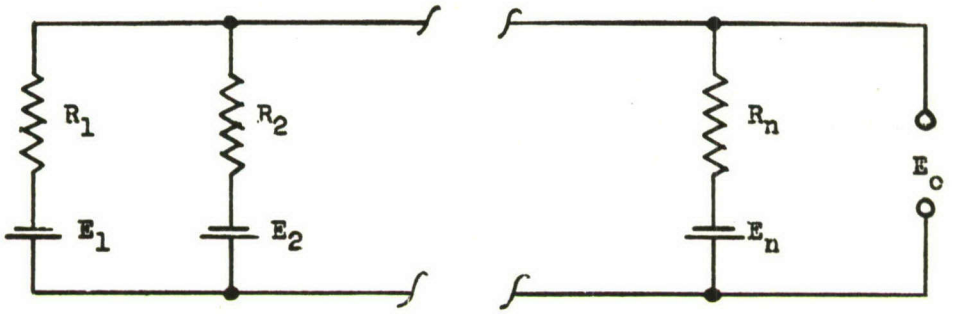
The contract specifications which governed the study of insulations were as follows:

1. Insulation Resistance - The resistance of the insulation used in the thermocouple system shall be at least 0.25 megohms under all engine

operating conditions. The insulation resistance of any subassembly of the thermocouple system shall not fall below 100,000 ohms during storage. These requirements shall prevail unless the development is able to prove that the resistance of the insulation selected is constant at some lower value throughout the operating range.

2. Fuel Contamination - The thermocouple shall not carbonize when subjected to the following test. Eight thermocouples shall be heated to a temperature of 200°F and immersed in a bath of JP-4 fuel at room temperature and allowed to soak for 10 minutes. The thermocouple shall be placed in the test section aft of a ramjet burner for one hour where temperatures shall be 1800 to 2300°F. This cycle shall be repeated 10 times and the insulation resistance shall not fall below 10,000 ohms.

The above specification deals specifically with a system having a resistance of at least 0.25 megohms. Since a system may consist of a number of components, the concept as used in the following discussion is worthy of clarification. A system as defined herein contains several paralleled units which in turn provide an approximate arithmetical average of the individually read thermocouples. Ideally, one represents a simple thermocouple harness as:



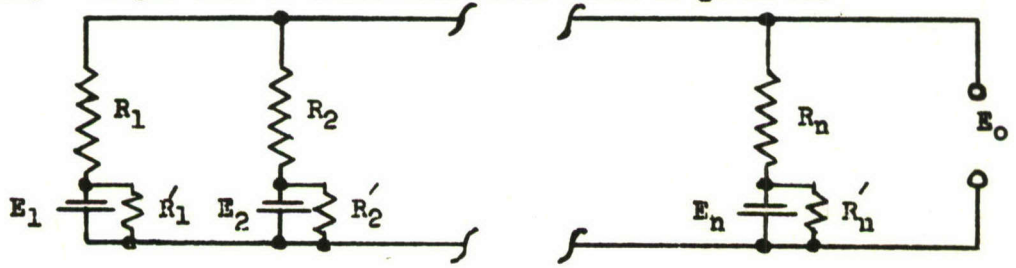
where the output voltage E_o is given by:

$$E_o = \frac{\sum_{i=1}^{n} \frac{E_i}{R_i}}{\sum_{i=1}^{n} \frac{1}{R_i}}$$

$$E_o = \frac{\sum_{i=1}^{n} E_i}{n} \quad \text{if } R_1 = R_2 = \ldots\ldots = R_n$$

$$R_o = \frac{R_1}{n}$$

If one now considers the case of the inter-element resistance (floating ground system) a single unit as considered above would be given as:



In this case, we represent that portion of the insulation nearest the thermoelements as a resistive path and assume it to represent the equivalent resistance between the thermoelements. The portion nearest the thermoelements was chosen because it represents the lowest equivalent value since it is at the maximum temperature. In this case, the output voltage is given by:

$$E_o = \frac{\sum_{i=1}^{n} E_i \frac{(R_i + R'_i)}{R_i R'_i}}{\sum_{i=1}^{n} \frac{1}{R_i + R'_i}}$$

which reduces to the prior case when $R'_i \longrightarrow \infty$. In any respect, this points up that R_i must be some comparable value of R'_i before it significantly changes the output voltage.

For a single standard design thermocouple, Figure (21), with a thermoelement diameter of 0.050 inches and an inner sheath diameter of 0.25 inches, the calculated resistivity must have a value of 5.4×10^6 ohm - cm. to provide an insulation resistance of 0.25 megohms (Figure 24). Figure (22) provides some resistivity values as found by a literature survey and G.E. tests. The only applicable material from this figure would be periclase (crystalline MgO) which is extremely brittle and extremely difficult to fabricate.

The resistivity of a refractory is affected by various factors. The presence of impurities will lower the resistivity as will an increase in the porosity which effects the amount of fuel absorption which will take place. A non-hygroscopic, inorganic refractory in a fused state is necessary to lessen or eliminate this effect as a powdered insulator will absorb fuel by capillary attraction. Swaging will also decrease the porosity of an oxide.

Resistivity is also affected by the surrounding atmosphere, especially at high temperatures, probably due to a chemical change in the surface of the material. This has little effect on a thermocouple enclosed in a metallic sheath as there is little exposed surface area.

Factors Affecting Choice of Insulation

1. Resistivity

The formulas of the preceding discussion show that the magnitude of the resistance of the insulation is primarily dependent on the value of the resistivity. This is shown graphically in Figures 23 and 24. An increase in the outer diameter of the insulation has little effect on resistance after an optimum value has been reached at about 0.2" to 0.3". A decrease in the diameter of the thermoelements is advantageous as regards resistance, but is detrimental structurally. A decrease in probe length also has a small beneficial effect.

The effectiveness of the two designs considered was compared. Figure (25) shows that the concentric design thermocouple gives a higher resistance than the standard design with 0.05" diameter thermoelements for any prac-

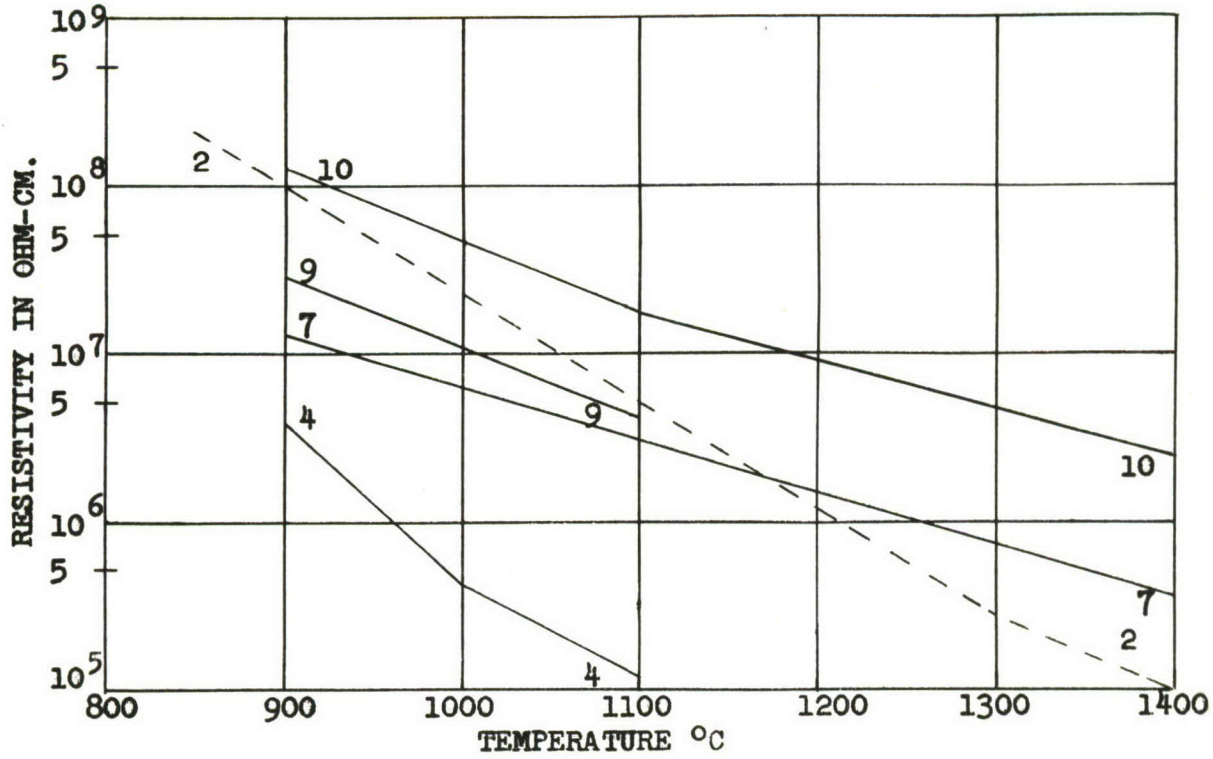


FIGURE 22. RESISTIVITY VALUES OBTAINED FROM LITERATURE AND BY TEST

TABLE 7. REFRACTORY DATA

KEY NO.	REFRACTORY	SOURCE OF DATA
1	FUSED INDUSTRIAL MgO	L.J. HOGUE: PROPERTIES OF HIGH TEMPERATURE INSULATION. G.E. REPORT NO. R56GL127
2	FUSED MgO	M. MARC FOEX: CONDUCTIBILITIES ELECTRIQUE DE LA GLUCINE ET DE LA MAGNESIE AUX TEMPERATURE ELEVEES. COMPT. REND 214,665-666 (1942)
3	FUSED MgO	H.M. GOODWIN AND R. D. MAILEY; ON PHYSICAL PROPERTIES OF FUSED MAGNESIUM OXIDE PHYSICAL REVIEW 23, 22, (1906)
4	SWAGED MgO	TESTS AT WEST LYNN
5	ALUMINA AL-1009	WESTERN GOLD AND PLATINUM COMPANY
6	ALUMINA (CORUNDUM)	R.J. RUNCK: HIGH TEMPERATURE TECHNOLOGY (EDITED BY I.E. CAMPBELL) P.58
7	SINTERED ALUMINA	E.C. HENRY: HIGH TEMPERATURE TECHNOLOGY P.457
8	ALUMINA	GARY STEVENS: HIGH TEMPERATURE TECHNOLOGY P.366
9	SWAGED ALUMINA	TESTS AT WEST LYNN
10	PERICLASE	E.G. ROCHOW: ELECTRICAL CONDUCTION IN QUARTZ, PERICLASE AND CORUNDUM AT LOW FIELD STRENGTH JOUR. APPL. PHY- 9, 10, (1938)
11	BERYLLIUM OXIDE	M. MARC FOEX: CONDUCTIBILITIES ELECTRIQUE DE LA GLUCINE ET DE LA MAGNESIE AUX TEMPERATURE ELEVEES. COMP. REND 214,665-666 (1942)

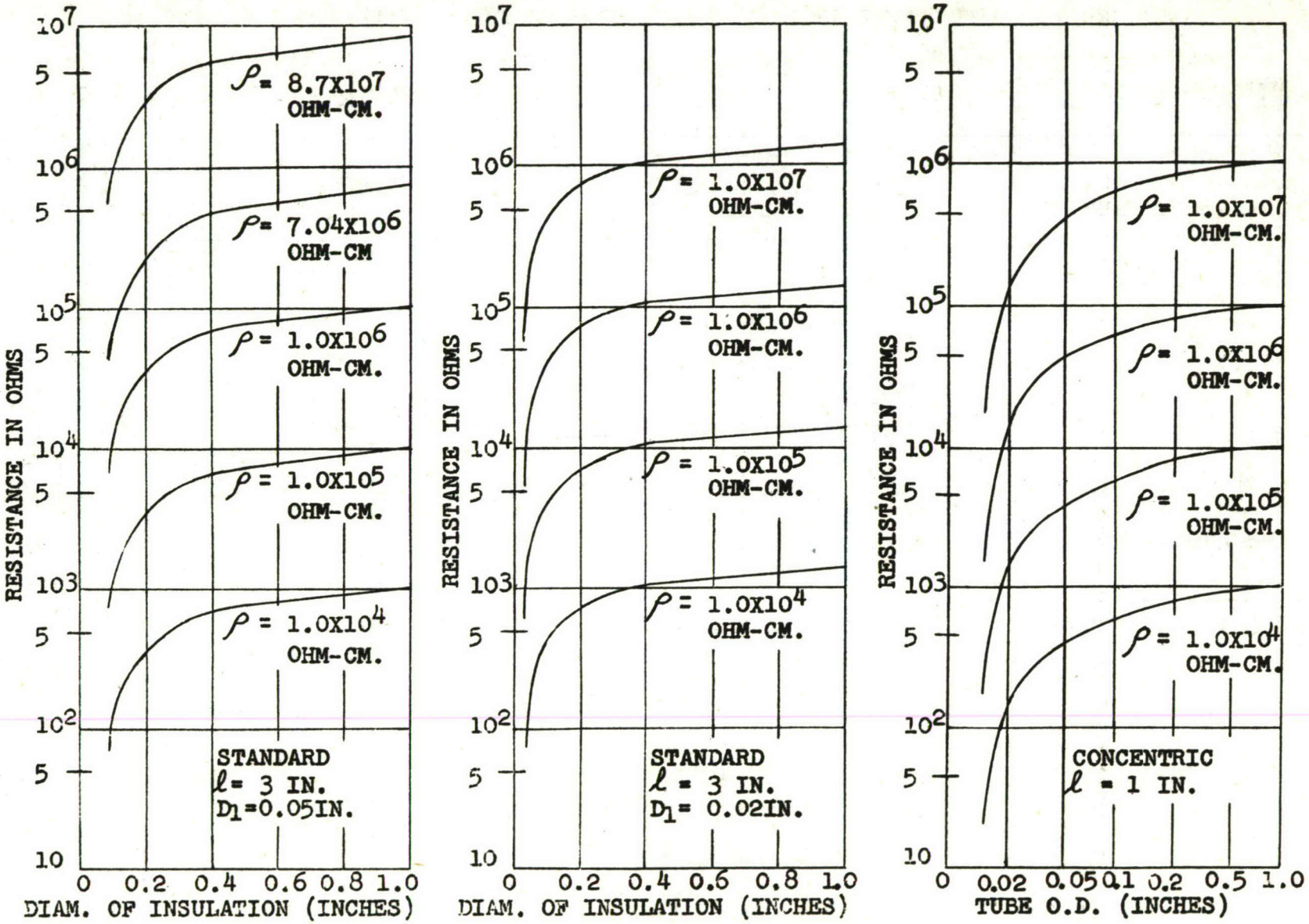


FIGURE 23. INSULATION RESISTANCE BETWEEN THERMOELEMENTS VS. DIMENSIONS AT VARIOUS RESISTIVITY VALUES

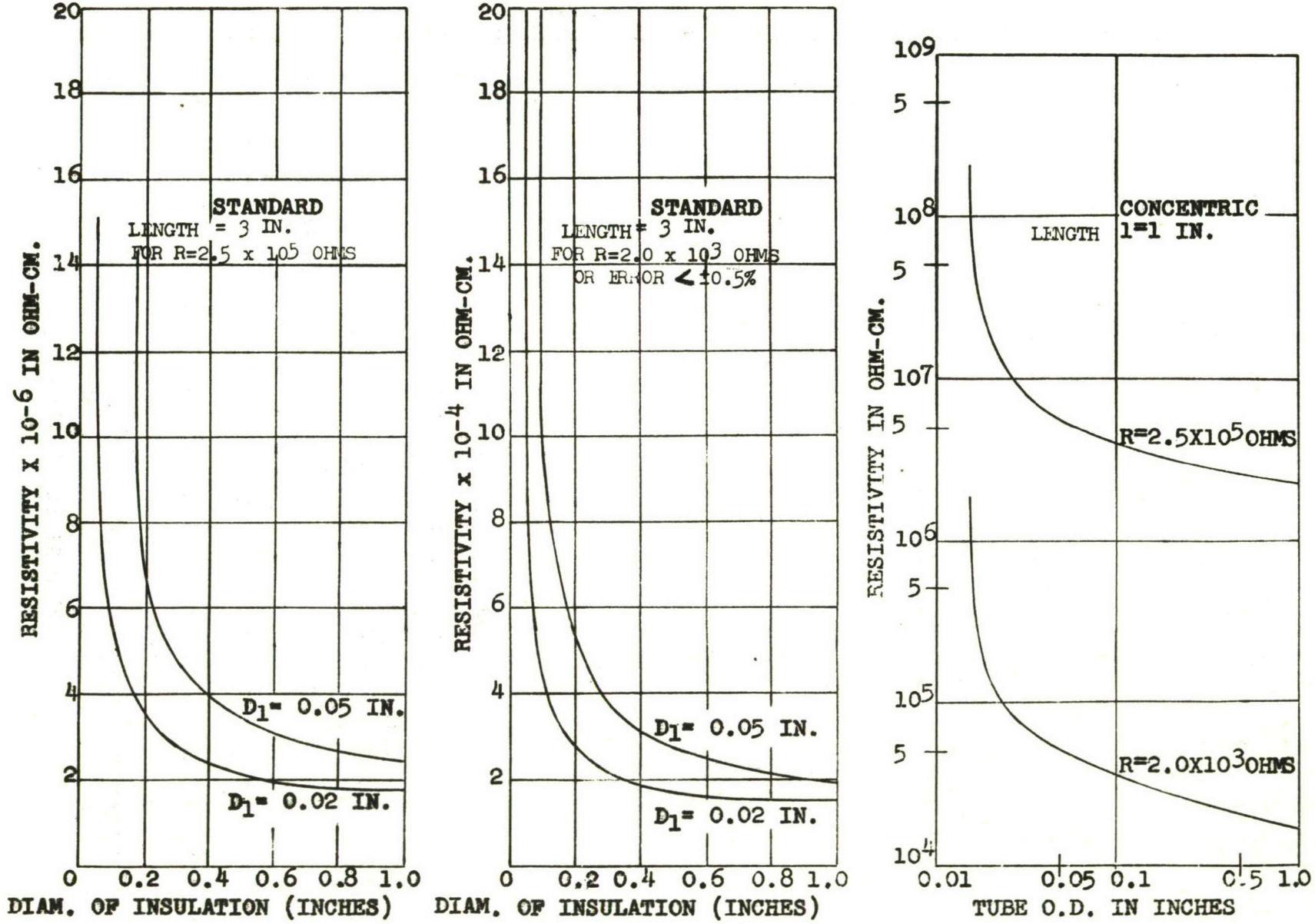
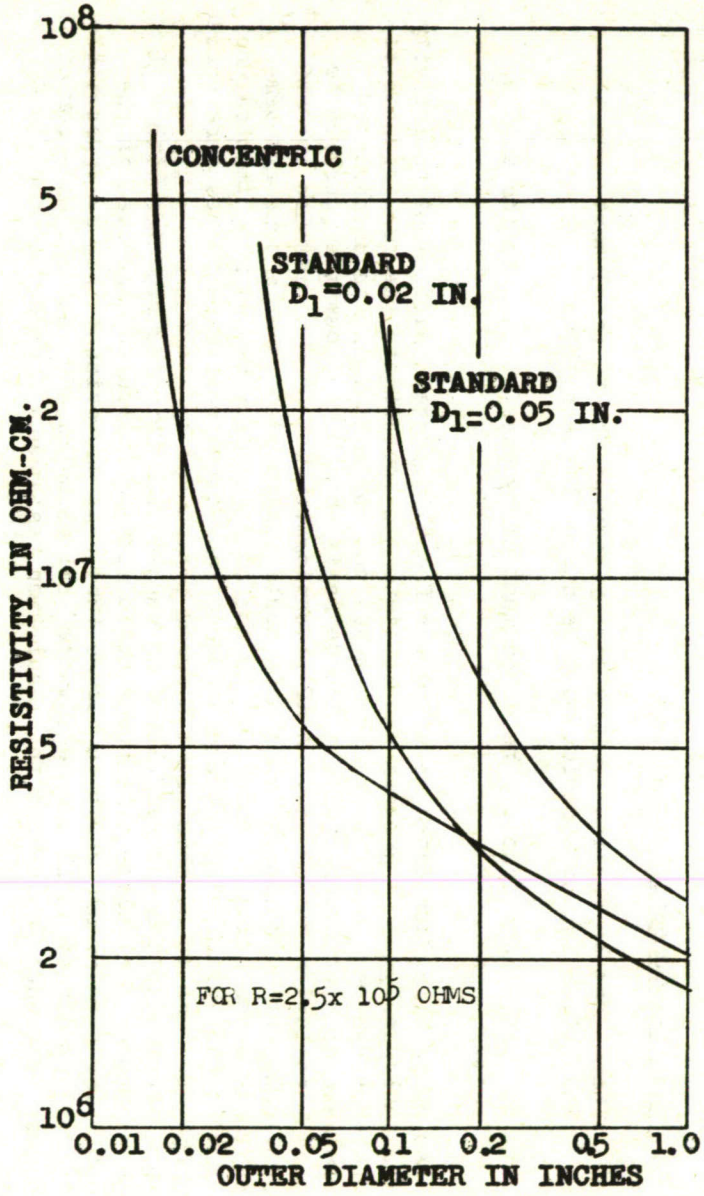


FIGURE 24. RESISTIVITY VERSUS DIMENSIONS AT VARIOUS THERMOELEMENT DIAMETERS



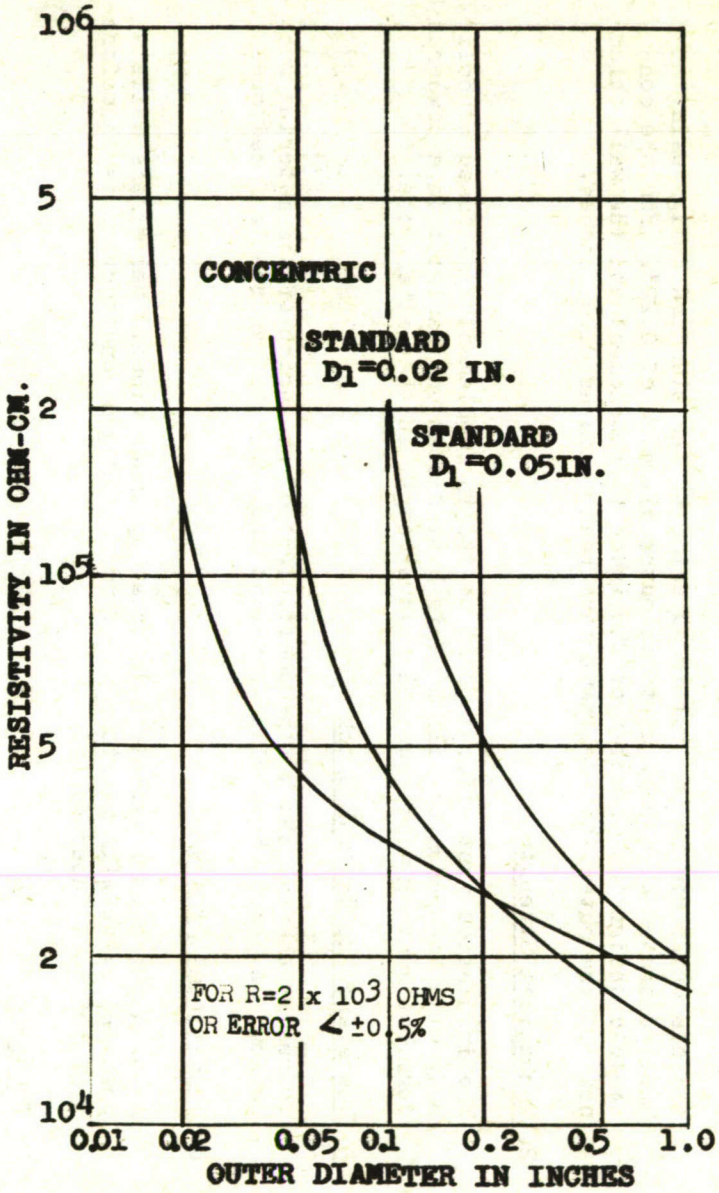


FIGURE 25. RESISTIVITY VERSUS OUTER INSULATION DIAMETER FOR VARIOUS SYSTEMS

ticable outer dimension, but is superior to the standard design using 0.02" diameter wire only up to an outer diameter of 0.22". For the concentric design the diameter of the inner thermoelement and the wall thickness of the outer thermoelement have been taken as 0.005 inches.

2. Mechanical Strength

The insulation must offer support to the thermoelements. A fused or solid body with low porosity will do this better than an insulator in a powdered form but swaging will increase this strength in the latter case.

3. Resistance to Thermal Shock

To resist thermal shock, the coefficient of expansion of the material must be low. A porous body will withstand the shock better than a fused one.

4. Vibrational Stress

A solid refractory will tend to break up under vibrational stress while a powdered oxide will maintain its form. A swaged construction is therefore superior to a fused ceramic.

5. Expansion

For the concentric design thermocouple, it is important that the coefficient of expansion of the thermoelements be close to that the insulation or one will pull away from the other at high temperatures. This is of less importance in the standard design thermocouple.

6. Chemical Compatibility

There must be chemical compatibility between the thermoelements and the insulation and no abrasion must be caused between them.

7. Finally, the refractory selected must allow ease of fabrication at low cost.

As no readily fabricated material was found to possess sufficient resistivity in the early analysis, a program was initiated to investigate the requirements of an operable system. A balanced circuit was set up, containing an uninsulated chromel-alumel thermocouple with a decade resistance box across the junction to simulate insulation resistance. A K2 potentiometer was used to measure the emf output. The hot junction of the thermocouple was maintained at a constant temperature in a controlled furnace, while the cold junction was at room temperature. The output for infinite resistance was recorded, then resistance values were varied from 250,000 ohms to 20 ohms and the error introduced by leakage through the insulation was calculated in each case. This was repeated with a 38 ohm resistance to simulate a temperature-indicating instrument included in the cicuit. The results are shown in Figure (26). It was evident that no appreciable error was introduced until the resistance fell below 10,000 ohms and an error of ±0.5% was introduced only when the insulation resistance dropped to about 1000 ohms.

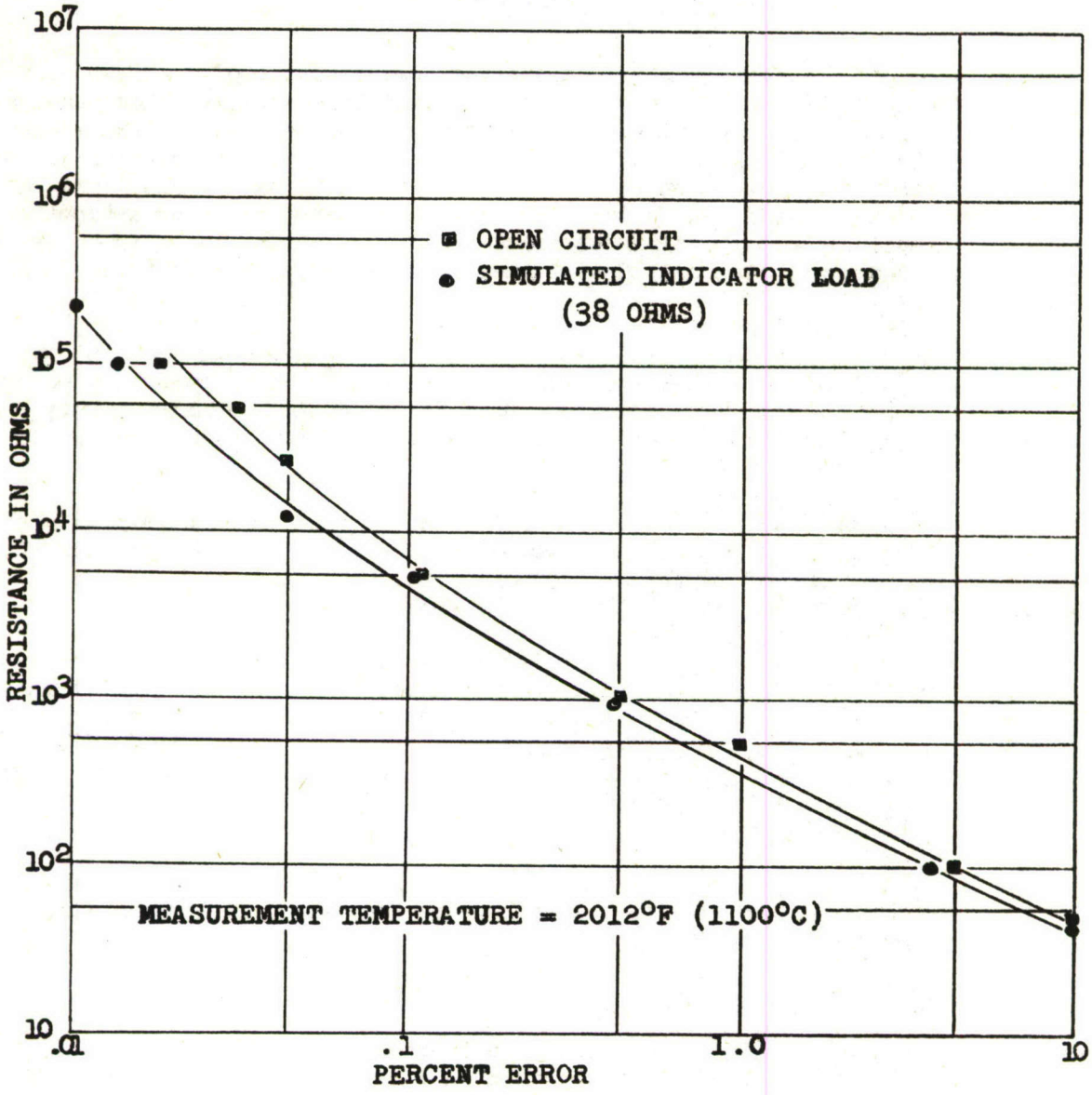


FIGURE 26. ERROR IN THERMOCOUPLE OUTPUT AS MEASURED BY SIMULATED RESISTANCE DECREASE

Testing of Refractories

Tests were made at West Lynn to compare the resistivities of a number of available refractories. Samples were made up in stainless steel sheaths; some containing parallel and some concentric thermoelements. In each case, a short sample was suspended by its leads beside a chromel-alumel thermocouple in a furnace. A previous furnace survey had shown that the area surrounding the sample would be at constant temperature. This temperature was read on a thermocouple potentiometer and the resistance between the thermoelements and later between the thermoelements and sheath was measured. The relation between resistance and temperature was plotted in each case.

Samples of magnesium oxide and alumina, both in a swaged construction, were tested in the standard parallel-wire form. The magnesium oxide, being hygroscopic, had to be thoroughly dried out before testing. Hylumina, a fused high purity alumina, and MgO combined with glass and with boron nitride were also tested in this form.

Periclase, single crystal magnesium oxide, was crushed under high-purity conditions and its resistivity compared with that of powdered MgO. Both were tested in swaged concentric constructions of approximately the same dimensions. Alumina was also tested as a concentric sample but of much smaller dimensions.

Results of these tests are shown in Figures 27 and 28. Resistivity decreases rapidly, but not uniformly, with rise in temperature. For most samples tested, the rate of decrease in resistivity lessens at higher temperatures. Of all refractories tested, alumina has the highest resistivity over the range considered. Although powdered periclase has a higher resistivity than magnesium oxide at temperatures below 850°C, it decreases rapidly in value at higher temperatures.

Refractories

The general comments on the oxides which were considered for use as insulation can be summarized as follows:

Magnesium Oxide

Powdered magnesium oxide is popular as a thermocouple insulator. It has a melting point of 5072°F (2800°C), can be used in a reducing atmosphere up to temperatures of 3092°F (1700°C) and, in an oxidizing atmosphere, up to 4352°F (2400°C). It is stable in contact with carbon up to 3272°F (1800°C).

The values reported for its electrical resistivity vary considerably. The highest value reported is 2.5×10^7 ohm - cm at 1832°F (1000°C) for fused MgO, while West Lynn tests of a swaged sample give a value of 4.2×10^5 ohm - cm at this temperature. Other data is shown in Figure 29.

The mechanical strength and thermal shock resistance properties of MgO are sufficient, though not as good as those of alumina. Also, MgO is hygroscopic, and this decreases its resistivity and increases fuel absorption. However, it is easy to fabricate and the present swaging method used by the General Electric Company compacts the oxide and thus decreases porosity, fuel absorption, increases electrical resistivity and mechanical strength.

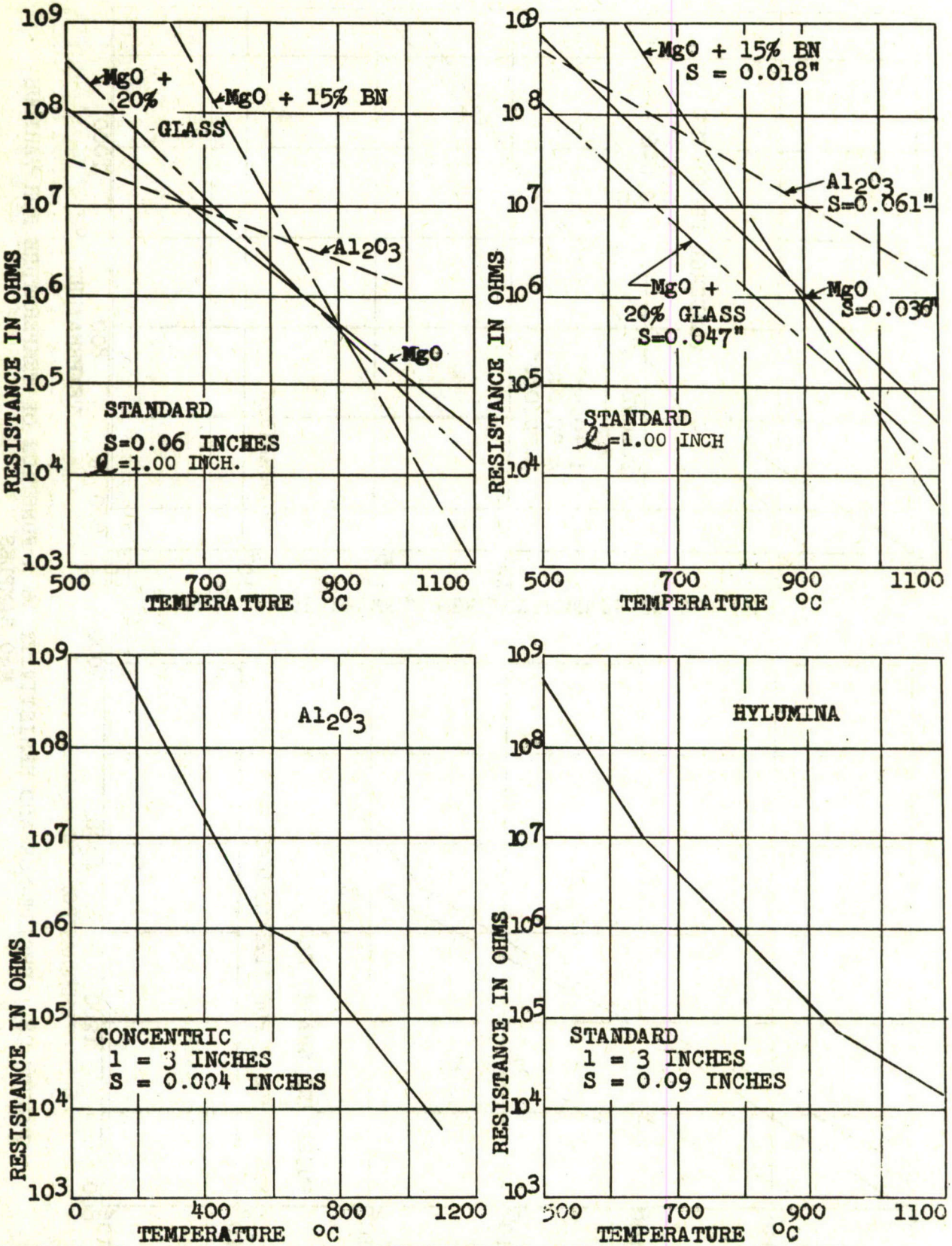
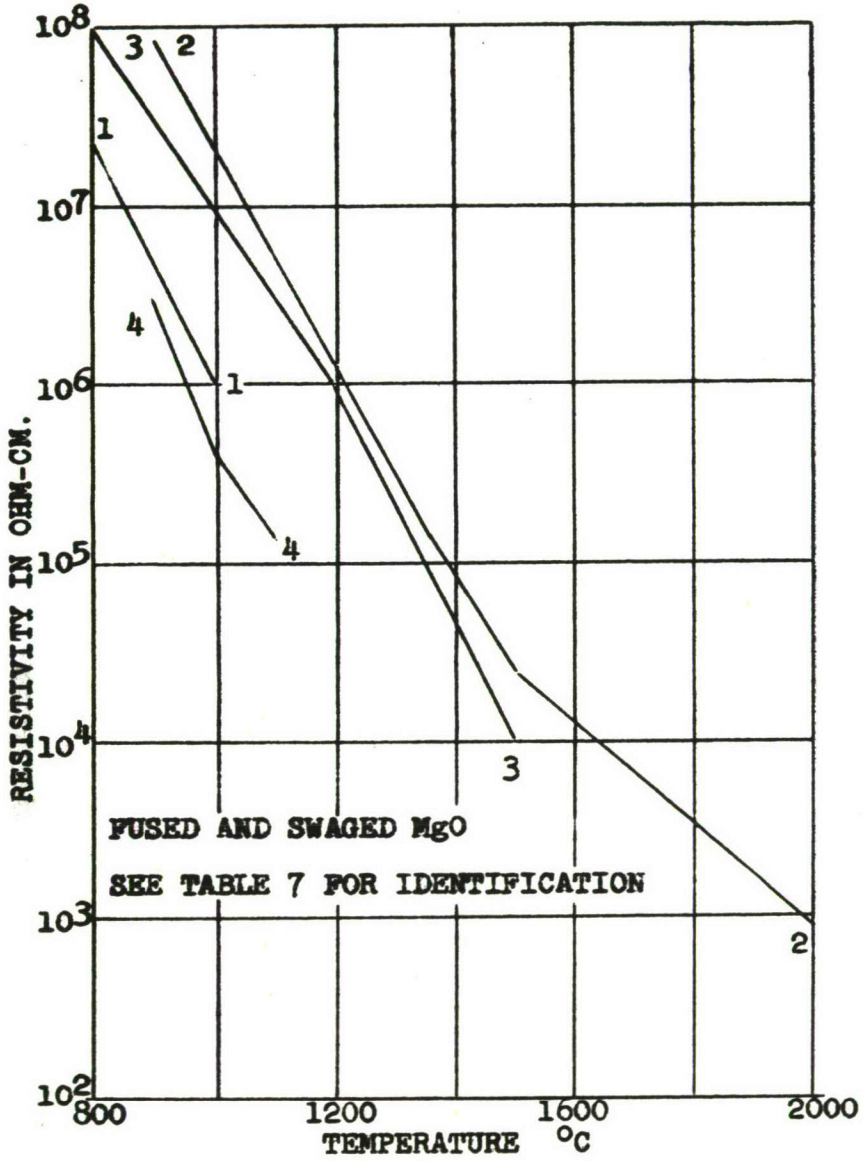


FIGURE 27. RESISTANCE AS A FUNCTION OF TEMPERATURE FOR VARIOUS MATERIALS



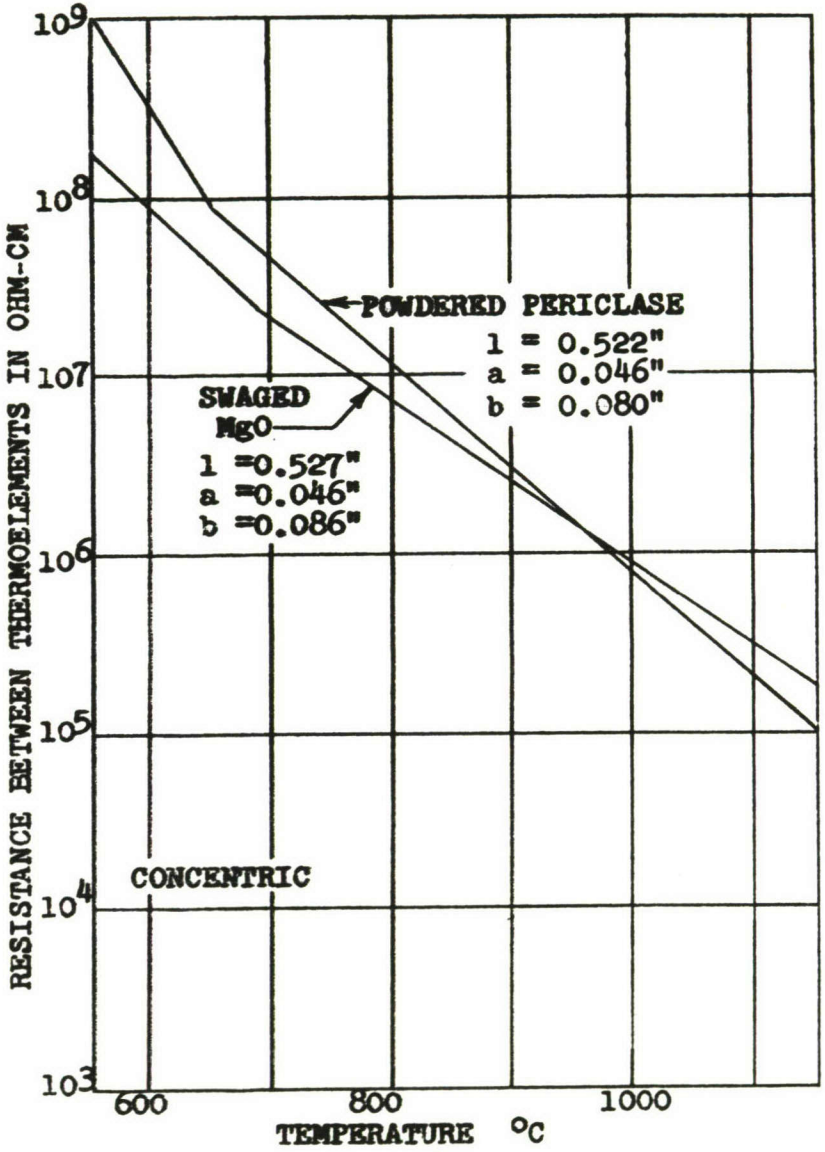


FIGURE 28. RESISTANCE AND RESISTIVITY AS A FUNCTION OF TEMPERATURE FOR VARIOUS MgO SAMPLES

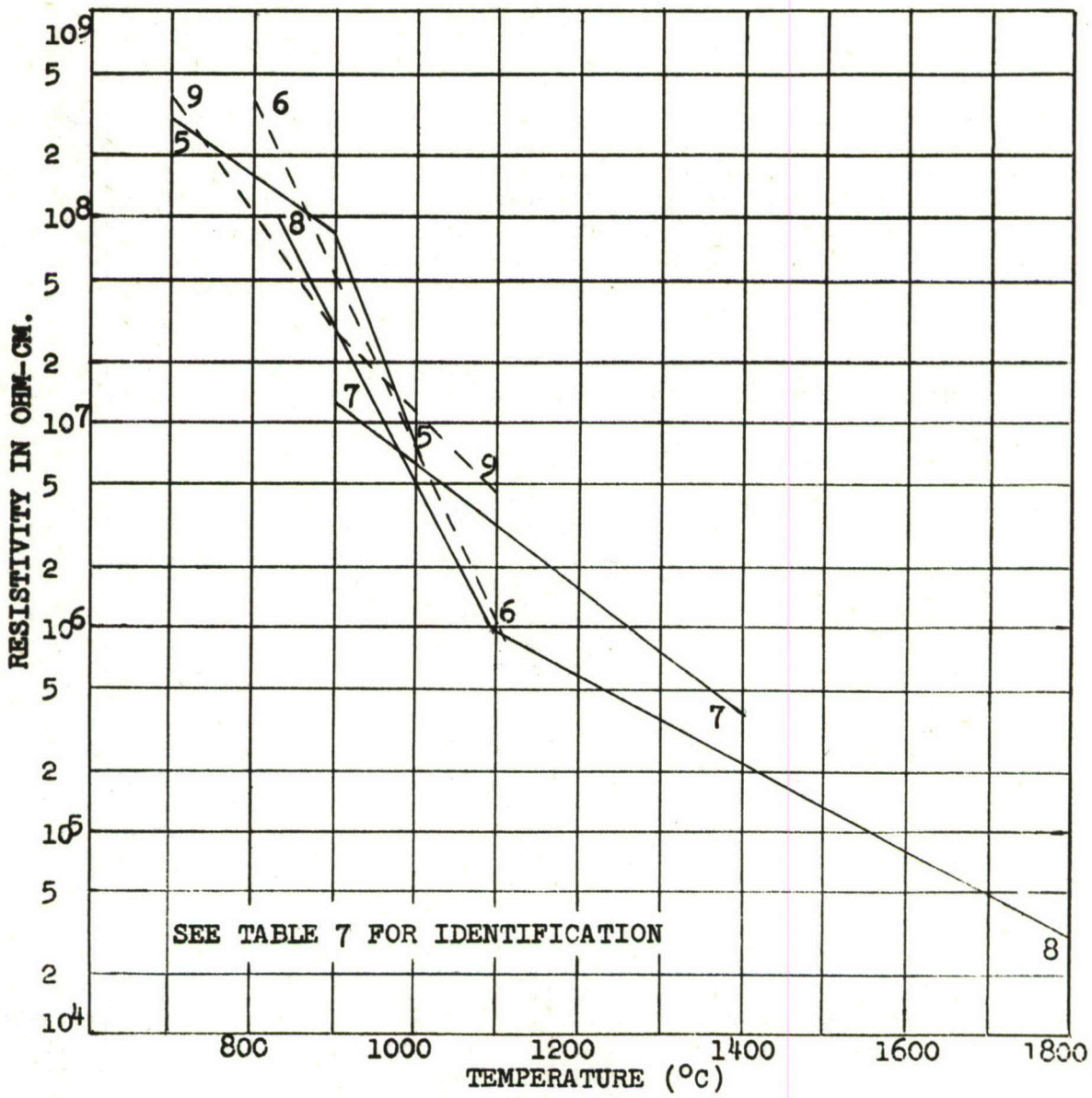


FIGURE 29. RESISTIVITY VERSUS TEMPERATURE FOR ALUMINUM OXIDE

Magnesium oxide has been combined with both glass and boron nitride to test the effect of these addatives on the resistivity. The results for MgO + glass were comparable with those of MgO alone but when boron nitride was combined with MgO the resistivity dropped more rapidly with increased temperature.

Periclase

Magnesium oxide appears in nature as the mineral periclase. It is formed by driving carbon dioxide from magnesite at temperatures between 752 and 1652°F (400° and 900°C). Its reported electrical resistivity, in its natural crystalline state is 1.79×10^7 ohm-cm at 2012°F (1100°C) and 2.50×10^6 ohm-cm at 2552°F (1400°C). This is higher than any other known refractory (Figure 22). However, in this crystalline form, periclase is very difficult and expensive to fabricate and entails the use of ultrasonic drilling. Although its mechanical strength is good, it is unlikely that it would survive a vibration test in this form.

Periclase was crushed to powder form and tested in a swaged construction but the results indicate that this destroys the high resistivity properties.

Aluminum Oxide (Alumina)

Aluminum oxide has a higher electrical resistivity than magnesium oxide, but once again, reported values vary with degree of purity and the form in which the alumina was tested. The swaged sample tested at West Lynn showed a resistivity of 1.12×10^7 ohm-cm at 1832°F (1000°C), and 4.19×10^6 ohm-cm at 2012°F (1100°C). A reported alumina, sintered at 3272°F (1800°C), although indicating a lower resistivity value at 1832°F (1000°C, decreases in value less rapidly with increasing temperature than the West Lynn sample and still has a resistivity of 4×10^5 ohm-cm at 2552°F (1400°C).

Alumina has a melting point of 3969°F (2015°C) and is stable in reducing or oxidizing atmospheres up to 3542°F (1950°C). It is one of the strongest refractories mechanically, certainly superior to magnesium oxide in this respect and in thermal shock resistance. It is more stable with most metals than MgO but less stable when in contact with carbon at high temperatures. Water absorption by alumina is negligible and fabrication should present no difficulties.

Beryllium Oxide (Beryllia)

This refractory has an electrical resistivity of 8×10^7 ohm-cm at 1832°F (1000°C) and 2.5×10^5 ohm-cm at 2552°F (1400°C). This is considerably higher than both MgO and alumina at these temperatures, but as beryllium oxide it is highly toxic and is dangerous to work with unless special precautions are taken. This increases difficulty and expense of fabrication.

The melting point of beryllia is 4622°F (2550°C), and it is chemically inert at high temperatures. It has a high resistance to reduction and is thermally very stable. At high temperatures, it has great mechanical strength though it is weak at low temperatures. Beryllia is volatilized by water vapor at temperatures above 3000°F (1650°C). A refractory grade (99.5% pure) is available commercially.

Conclusions

It was determined that thermoelements of small diameter would require insulation of a lower resistivity for any given probe size than would thicker wires. The smallest diameter feasible for the standard design with parallel thermoelement was 0.02". At outer diameters greater than 0.22" the standard design was more efficient than the concentric whose tube O.D. was this size. Sheath material would add to the size in both cases, but more so in the case of the concentric as further insulation would be required between it and the tube. It was determined, that a parallel wire thermocouple of maximum feasible outer diameter, containing thermoelements of minimum feasible diameter would best meet specifications. A minimum feasible length should also be maintained.

For a probe of this design, aluminum oxide was selected as the most suitable type of insulation. It has the highest resistivity after periclase and boron nitride, which are not recommended for reasons already stated. Alumina also has suitable physical and chemical properties over the range of temperature required.

Section V - Sheath Material

The sheath material dictated that an analysis similar to that in the general introduction be made. This assumed that the sheath material would be subjected to peak temperatures. The recommendation of a noble metal sheath material seemed impractical so that a detailed analysis of the problem was needed.

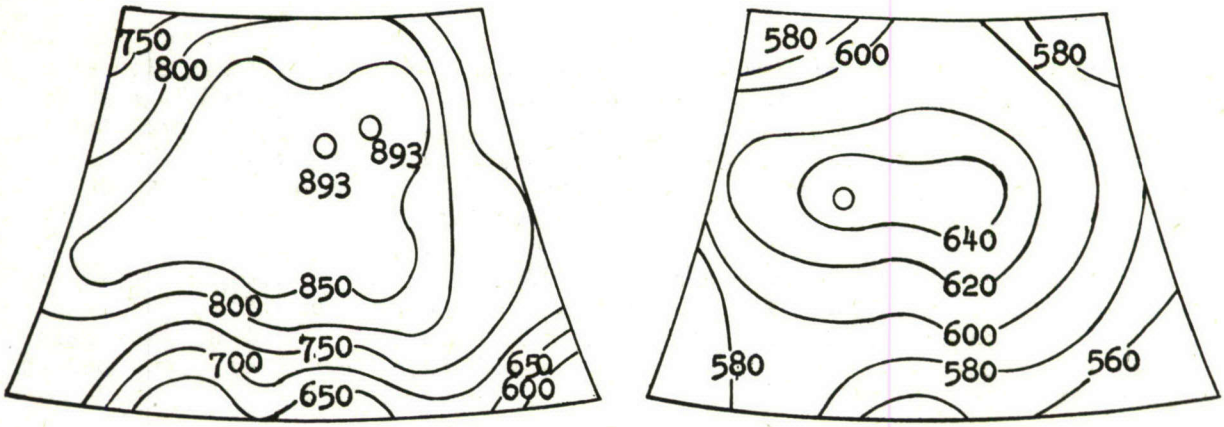
The specifications applicable to the sheath material were as follows:

1. Steady state range = 0 to 2300°F
2. Maximum transient range = up to 2500°F
3. Gas flow rate - The thermocouple system shall be capable of measuring the temperature of gases whose velocities vary from 0 to Mach. 0.8.
4. The system shall not require special cooling provisions.
5. Prospective materials shall be studied in view of structural strength at high temperatures and their adaptability to the various thermocouple fabrication processes that may be employed.
6. The various materials studied shall be described and notations included regarding their applicability to the problem.
7. In studying and determining the final assembly and composition of the thermocouple, prime consideration shall be given to the probability of mechanical failure within the limits of engine operation and prevalent temperatures. The development can not be considered successful unless the thermocouple is designed to be extremely reliable when used for measuring turbine inlet temperatures.

An analysis of the pre-turbine application and more specifically the definition of the environment of a probe was undertaken. It was reasonable to assume that at the operational temperatures, gradients of 200 to 400°F (93 to 204°C) existed in a combustion chamber. It was also known that a clear definition of the temperature and velocity gradients at any time was impossible because of their dependence on flow conditions from the compressor. Pulsation, surging or shock from the compressor delivery radically altered the conditions at any time.

In an effort to define the existing conditions, Figure 30 shows a temperature and velocity contour at a segmental entry to a turbine under specific conditions (83). From this figure, it was determined that a thermocouple tip in a pre-turbine application may see temperatures of the order 1800 to 2300°F (982 to 1260°C), however, the sheath material would possibly be subjected to a maximum of 1600 to 2100°F (879 to 1149°C) at its very end. The rest of the sheath material would be subjected to temperatures which depend on the inside temperature contour and the ambient temperature outside the combustion chamber. Under these conditions, a base-metal which was operational to a maximum temperature of 1149°C (2100°F) was needed.

When considering any high temperature application, the oxidation characteristics of a material were first considered, and its mechanical properties second. Consideration of mechanical properties as a prerequisite was useless if the material deteriorated through oxidation.



TEMPERATURE °C VELOCITY FT./SEC.

FIGURE 30. TEMPERATURE AND VELOCITY CONTOUR AT THE SEGMENTAL ENTRY TO A TURBINE

PERCENTAGE OF ORIGINAL SAMPLE THICKNESS REMAINING** AT TEMPERATURE

ALLOY	1800°F	1900°F	2000°F	2100°F	2200°F	2400°F
WROUGHT Ni. BASE						
INCONEL	90	92	95	65	67	70
INCONEL W	-	-	95	87	92	92
INCONEL X	80	85	90	85	82	82
INCONEL 700	-	85	85	50	15	COMP.OX.
INCONEL 702	-	-	97	92	85	90
HASTELLOY B	97	87	65	60	55	-
HASTELLOY R	-	-	70	35	-	-
HASTELLOY X	100	97	95	92	90	-
M-252	95	97	97	98	92	-
WROUGHT Iron BASE						
A-286	-	97	80	65	-	-
N-155	-	97	90	COMP.OX.		
310 SS	-	90	80	70	50	50
321 SS	95	82	40	COMP.OX.		
INCOLOY T	-	100	82	87	55	-
WROUGHT Co. BASE						
L-605	-	97	96	95	COMP.OX.	
t-1570	87	87	87	70	-	-
V-36	87	77	70	COMP.OX.		
S-816	97	87	77	COMP.OX.		
CAST COBALT BASE						
HE-1049	100	100	100	COMP.OX.		
X-40	95	92	92	47	-	-

TABLE 8. OXIDATION RESISTANCE OF IRON, NICKEL AND COBALT BASE ALLOYS*
*100 HOURS IN SLOW MOVING AIR **ORIGINAL SAMPLE THICKNESS-0.020"

During this phase of the development, attention was given to three classes of materials, iron, nickel, and cobalt base alloys. Table 8 was prepared to show the comparative oxidation resistance of these three classes of materials. From this table considering the maximum indicated table temperature of 1316°C, four wrought nickel base alloys appear to be the best, these are Inconel W. Inconel 702, Inconel X, and Inconel in the order of their desirability.

For consideration of the intergranular oxidation, Table 9 was prepared for those materials shown in Table 8. Considering only those materials exhibiting superior oxidation characteristics, intergranular oxidation reduced the materials recommended for consideration to Inconel or Inconel 702, and of these two, Inconel 702 is the least oxidizable.

When it was assumed that the maximum temperature the sheath tip was at 1149°C (2100°F) because of combustion chamber temperature gradients, from Table 8 in the order of their oxidation characteristics, the possible choices were M-252, L-605, Inconel 702, Hastelloy X, Inconel W, Incoloy T, Inconel X, J 1570, 310SS, A-286, Inconel, and Hastelloy B. Reconsidering the possibility of intergranular attack and assuming that no attack was desired for reliability, this list of materials reduced to Inconel 702, Hastelloy X, and Inconel. The first choice would again be Inconel 702, however, the other two materials were considered for further application to the problem.

A variety of mechanical properties were possible with the latter three alloys whose compositions are:

Alloy	C	Ni	Cr	No	Co	Mu	Si	Ti	Al	W	Fe
Inconel 702	.02	79.7	15.8			.11	.09	.45	3.73		.04
Inconel	.05	77.5	14.5								6.50
Hastelloy X	.10	Bal.	21.88	9.03	1.01	.50	.48			.43	18.86

The alloy Inconel 702 is hardened by what is probably a nickel-aluminum-titanium compound precipitate. Inconel and Hastelloy X exhibit solution and work hardening. For high temperature service applications at 1800 - 2000°F, only solution hardening can be depended upon for strengthening due to stress-relieving, averaging, and re-solutioning effects making Inconel 702 peculiar in this case.

An analysis of the strength properties of these alloys was then considered The comparison of the load carrying capabilities, assuming the arbitrary maximum temperature limitation for each alloy based on an assumed stress of 10,000 psi for 10 hours were found to be as follows:

Alloy	Mechanism of Strengthening	Max.Service Temp °F 10,000psi, 10 hours
Inconel 702	Precipitation hardening	1650
Inconel	Solution and work hardening	1450
Hastelloy X	Solution and work hardening	1650

TABLE 9. INTERGRANULAR OXIDATION OF IRON, NICKEL, AND COBALT BASE ALLOYS

ALLOY	PERCENT OF ORIGINAL THICKNESS EXHIBITING INTERGRANULAR ATTACK 1800°F	1900°F	2000°F	2100°F	2200°F	2400°F
Wrought Nickel Base						
Inconel	0	0	0	0	0	0
Inconel W	-	-	-	40	30	40
Inconel X	10	25	35	40	30	40
Inconel 700	-	0	20	20	15	-
Inconel 702	-	-	0	0	0	0
Hastelloy B	0	5	15	23	30	-
Hastelloy R	-	-	0	0	-	-
Hastelloy X	0	0	0	0	0	-
M-252	15	43	95	100	-	-
Wrought Iron Base						
A-286	-	30	50	50	-	-
N-155	-	8	10	Comp. Ox.		
310SS	-	5	5	10	10	13
321SS	0	5	25	Comp. Ox.		
Incoloy T	-	35	32.5	40	40	-
Wrought Cobalt Base						
L-605	-	-	8	40	Comp. Ox.	
J-1570	28	28	28	30	-	-
V-36	0	0	0	Comp. Ox.		
S-816	0	0	0	Total Ox.		
Cast Cobalt Base						
HE-1049	15	23	30	Total Ox.		
X-40	10	10	10	30	-	-

The high oxidation resistance of these alloys permits their use at low stress levels (2000 - 3000 psi) up to 2000°F and in the case of Inconel 702, up to 2200°F. For very short periods of time, these temperatures can be raised an additional 200°F.

Having chosen the materials which were most probable for application to this development, confirmation testing was undertaken. Figures 31 and 32 illustrate the comparative surface effect of an oxidizing atmosphere on the three materials (77). Figure 33 illustrates a series of photomicrographs of Inconel 702, made at a higher operational temperature. These show that even at 2450°F (1343°C) serious intergranular attack does not occur until after approximately 96 hours. These tests served to confirm the prior deductions of good high temperature oxidation resistance.

The preceding analysis provided materials of relatively low strength at elevated temperatures. Attention was then turned to the possible factors which may allow these materials to be applicable in this development. One approach was to idealize a condition in order to obtain a relative magnitude of the actual strength requirements.

Assuming these ideal conditions, consideration was given to a flat surface in a gas stream. This would be the case of maximum requirements. Structure-borne excitation was not considered initially and the assumptions were:

1. Air was the force producing medium.
2. The probe had a flat front surface for purposes of estimating a maximum force.
3. Air impinges on the flat surface and none rebounds.
4. Velocity undergoes a constant deceleration.

Letting:

M = Mass of the air

ρ_a = Density of the Air

A = Incremental cross-section

X = Incremental length

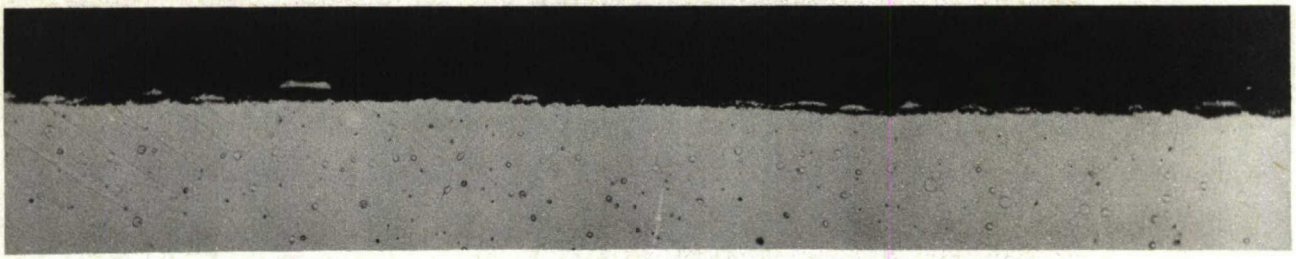
V = Velocity of the air

$\overline{V}$ = Average velocity of the air = $\frac{v_1 - v_o}{t_1 - t_o}$

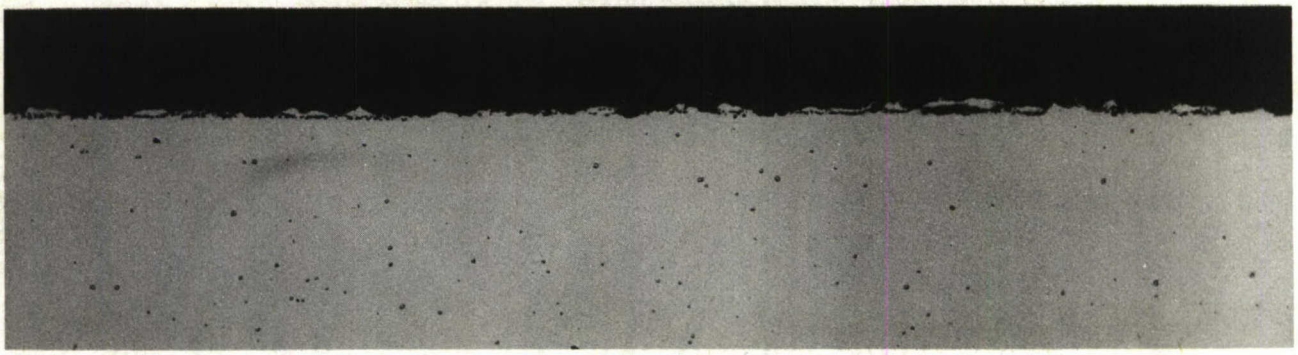
the usual analysis provides the force relation

$$F = A\overline{V} \triangle V$$

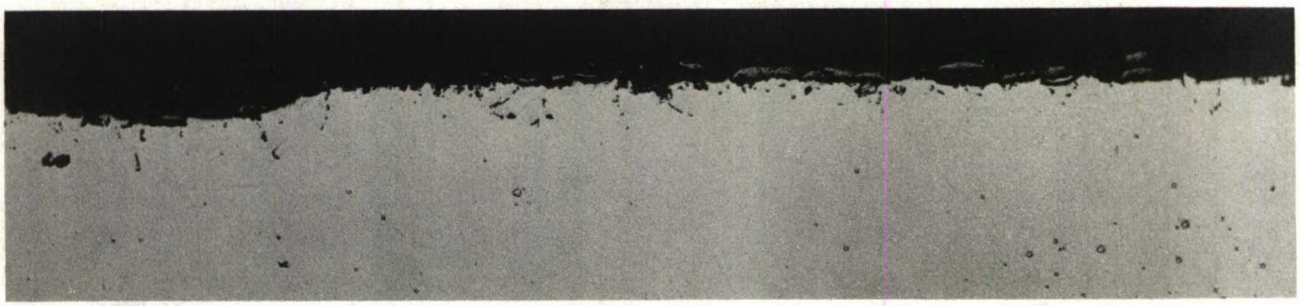
By substitution of the conditions specified by this contract, it was found that a force of 13 pounds would be distributed along a surface 3 inches x 1 inch.



INCONEL 702-2000°F - 100 HOUR EXPOSURE



INCONEL 702-2400°F - 100 HOUR EXPOSURE



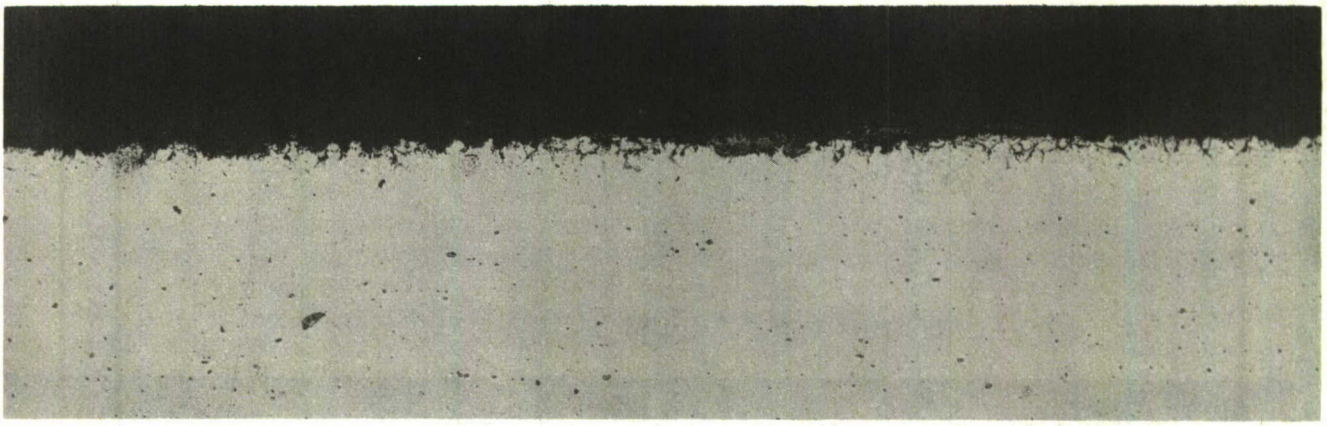
INCONEL - 2100°F - 100 HOUR EXPOSURE



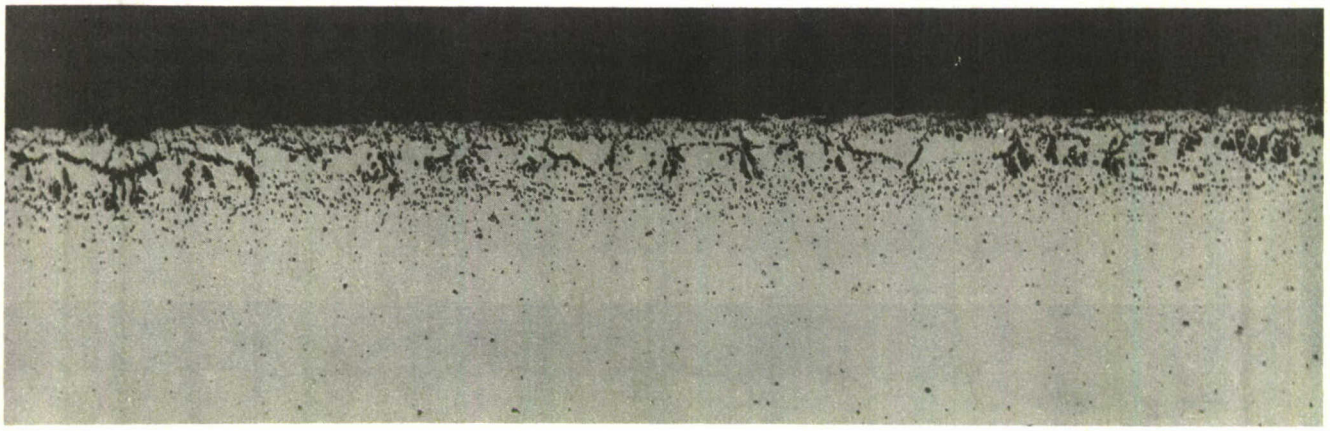
INCONEL - 2400°F - 100 HOUR EXPOSURE
Note that the Inconel Surface is roughened considerably

Mag. 100X

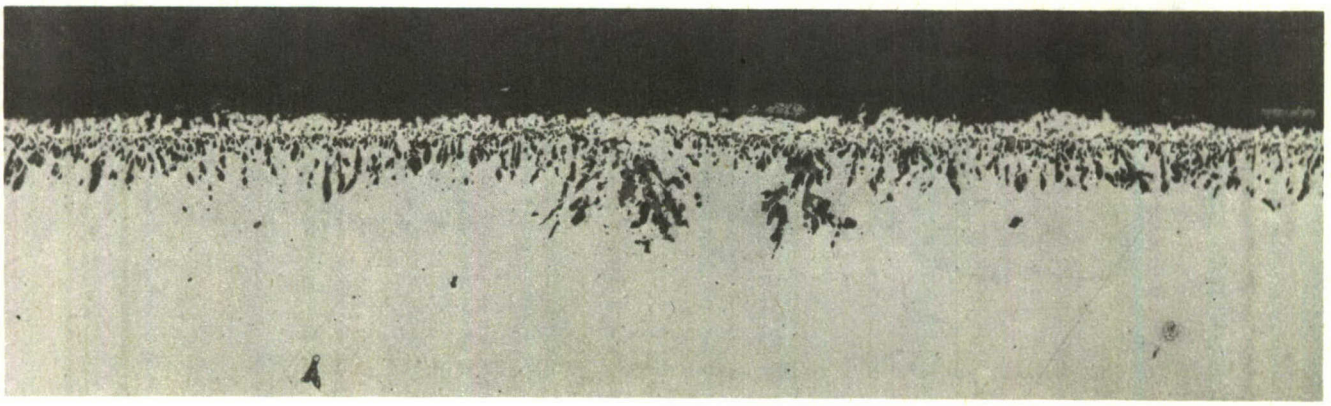
Figure 31 - Surface Oxidation of Inconel and Inconel 702



INCONEL X-1800°F - 100 HOUR EXPOSURE (Note Intergranular attack starts)



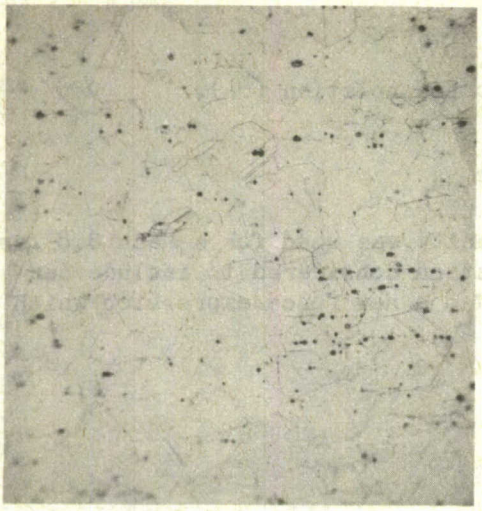
INCONEL X - 2100°F - 100 HOUR EXPOSURE



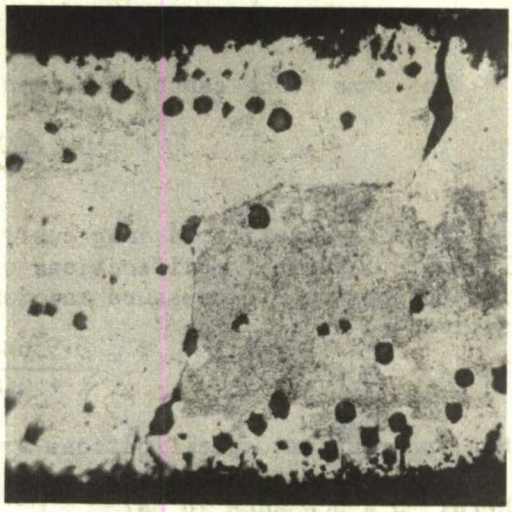
INCONEL X - 2400°F - 100 HOUR EXPOSURE

Mag. 100X
(Unetched)

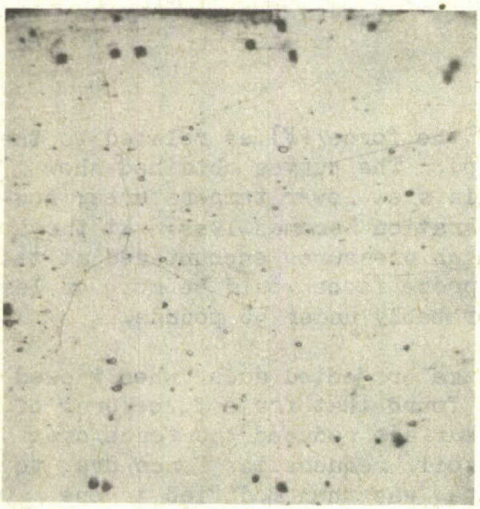
FIGURE 32 SURFACE OXIDATION OF INCONEL X



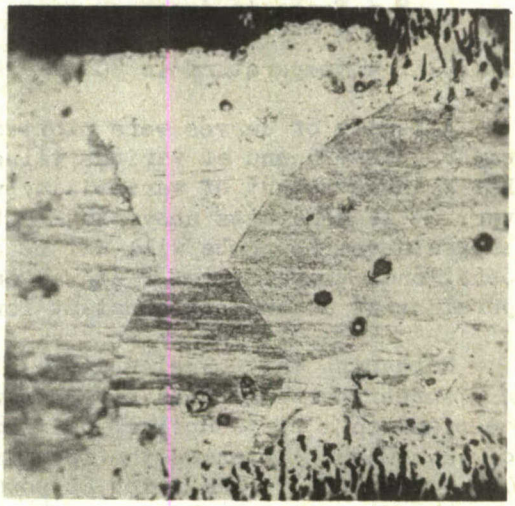
As Received



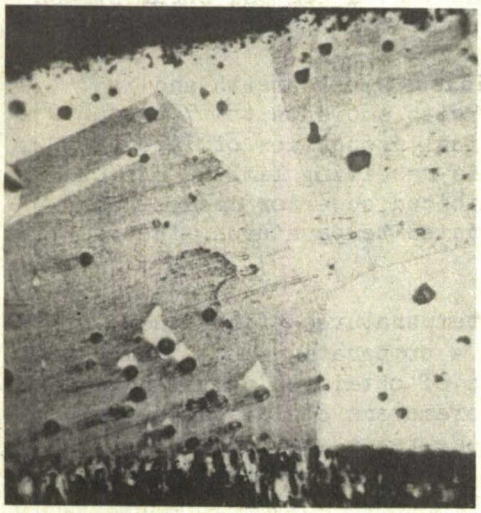
48 Hours



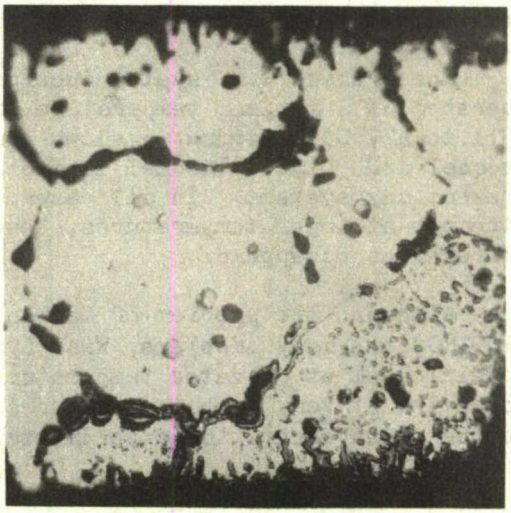
4 Hours



72 Hours



24 Hours



96 Hours

FIGURE 33 - INCONEL 702 PHOTOMICROGRAPHS
(Combustion Test @ 2450 $\pm 25^{\circ}F$)

The same force can be obtained by using a reported relation (84).

$$F = \frac{C_D \rho_a V^2}{2}$$

In this relation, a drag coefficient, C_D, of unity was used for a Mach 0.8 gas flow rate. Further modifications of the first equation considered to include density changes due to pressure and temperature provided a new force expression which is given as -

$$F = \frac{3.95p \times 10^5}{1 + 0.00367T}$$

when the contract specifications are used.

where: p = pressure in psi

F = Force in dynes

T = temperature in °C

A family of curves were plotted (Figure 34) of the force (F) as related to the temperature (T) and at various values of pressure (p). The curves obtained show that a large amount of variability with pressure exists at lower temperatures; however, at temperatures above 1832°F (1000°C) the separation becomes less. At the low temperatures the probe will not be exposed to the high pressures encountered at the operational temperature. It was deduced that the probe force would be more or less operating at a somewhat constant force value most probably under 50 pounds.

Comparing the force on various shapes of the same projected area, when viewed on a screen perpendicular to the air stream, it was found that for a force/drag of one pound on a flat surface, pointing the upstream surface reduced the force/drag to 0.2 pounds. Altering the model shape to an air foil, reduces the force/drag to 0.02 pounds (85). The prior 50 pound probe force/drag was then modified to one pound by designing a probe of the shape of an air foil.

From the usual stress calculations, it was found that a 282 psi shear stress existed for a rod and 178 psi for the air-foil.

The present G.E. system incorporates a 321 stainless steel sheath and is operated at a maximum temperature of 1600°F (871°C) with ambients to 700 to 800°F (371 to 427°C). Figure 35 shows comparative mechanical properties of Inconel 702, Inconel and 321SS. Inconel is included because it is receiving limited use on present day systems. In all cases, Inconel 702 exhibited superior mechanical strength at lower temperatures, however, at the elevated temperatures, the relative differences disappear.

Although the problem of mechanical testing at temperatures higher than 2000°F (1093°C) has many problems, West Lynn did undertake a comparative short time axial loading test at elevated temperatures with the hopes of obtaining comparative information at very high temperatures. Since other parameters could also contribute to the measurement, the experimental validity of these tests was doubtful.

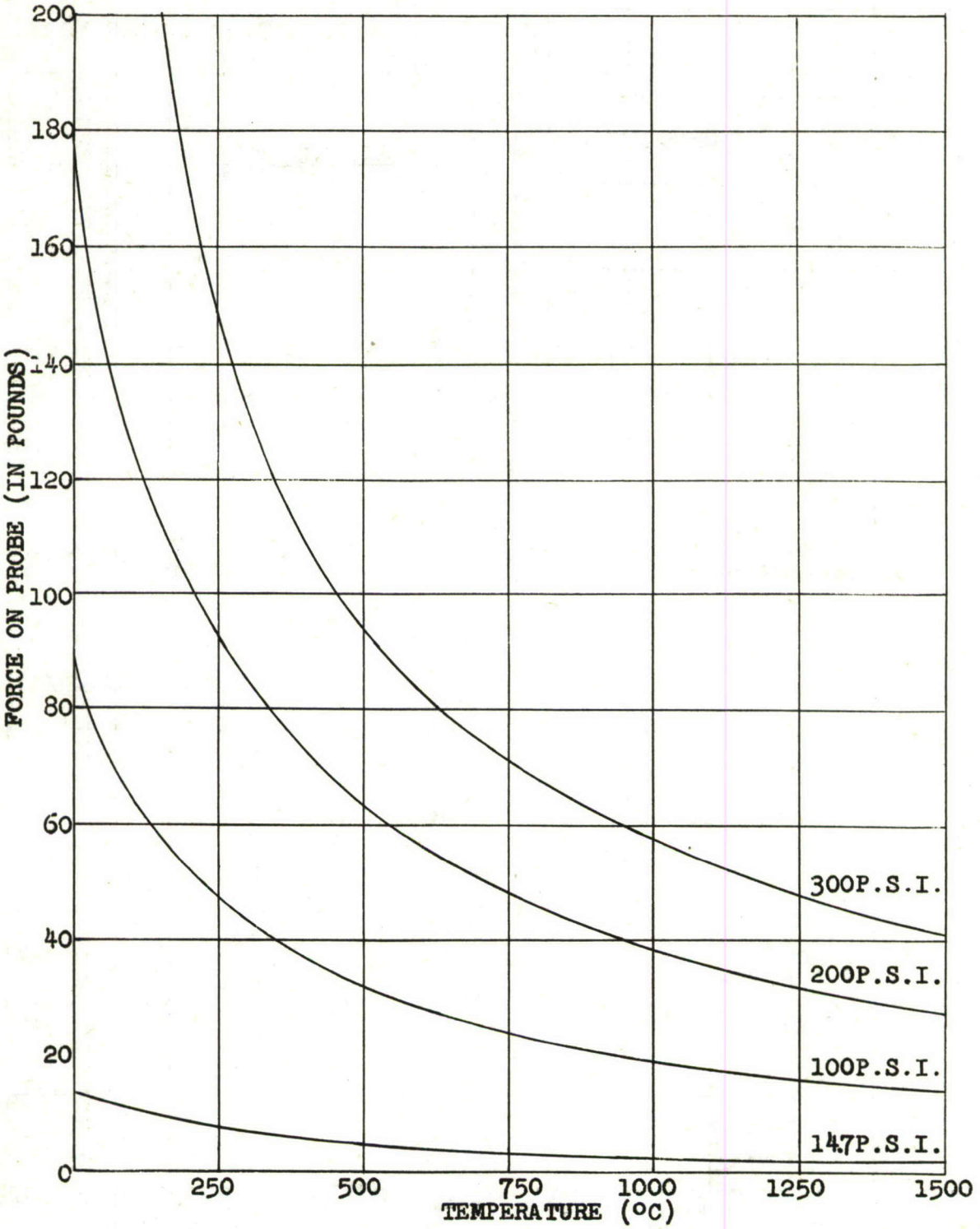


FIGURE 34. PROBE FORCE AS A FUNCTION OF TEMPERATURE AND PRESSURE

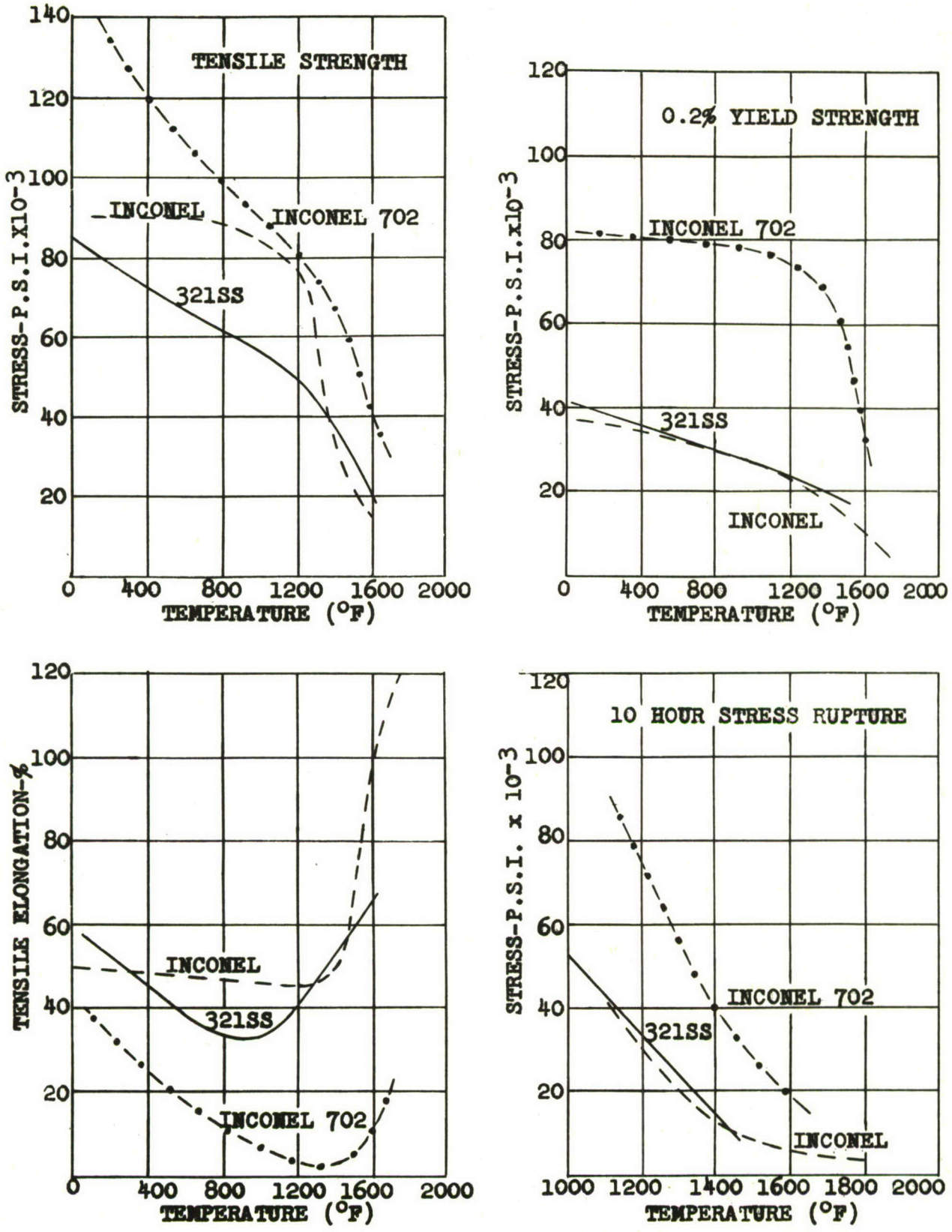


FIGURE 35. COMPARATIVE MECHANICAL PROPERTIES OF INCONEL, INCONEL 702 AND SS321

In figure 36 the arrangement of the test apparatus for the high temperature axial loading test is illustrated. Testing of the sample was started when the furnace attained a relatively stable predetermined value. The test provided the results of table 10. Although these data were extremely difficult to obtain and interpret, the indication in each case was that in the low stress regions, Inconel 702 is superior to the present design whether it is the basic sheath materials or in a composite prototype. In the extremely low stress regions, Inconel 702 appears to be better by one order of magnitude when compared to SS321.

The problem had been investigated and based on all the tests and discussion above. The most probably sheath material for recommendation was Inconel 702.

Cermets & Alloys

Figure 37 illustrates the results of two hours in combustion for some high temperature alloys and cermets discussed in the introduction of this section. The cermets were not completely oxidized so that an axial strength test was made and accounts for the breakage shown in the figures. It was found that this aggregates of metal and ceramic possess no measurable ductility. Further testing was then limited to more detailed confirmation studies and new materials which were supplied by various vendors familiar with the problem of this development.

Kennametal materials were obtained as shown in the as received condition in figure 38. These were combustion tested at 2450°F (1343°C) with the results shown in figure 39. Both cermets exhibited unstable dimensional characteristics and spalling of oxide coatings which were formed during combustion. Aside from the dimensional instability and spalling, these materials did not fracture during three thermal shock cycles. They did, however, exhibit cracking deep into the sample body at the third cycle which was considered a failure.

In figure 40, there are illustrated the results of additional tests of the Haynes Stellite Company LT-1 cermet (77% chromium and 23% aluminum oxide by weight). This material exhibited dimensional instability and mild creep characteristics early in the test cycle (after 25 hours 2450°F) (1343°C). It can also be observed in figure C that cracking of the body occurred. Sample B survived three thermal shock cycles after 75 hours of combustion while sample C fractured after four cycles and 125 hours of combustion.

Several new materials were provided as experimental samples by the Haynes Stellite Company. One of these was a cermet designated LT-1B (60% chromium, 20% molybdenum and 20% aluminum oxide). This material exhibited characteristics similar to those discussed above, however, it only survived two thermal shock cycles with the results shown in figure 41. Another material provided by the Haynes Stellite Co. was designated at LT-2 (60% tungsten, 25% chromium and 15% aluminum oxide). This cermet exhibited destructive oxidation characteristics as shown in figure 42.

It was concluded from these tests that the most probable cermet studied was LT-1, however, all of those tested exhibited dimensional instability and their use in this development was not recommended.

Another probable solution in order to attain a reliable high temperature sheath material was through coating. An attempt was made to the deter intergranular corrosion of Inconel 702 to extend its life beyond 96 hours at the elevated temperatures.

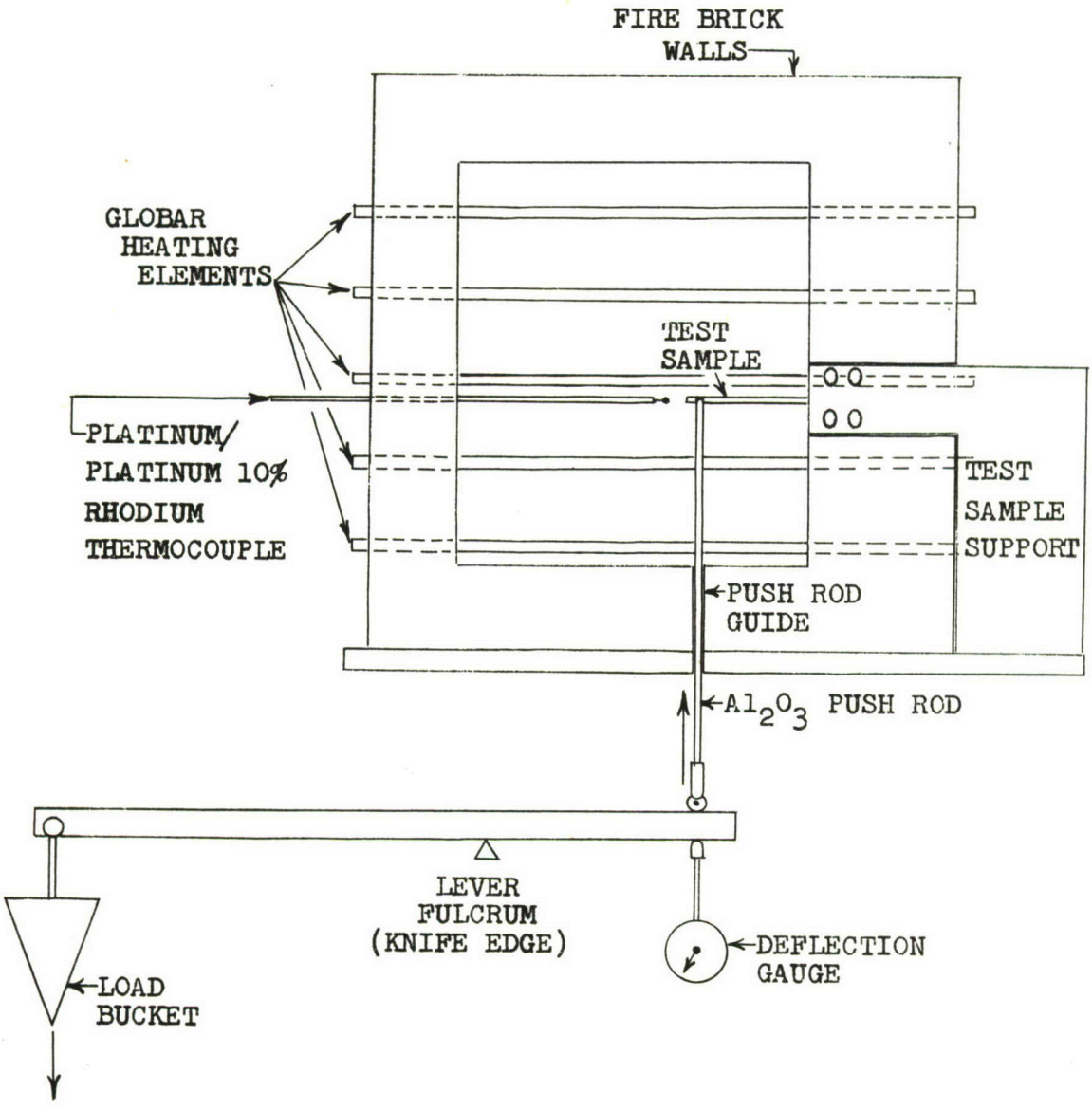
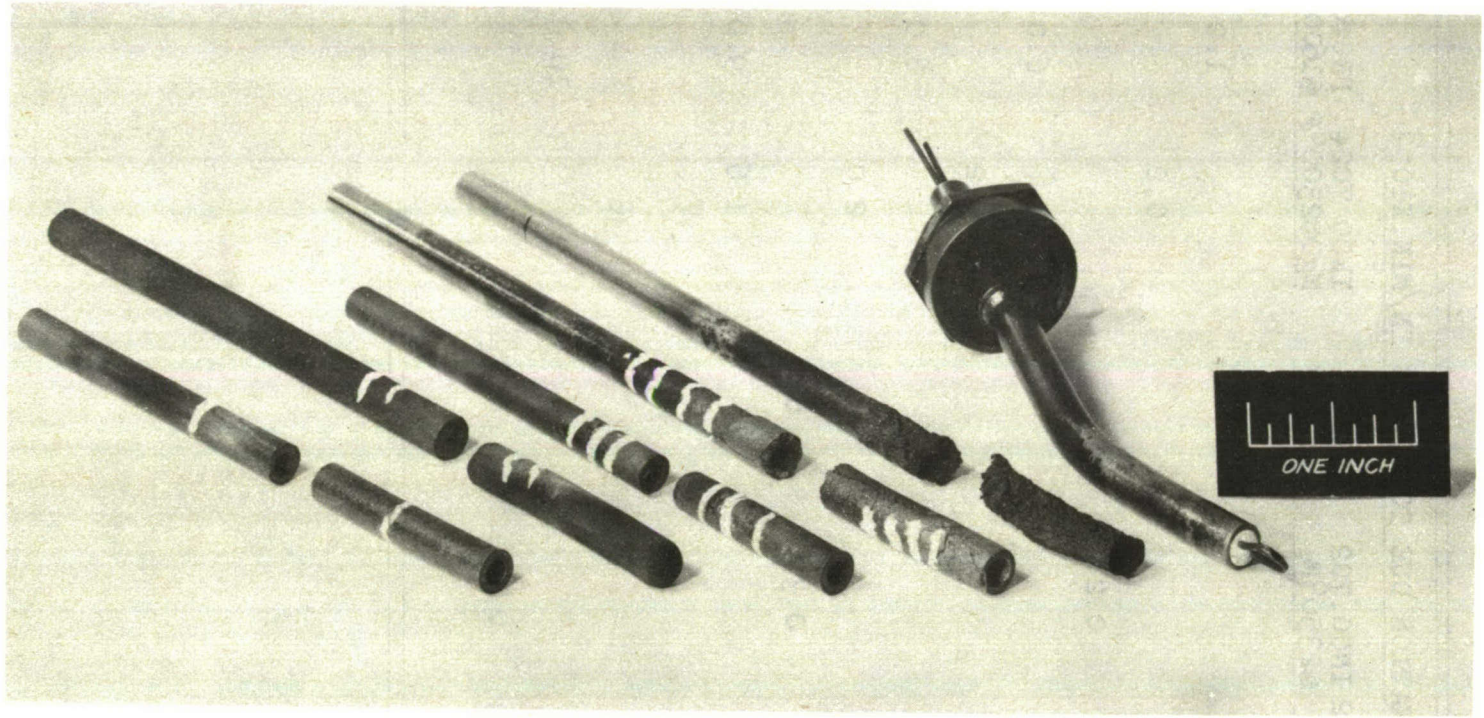


FIGURE 36. HIGH TEMPERATURE AXIAL LOAD TEST

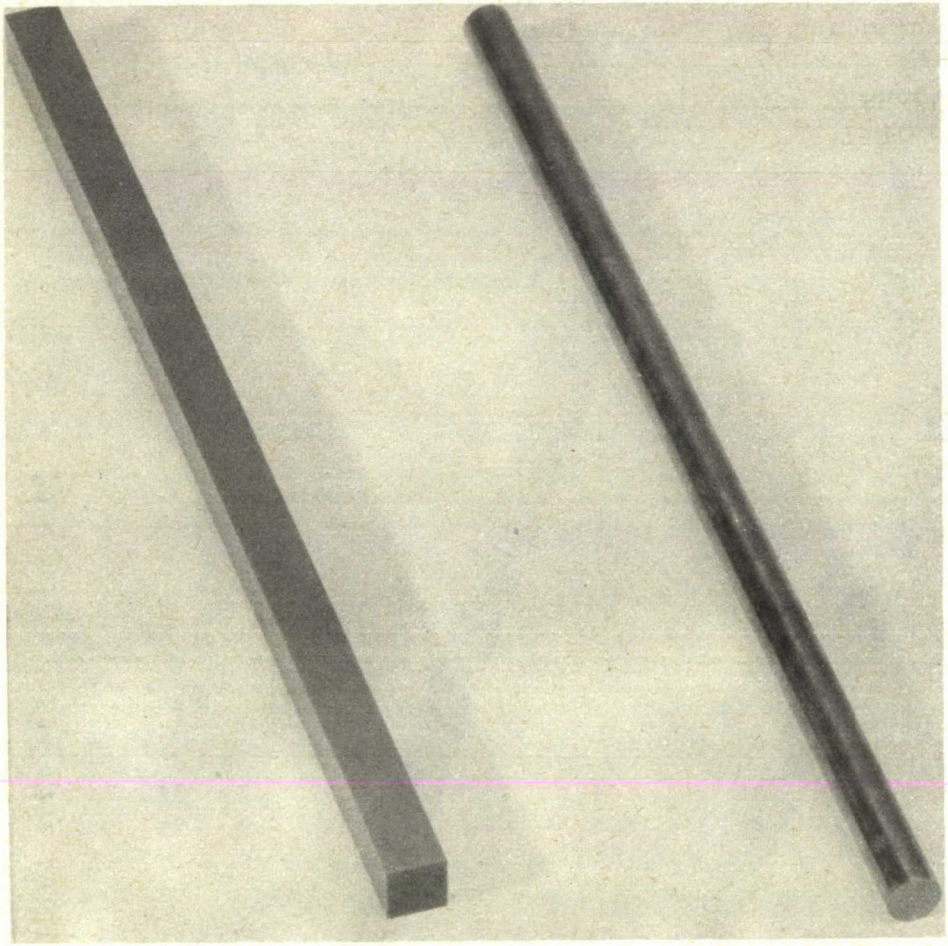
TABLE 10. COMPARATIVE RESULTS AS CALCULATED FROM HIGH TEMPERATURE SHEATH MATERIAL TESTS

	SHORT TIME DEFORMATION DUE TO STRESS IN/MIN.X10^{-3}					
BENDING STRESS-PSI	INCONEL 702 @2300°F	INCO.702 @2350°F	SS321 @1600°F	INCO 702+ MgO@2300°F	PROTOTYPES @1600	PROTOTYPES @1800
1290					1.0	5.0
2070				0.2		
2230	0.2	0.2	2			
2580					6.0	9.0
3100				0.2		
3870					8.0	12.0
4140				2.0		
4460	1.0	0.3	6			
5160				1.6	9.0	16.0
5170						
6200				38		
6500					10.0	6.0
6700	1.0	0.7	6.4			



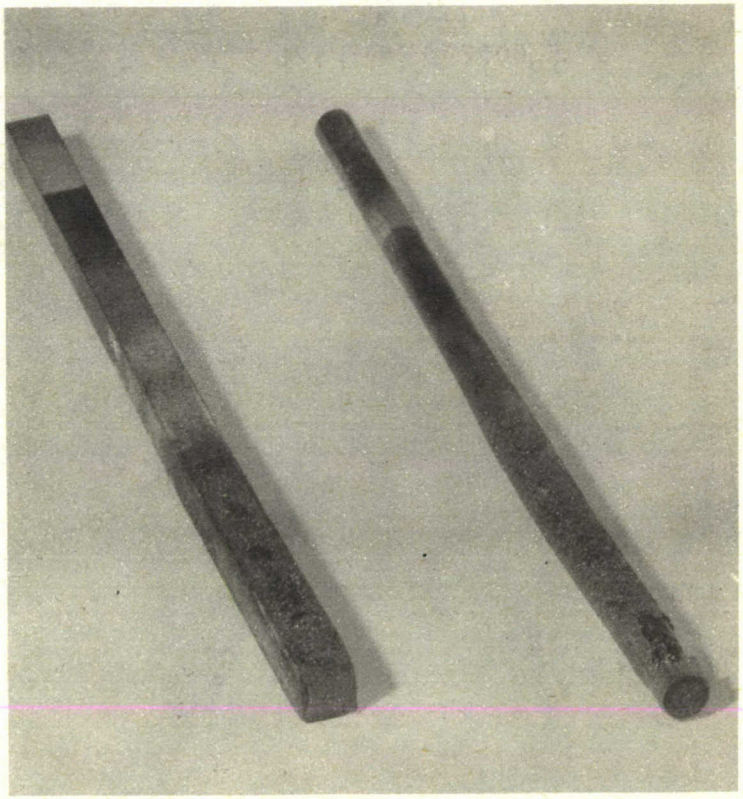
1. K-162B Cermet
2. LT-1 Cermet
3. K-151A Cermet
4. Hastalloy X
5. L-605
6. Prototype

FIGURE 37 - RESULTS OF COMBUSTION TESTING OF SHEATH MATERIALS AT 2400°F
(Prototype at 1600°F)



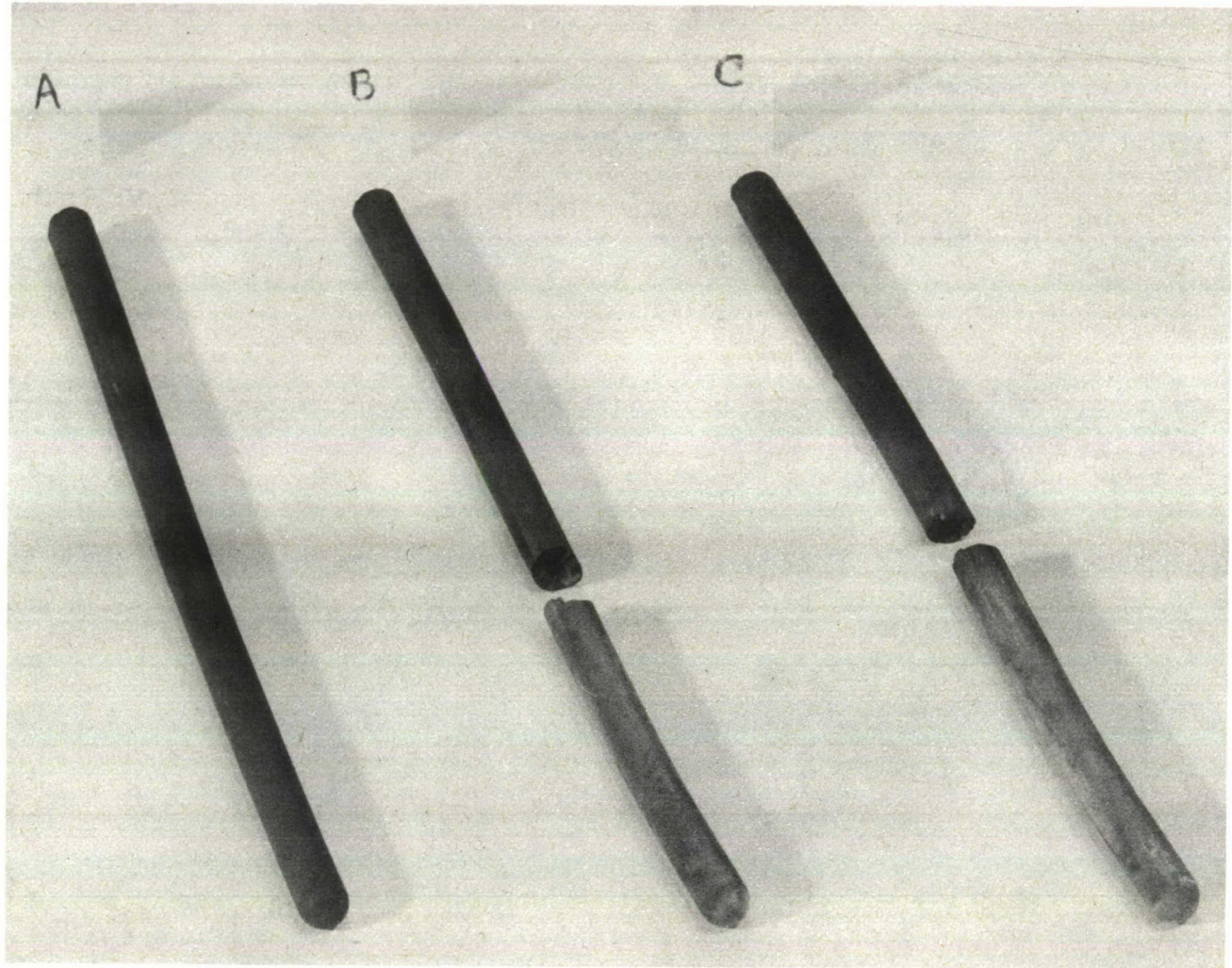
K-151-A K-162-B

Figure 38 - Kennametal Cermets as Received Condition



K-151-A K-162-B

Figure 39 - Kennametal Cermets After 25 Hrs. Test at 2450°F.



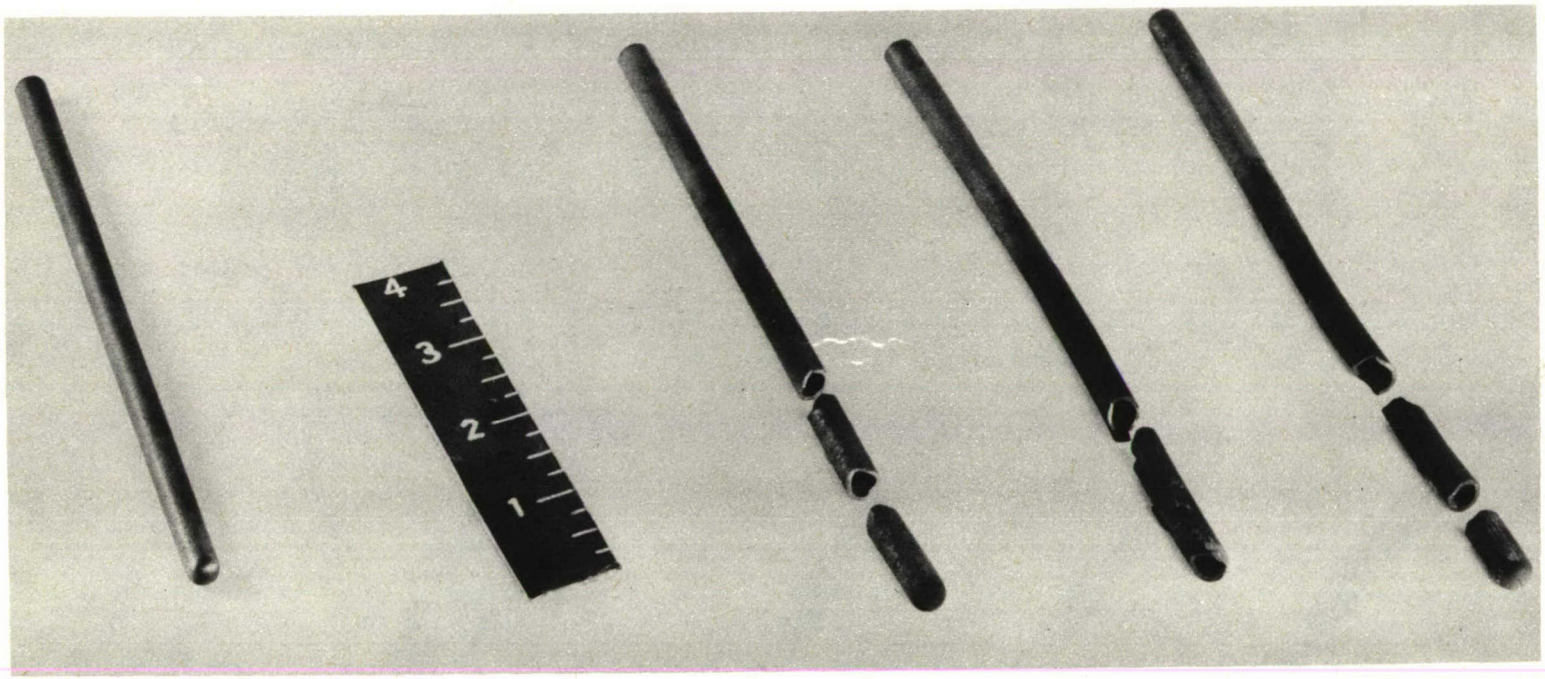
As Received

75 Hrs. @ 2400°F
3 Shock Cycles

125 Hrs. @ 2400°F
5 Shock Cycles

Composition: 77% Chromium, 23% Aluminum Oxide
(Shock Cycle was from the indicated temperature into room temperature water)

FIGURE 40 - HAYNES STELLITE LT-1 CERMET TEST RESULTS



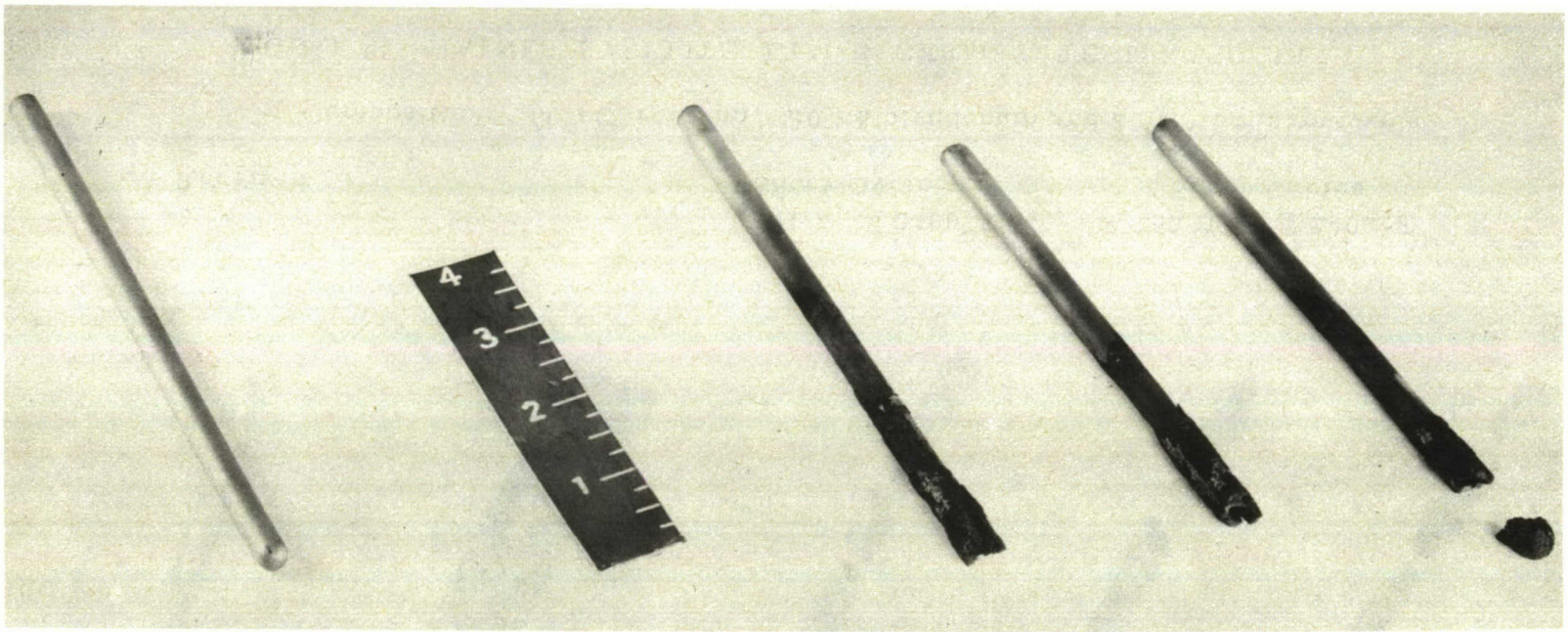
As Received

25 Hrs. @ 2400°F
1 Shock Cycle

50 Hrs. @ 2400°F
2 Shock Cycles

Composition: 60% Chromium, 20% Molybdenum and 20% Aluminum Oxide

FIGURE 41 - HAYNES STELLITE LT-1-B CERMET TEST RESULTS



As received

24 Hrs. @ 2400°F

Composition: 60% Tungsten, 25% Chromium, and 15% Aluminum Oxide

FIGURE 42 - HAYNES STELLITE LT-2 CERMETS TEST RESULTS

Figure 43 illustrates Inconel 702 coated with a dense alumina coating designated as LA-1 by the Linde Air Products Company who supplied the coated samples. Figure 44 illustrates the results of combustion testing these samples for 15 hours at 2400°F (1316°C).

As a result of these tests, the Linde Air Products Company furnished a new porous coating designated as LA-3. The results of testing these coatings are shown in figure 45. Sample B exhibited a small amount of spalling, however, these tests were much improved from those with the LA-1 coating. Figure 45 shows the complete failure of the LA-3 coating after three thermal shock cycles such as the cermets were subjected to earlier.

These tests confirm that when heating or cooling a metal protected with a ceramic coating, sharp temperature gradients exist across the low conductivity ceramic. This difference in temperature coupled with a difference in expansion coefficient results in very high stresses. The expanding metal stretches the coating until rupture occurs.

It was concluded that Inconel 702 appeared most favorable after an analysis of the sheath problem and tests which are discussed above. From the standpoint of reliability in a pre-turbine application, it was further concluded that as a result of the limited testing accomplished during this development, no tested cermet or coating showed sufficient success to warrant recommendation.

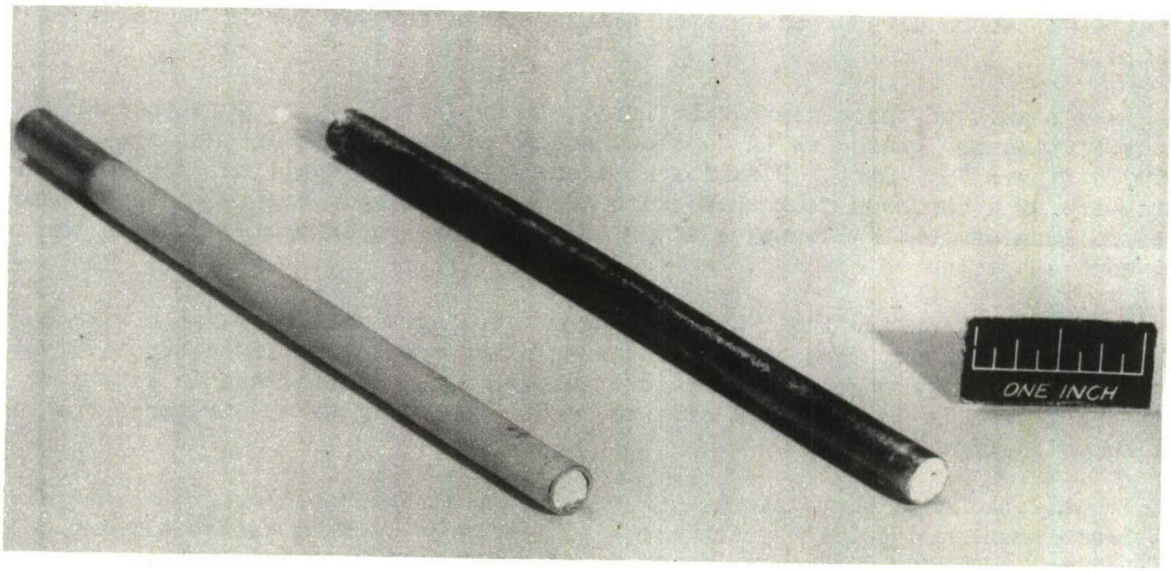


FIGURE 43 LA-1 COATED INCONEL 702 - AS RECEIVED CONDITION

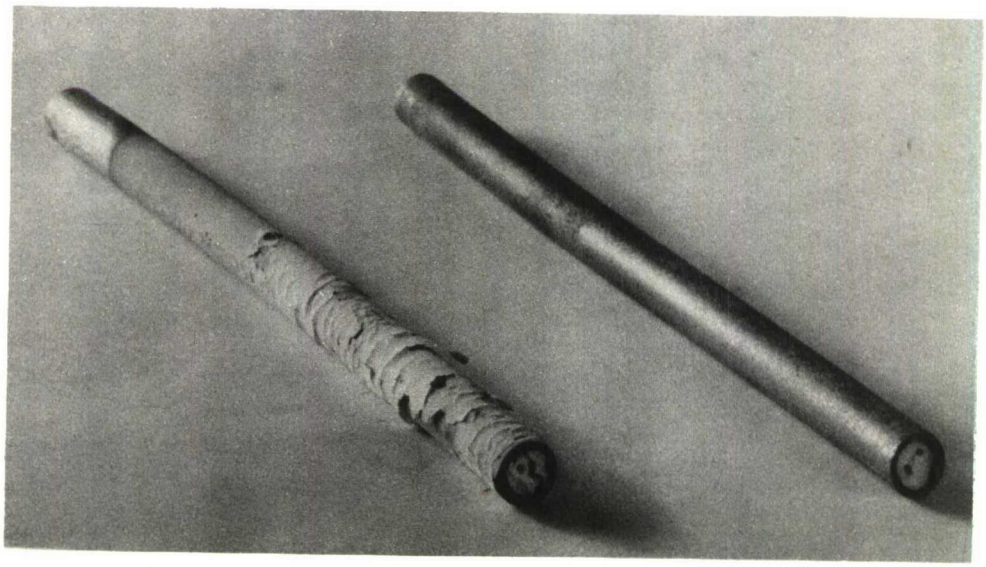


FIGURE 44 - LA-1 COATED INCONEL 702 - AFTER 25 HOURS @ 2400°F AND THERMAL SHOCK TO 68°F

Coating Supplied By: Linde Air Products Company

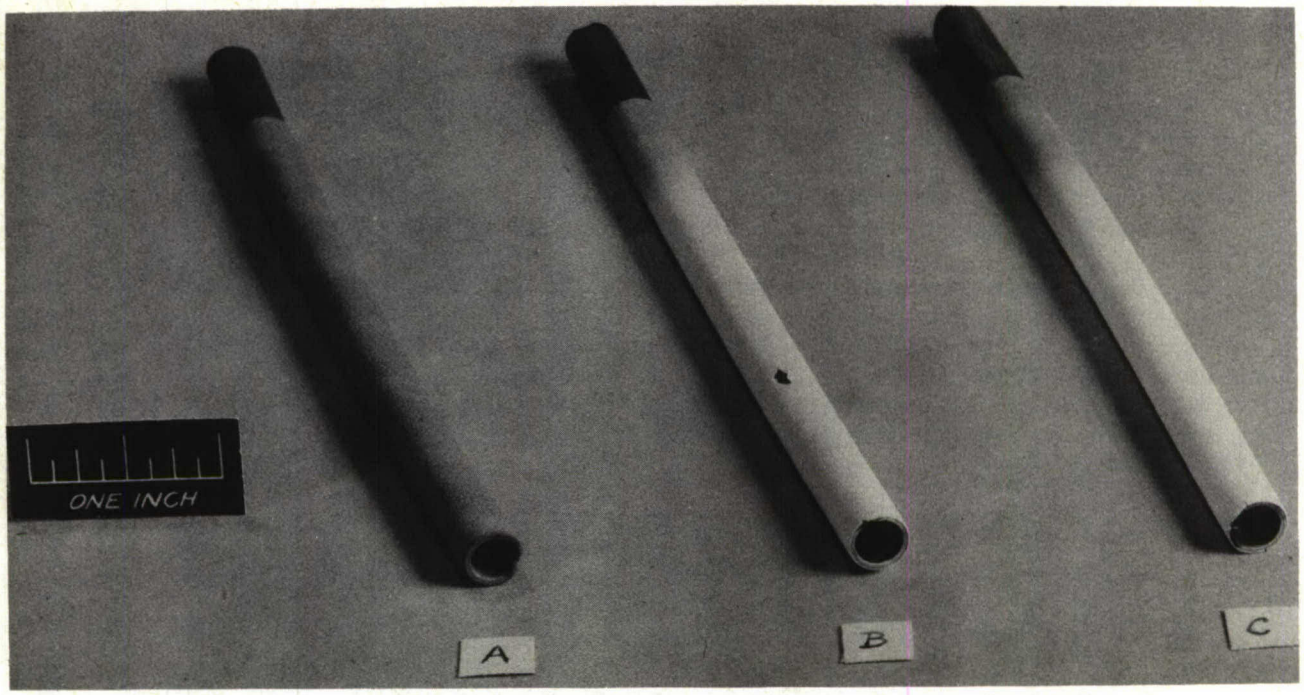


FIGURE 45 - LINDE AIR PRODUCTS LA-3 COATED INCONEL 702

A. As Received
B. Eight Hours Combustion @ 2300°F - One Thermal Shock to 68°F.
C. Sixteen Hours Combustion @ 2300°F - One Thermal Shock to 68°F.

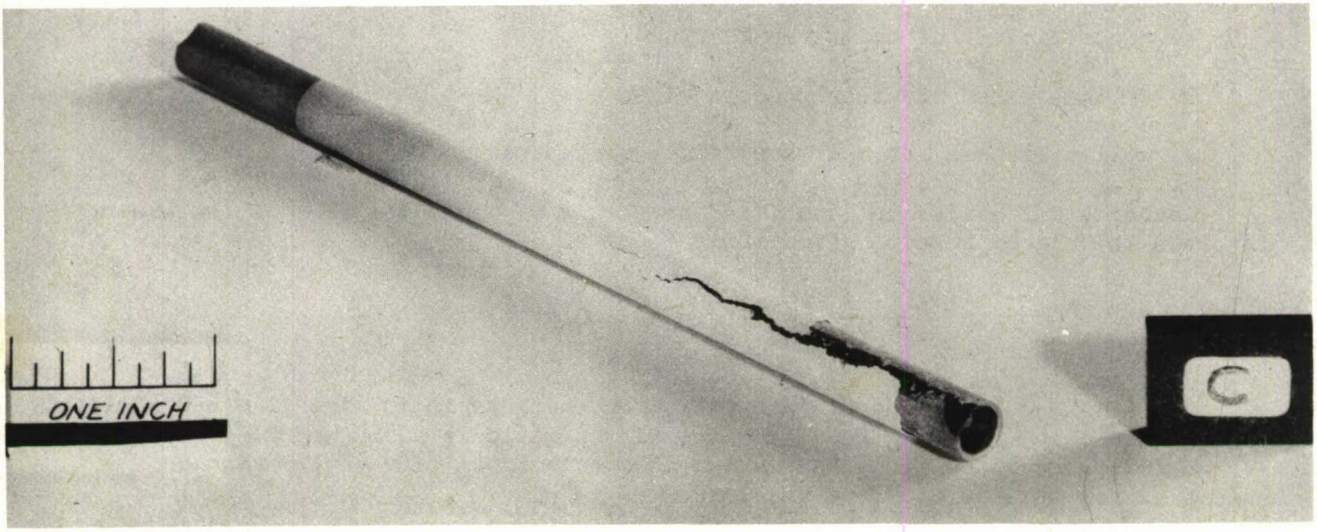


FIGURE 46 - LINDE AIR PRODUCTS LA-3 COATED INCONEL 702 (After Combustion Test at 2450°F and Three Thermal Shock Cycles to 68°F).

Section VI - System Design

This development contract considered two types of systems from the standpoint of design. These systems were:

a. One type of thermocouple with a maximum time response of 1.2 seconds at a maximum flow rate of six pounds per foot square per second.

b. One type of thermocouple with a recovery factor of not less than 0.98.

The characteristic time of a thermocouple is a transient behavior which is usually identified by the Greek letter, τ (tau). When considering only a condition of convective heat transfer to or from the couple, a heat balance can be written to obtain results similar to those of several investigators (5) (15) (16) (61) and (62).

$$(t_i - t) = (t_i - t_2)\left(1 - e^{-\tau/\beta}\right)$$

$$\beta = \frac{\rho D c}{4h}$$

where:

t_i = initial temperature as indicated before a temperature change occurs.

t = temperature indicated by a thermocouple at a time after the change occurs.

t_a = temperature of the air stream after a temperature change occurs.

c = specific heat of the thermocouple material.

ρ = density of the thermocouple material.

h = coefficient of heat transfer.

D = Diameter of the thermocouple wire.

τ = time elapsed after a temperature change occurs.

Characteristic time is identified as when $\tau = \beta$ and the ratio of temperature involved in this expression gives that

$$\frac{t_i - t}{t_i - t_2} = \left(1 - e^{-\tau/\beta}\right)$$

If $\tau = \beta$ the value of this ratio for characteristic time if 0.632 similarly if $\tau = 2\beta$, and $\tau = 3\beta$ the value of the ratio is 0.865 and 0.95 respectively. In the following discussion, the maximum characteristic time of 1.2 seconds specified for this development was used.

Two systems of different materials were compared by allowing the following conditions:

1. All temperatures equal for two thermocouples of different materials.

2. Both thermocouples were of the same diameter.

3. Both thermocouples had the same heat transfer coefficients.

A ratio of the two systems provides:

$$\frac{\tau_2}{\tau_1} = \frac{\rho_2 C_2}{\rho_1 C_1}$$

indicating that the ratio of characteristic times are equal to the ratio of density and specific heat.

Listed in Table (11) are characteristics of commercial thermocouple materials as well as estimates for thermoelement materials recommended under this development.

If the ratio of a chromel/alumel system with an average ρC of 62 and a palladium/platinum 15% Iridium system which has an average ρC of 44 are taken

$$\frac{\tau_{C/A}}{\tau_{pd/pt\ Ir}} = 1.41$$

or

$$\tau_{C/A} = 1.41\ \tau_{pd/pt\ Ir}$$

In figure (47), are shown characteristic times vs. mass velocity from ref. (14). These values are both calculated and experimental for a chromel/alumel, 16 gauge, loop junction. Also shown are the expected characteristic times for either a platinum/platinum rhodium or a palladium/platinum-iridium system at the maximum temperature of 1600°F (871°C).

This figure illustrated that a characteristic time lower than the specified 1.2 seconds could be predicted for a 16 gauge palladium/platinum 15% iridium thermocouple at as low a temperature as 1400°F (760°C) and a 6 lb/ft ^{2} sec. mass flow. It was therefore not anticipated that the time response requirement in this development would present any problem.

In order to better understand the factors which more directly effected the speed of response of the thermocouple junction, the following simplified problem analysis was prepared. This analysis was made in preparing specific recommendations for characteristic time improvements.

Considering a heated thermocouple placed in a cooling, moving air stream. Radiation and conduction losses neglected; the only mechanism available for removing energy from the couple was the moving air stream. Density and viscosity variations were likewise neglected. The air stream was considered to be tube-like with:

$$dm = \rho_g A_g\ (dl)$$

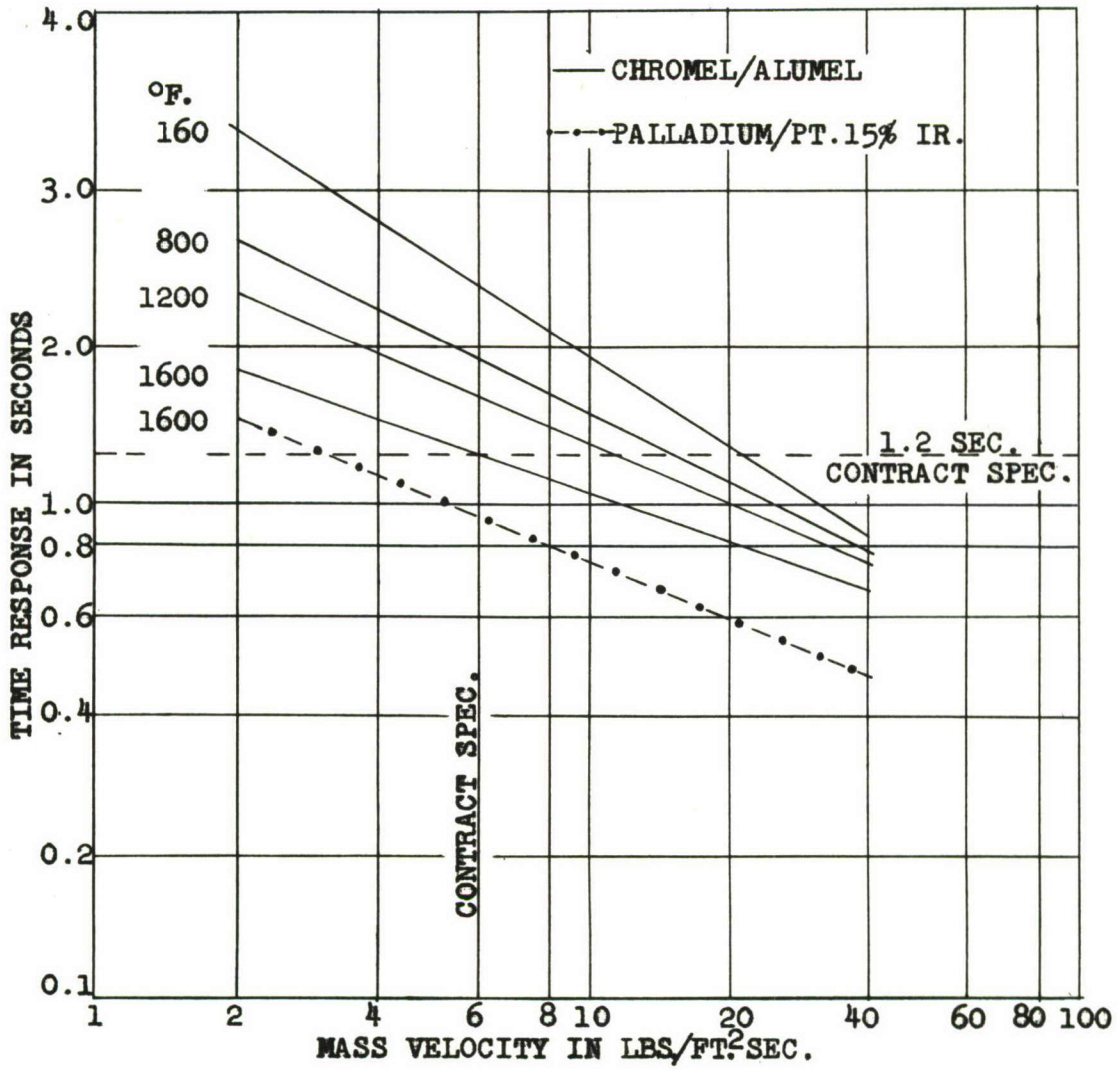


FIGURE 47. EXPERIMENTAL TIME RESPONSE

TABLE 11

MATERIAL CHARACTERISTICS FOR TIME RESPONSE ESTIMATES

MATERIAL	DENSITY LBS./FT.3	SPECIFIC HEAT B.T.U./LB./°R.	ρc B.T.U./FT.^{3}/°R.
CHROMEL	545	0.106	57.770
ALUMEL	537	0.124	66.588
PLATINUM	1334	0.0324	43.222
PLATINUM 13% RHODIUM	1261	0.0357	45.018
PALLADIUM	744	0.596	44.342
PLATINUM 15% IRIDIUM	1343	0.0323	43.379

where dm is an element of mass, A_g is the area of the stream (equal to the area of the junction A_j), ρ_g was the density of the air, and dl is a unit of length along the tube. Differentiating this equation with respect to time given the rate of change of mass flowing pass the thermocouple. Using this relationship in the energy equation for heat flow gave, after integration, the result:

$$T-T_f = (T_i - T_f) \exp(-) (t/C_j/S_g \rho_g A_j V_g)$$

where:

t = Instantaneous time greater than zero

T = Temperature at any time (t) greater than zero

T_i= Initial temperature

T_f= Final temperature

C_j= Heat capacity of the junction

A_j= Area of the junction

S_j= Specific heat of the gas

ρ_g= Density of the gas (considered constant)

V_g= Velocity of the air stream

exp= Base of the Natural log (e)

The denominator of the exponent of (e)is called the time constant.

That is: $\tau = C_j/S_g \cdot \rho_g A_j V_g$

A similar expression to this has been given by Dahl and Fiock, (82) and mention was made that the coefficient of heat transfer (h_c) is dependent on the mass flow rate. The quantity $\rho_g V_g$ is the mass flow rate, so h_c does, in fact, contain that term.

In practice, the equation above cannot be used to rigorously define the time response constant τ. Heat transfer of this type is extremely complex, and in addition to the assumptions made, it has also been shown that τ depends on the temperature interval. The value of the equation lies in the fact that it points out some variables which are significant for rapid response, and it therefore provides a direction for proper thermocouple design.

Although the equation cannot be used to measure τ theoretically, examination of it showed that the quantity can be determined experimentally. When t is equal to τ, as pointed out earlier, the temperature of the thermocouple will have reached a value: $T = T_f + (0.362)\ (T_i - T_f)$. Thus, by measuring the time it takes the probe to traverse approximately 63% of the temperature interval, the τ is determined. Actually, since τ is a constant of a particular system (couple and measuring equip-

ment), any arbitrary change in the temperature interval can be used together with the corresponding time interval to calculate γ. This will hold true only if the experimental temperature-time curve is logarithmic as the theory suggests.

Test Results

In order to evaluate the speed of response of various thermocouple junction configurations, a test facility was set up to measure the speed of response under contract conditions. This facility is shown in Figure (48). The equipment was operated and measurements were correlated with the National Bureau of Standards for several types of thermocouple junctions. Table (12) shows the test results as compared to those of the National Bureau of Standards for three different types of thermocouple junctions. Figure (50) shows a sketch of these three junction types. In Figure (48) the high steady-state temperature was provided by an electric oven; the lower temperature was a cool, moving air stream. An orifice plate used in conjunction with a U-tube manometer provided for mass flow calibration. The emf of the thermocouple was fed into a recording oscillograph. Decade resistance boxes are used to provide both proper impedance matching and desired recording sensitivity.

Since the time response was defined as that time required to reach 63% of the temperature change, it was, in general, incorrect to use 63% of the emf change. For chromel-alumel couples which exhibit a linear emf-temperature relationship, a conversion was not necessary.

Errors could be introduced if the temperature or the velocity of the air stream were to vary significantly with time. The recording device was such that any drift was detected on the trace and necessary corrections made.

Since there were no pressure sensing devices situated near the couple, it was not possible to guarantee that the probe was "seeing" the mass flow indicated by the orifice plate. A simple "dip-stick" measuring device insured that the thermocouple was at the same position in the air stream, and the results indicated excellent reproducibility. Comparison of results with the Bureau of Standards indicated the necessary corrections.

It was also found that the galvanometer reached equilibrium in a time approximating its natural frequency. With the impedance match used (63% critical damping) the time lag was approximately 0.005 seconds.

The slope of the emf (temperature)-time curve was such that an error in measurement of temperature corresponding to an error in length of 1/60 of an inch produced errors in time responses of between 1% and 2%. Using an engineers' scale kept these errors to within these limits.

Time Response Conclusions

An analysis was performed indicating that the response of a palladium/platinum 15% iridium thermocouple should be faster than those observed by chromel-alumel by a factor of 1.41. Several responses of various chromel-alumel designs were measured and with an 18 gauge, machined loop system, a 1.17 second response was attained. It is concluded, that the time response specification of 1.2 seconds could be attained using 16 gauge wire in a machined loop configuration.

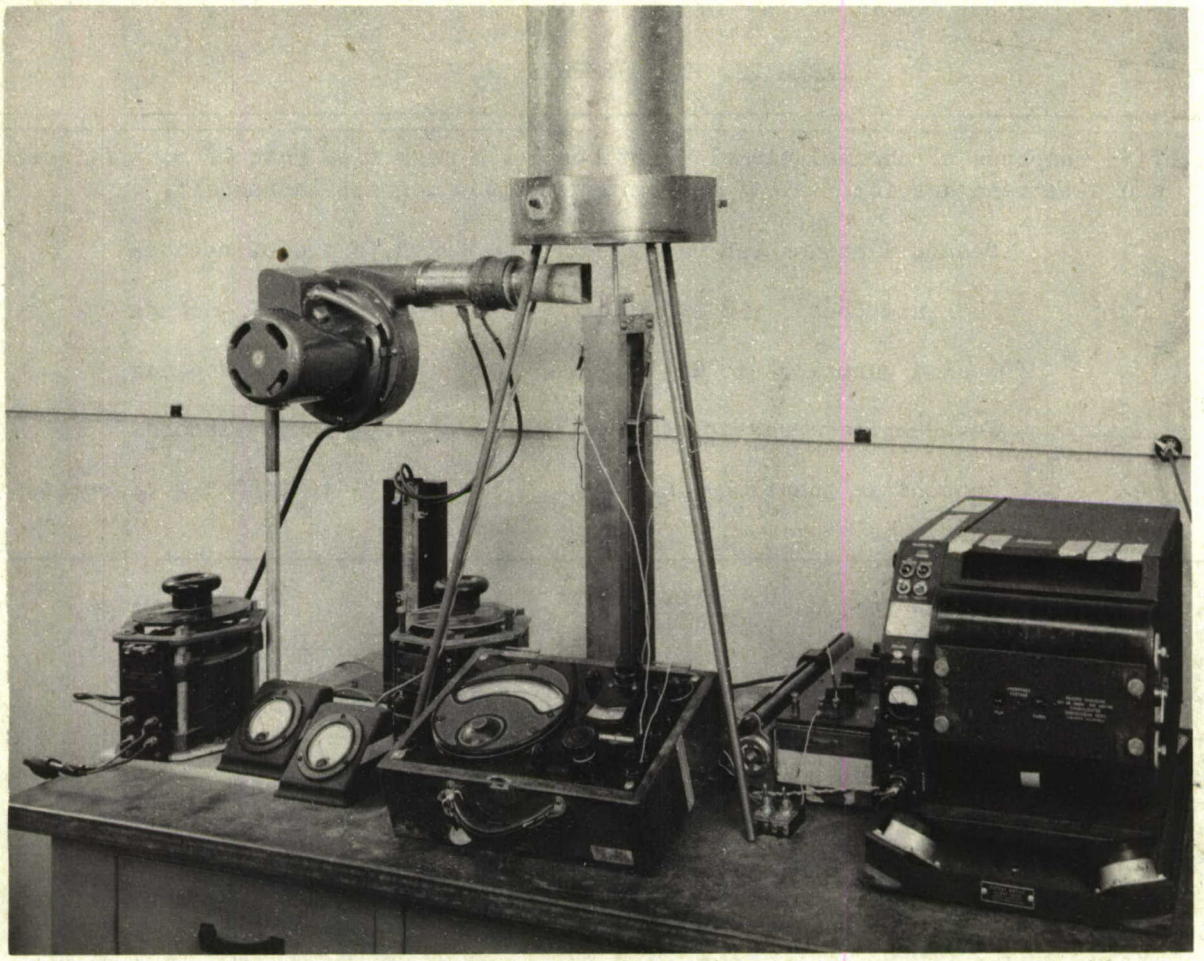
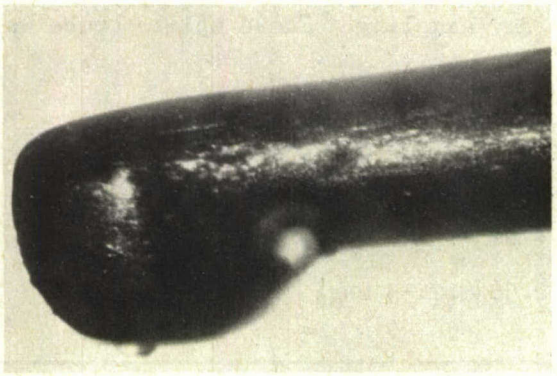
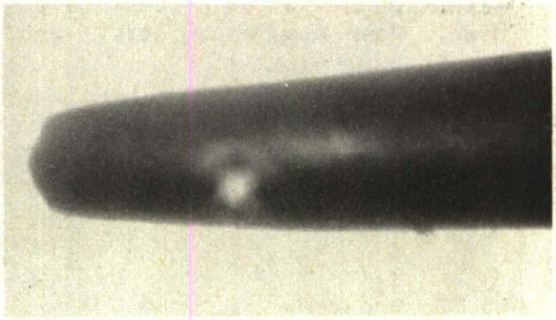


FIGURE 48. SPEED OF RESPONSE TEST



TYPE 2



TYPE 1

FIGURE 49. CONCENTRIC SUB-MINIATURE THERMOCOUPLE JUNCTIONS (APPROXIMATE O.D. AT TIP ≈ 0.020 INCHES)

TABLE 12. TIME RESPONSE RESULTS

a. Time response of chromel-alumel junctions for a mass flow rate of 6 lb/ft^2-sec. and a temperature interval of approximately 1000 degrees Fahrenheit.

Beaded Junction (26 GA)	0.78 ± 0.02 seconds
Machined Loop (18 GA)	1.17 ± 0.02 seconds
Beaded junction (18 GA)	1.92 ± 0.02 seconds
Fused splice junction (18 GA)	2.59 ± 0.03 seconds
Concentric junction (.028 OD)	0.71 to 0.50 ± 0.02 seconds

b. Variation of time response as a function of mass flow rate. Fused splice probe was used.

Mass flow rate: (lb/ft^2-sec.)	Time Response: (seconds)
3.0	3.66
4.5	2.97
6.0	2.56
7.0	2.37

c. Variation of γ as a function of day to day sampling. Fused splice probe was used. Mass flow was 6 lb/ft^2-sec.

Day	Time Response (Sec.)
1	2.58 & 2.61 sec.
2	2.56 * 2.58 sec.
3	2.56 & 2.59 sec.

d. Calculation of time response using arbitrary percentage changes in temperature.

Fused splice	Machined loop	Temp % change
2.58 sec.	1.17 sec.	63%
2.58 sec.	1.14 sec.	39%
2.61 sec.	1.14 sec.	28%
2.60 sec.	1.15 sec.	18%

---

e. Comparison of time response results against tests made at the National Bureau of Standards. The mass flow rate was 6 lb/ft^2-sec. The temperature interval was approximately 1000 degrees Fahrenheit.

Couple		General Electric Data	National Bureau of Standards
Beaded junction		0.78	0.72
26 GA)		0.78	0.72
			0.68
	Average	0.78 sec.	0.71 sec.
Machine loop		1.16	1.12
(18 GA)		1.17	1.00
			1.07
	Average	1.17sec.	1.06 sec.
Fused Splice		2.58	2.49
(18 GA)		2.61	2.35
			2.15
	Average	2.59	2.33 sec.

There is a constant conversion factor between the two sets of data. This conversion factor is:

$$\frac{G.E.}{1.1} = N.B.S.$$

TABLE 12. CONTINUED

f. Time Response of Concentric Design

Junction Form*	Unit No.	Record No.		Time Response-sec.		T. °F
1	1	3459		0.79		1000
1	1	3462		0.77		1000
1	1	3466		0.77		1000
			Average	0.77	Corrected Ave.	0.71
2	2	3469		0.54		1000
2	2	3472		0.53		1000
2	2	3475		0.54		1000
			Average	0.54	Corrected Ave.	0.49
2	3	3478		0.57		1000
2	3	3481		0.57		1000
2	3	3484		0.55		1000
			Average	0.56	Corrected Ave.	0.51

*See Figure 49.

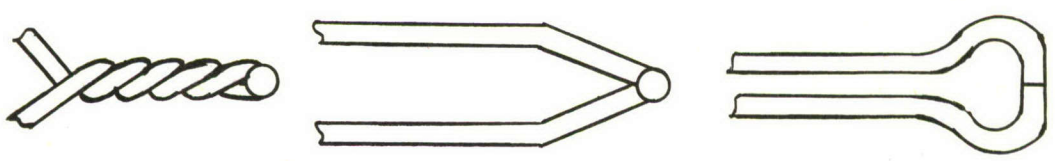


FIGURE 50. JUNCTION TYPES USED FOR TIME RESPONSE DETERMINATION

High-Recovery System

In this section, consideration is given to the system which required a recovery factor of not less than 0.98.

In speaking of gas temperature measurements in a high-velocity gas flow, there are two existing states. There is the static temperature which would be measured if the measurement was taken by moving a device along with the gas stream. The other is a total temperature where the measurement is made by a stationary measuring device. The total temperature device brings the gas to rest and the kinetic energy is converted to an adiabatic temperature rise.

The determination of these states of temperatures is a difficult task. The static temperature is the most difficult with a stationary probe, because of the gas velocity reduction by the boundary layer. This temperature is usually determined by measuring the static pressure and either the density, velocity or index of refraction of the gas.

The conventional probe usually indicates somewhere between the static, T_s, and total temperatures, T_t, depending on the shape, orientation, radiation and other factors of the probe. The stagnation, T_{st}, and static temperatures, T_s, are related by the following equation:

$$\frac{T_{st}}{T_s} = 1 + \frac{\gamma - 1}{2} M^2$$

where M = free stream mach. number.

Letting $\gamma = C_p/C_v = 1.4$ for air, the relationship can be written -

$$\frac{T_{st}}{T_s} = 1 + 0.2M^2$$

which holds for sonic as well as subsonic flows.

We define the recovery factor as the ratio of the indicated temperature rise, $T_t - T_s$, to the adiabatic temperature rise, $T_{st} - T_s$ or

$$r = \frac{T_t - T_s}{T_{st} - T_s}$$

This relation indicates that a system of maximum efficiency can have the ratio of one. Under this condition, the indicated temperature would be as near the stagnation temperature as possible.

Applying the conditions of this contract

$$r > 0.98$$

and $$M = 0 \text{ to } 0.8$$

From the recovery factor definition above, we have that:

$$\frac{T_{st}}{T_s} = 1.128 \text{ or } T_{st} = 1.128\ T_s$$

and:

$$T_t = 1.125\ T_s$$

It is now possible to proceed in determining what is needed for a high recovery system. From the discussion above and experimental data on high recovery systems, it is found that the system is required to be of some aspirated or stagnation design. The aspired or stagnation design provides for the reduction of differences in the indicated and true temperature by consideration of the following factors:

1. Reduction of the effect of adiabatic temperature rise, due to bring the gas to rest.

2. Reduction of radiation losses.

3. Reduction of conduction losses.

The first of these factors is affected by establishing a stagnation zone ahead of the temperature sensing element. The calibration of such a probe shows better reproducibility than that of a probe for which the flow characteristics in the boundary layer determine the recovery factor. A probe of this type is shown in Fig. 51.

The other factors can be affected by considering the following characteristics as they are related to the system.

1. The thermoelements should have low heat capacity to reduce couple time lag. Although it is not intended to consider time lag in the high recovery probe. An attempt must be made to provide an acceptable response.

2. To reduce conduction losses, the thermoelement leads should be partially exposed to the temperature of the stagnation chamber.

3. Radiation losses are reduced since the stagnation chamber serves as a radiation shield also. The radiation shield should be of a low heat conductivity and low surface emissivity so that the thermoelements "see" as small a temperature difference as possible. A low temperature difference reduces the radiative heat transfer.

4. A number of vent holes should be provided in the stagnation chamber to replace the air. The temperature of the air in the chamber will tend to drop below the stagnation temperature due to heat conduction and radiation if not replaced. These holes must be of small size so as not to cause the air in the probe to assume an appreciable velocity. The small velocity effect of these holes are advantageous, however, as they reduce the time lag by increasing the convective heat transfer.

5. The heat losses from the probe can be reduced by having a blunt probe with a strong normal shock wave in front which effectively raises the boundary layer temperature. The effect of a strong normal, shock wave also provides insensitivity to flow inclinations.

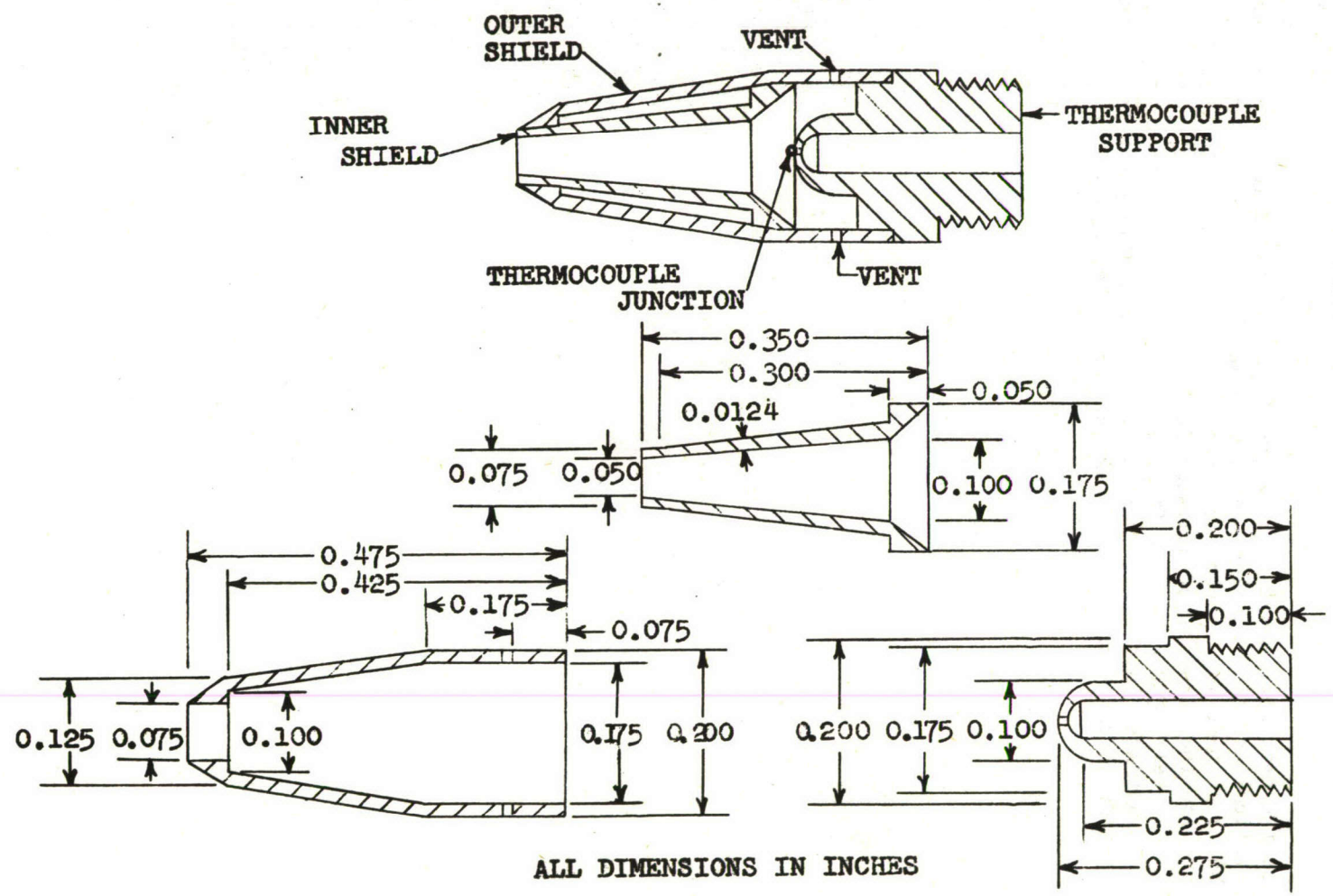
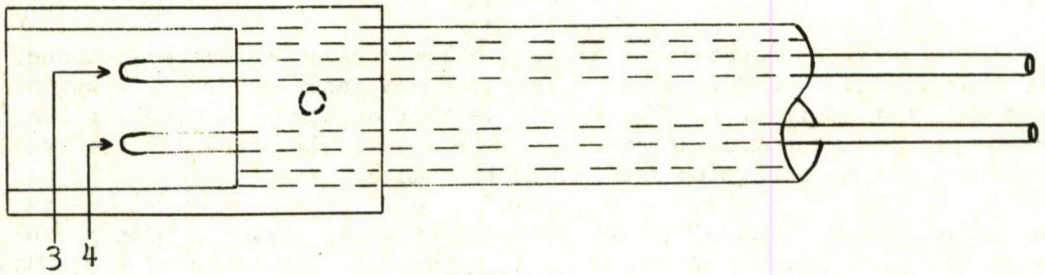


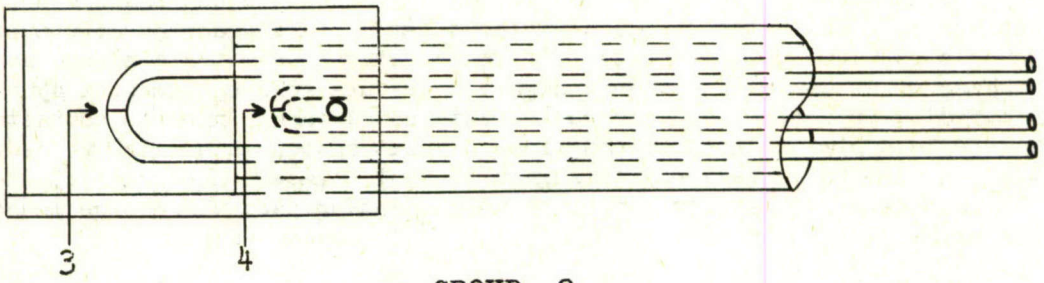
FIGURE 51. TOTAL TEMPERATURE PROBE

High Recovery Design Conclusions

Since the design of a system is a judicious choice of factors, and material characteristics, definite conclusions can not be made in the strict sense. An attempt has been made in this section to point out the controlling factors and ways to provide that a probe of suitable design be provided. Figure 51 illustrated a relatively complex design from the manufacturing standpoint, however, Figure 52 illustrates that the requirements of high recovery can be attained by minor modification of the present G.E. high recovery probe.



GROUP -1



GROUP -2

GROUP	JUNCTION NO.	CHARACTERISTIC TIME (SECONDS) @MASS FLOW RATE (LBS./FT.^{2}-SEC.)				RECOVERY FACTOR
		2	4	6	8	
1	3	7.2	4.7	3.7	3.0	0.95
	4	8.3	5.8	4.3	3.6	0.95
2	3	4.3	2.9	2.5	2.1	0.96
	4	15.4	10.3	8.3	6.9	0.96

FIGURE 52. GENERAL ELECTRIC HIGH-RECOVERY SYSTEMS

Section VII - Connectors

The thermocouple connector has three problem areas; contact resistance, spurious voltage, and mechanical life. The problems are not insurmountable, however, they are of such a nature that it is highly improbable that absolute elimination can be attained. They can be reduced to a minimum only by extreme designing care and observation of the following precautions resulting from field test data.

The contact resistance of a connector operating in a region of high temperature and vibration can increase from any of several causes; oxidation of the contacts, loss of contact pressure due to loosening or wear of the contact parts or relaxation of the spring member. The contact may also be damaged mechanically by forcing the contacts together improperly, over-stressing the spring or by inserting an oversized test lead into the socket. This problem can be overcome by proper material selection and elimination of mechanical damage.

Spurious voltage can be introduced into the thermocouple circuit at the connector by formation of a secondary thermocouple. If the contact members are of materials which do not match the lead wires, a temperature gradient at the connector would cause a spurious voltage error. If other extraneous materials such as studs, nuts, washers or solder are used in a high temperature gradient zone, a spurious voltage may also result. These errors are eliminated when connector contacts are made of materials similar to the lead wires and extraneous materials avoided. The connector can also be installed in a region of small temperature gradient while locations such as a firewall or a thermocouple mounting pad, where high temperature gradients exist, are to be avoided.

The mechanical design of a thermocouple connector should be such that it encloses the contacts protecting them from the products of combustion, dirt and foreign metallic particles. These can short-circuit the thermocouple circuit to ground or cause excessive wear of the contacts. Means should also be provided to prevent the contact pin from entering the socket at such an angle as to over-stress the contact spring itself. When galling of the thread occurs at high temperature, it would be an advantage to be able to replace the coupling nut and return the unit to service.

The specifications applicable to this phase of the development were as follows:

1. Spurious Emf. - Each connector of the thermocouple system shall be tested for spurious junction effect. This test shall be conducted in a similar manner to the procedures used in WADC TR 53-341. The amount of emf generated when a temperature gradient of 100°F is imposed across any one harness connection shall not introduce an error in excess of plus or minus 5°F. When a 1000°F gradient is imposed, the amount of emf generated by any firewall connection, if applicable, shall not exceed plus or minus 5°F.

2. Torque Resistance - The operation of each threaded connector used in the thermocouple system shall not be affected by being torqued to 100 in-lbs. Upon heating in an airframe installation, or its equivalent, disassembly of the connector shall not result in damage when the initial torque value is 100 in-lbs. At torque settings of 30 in-lbs. to 100 in-lbs., the contact resistance shall not vary from the design contact resistance by more than plus or minus 0.1 of an ohm at all ambient temperatures from 500 to 1500°F. In addition, if some type of spring loaded socket is determined to be more advantageous

for this application, testing shall be conducted to prove that a reliable positive contact is maintained at the maximum operating temperatures as well as at room temperatures.

3. Maintenance - The complete thermocouple system shall be assembled and disassembled 50 times without damage occuring to any one component. It shall take no more than 12 minutes to assemble and disassemble the complete system on an engine installation.

Evaluation

There is no recognized method for evaluating thermocouple connectors to insure that they will perform satisfactorily under the high ambient temperatures and vibration forces that are found on jet engines. In lieu of accepted tests, a comparison test was used as developed for evaluating improvements on thermocouple connectors. The test consists of cycles of vibration at 45 g's, 190 cps and 25 mil vertical displacement and then heating the connector assembly to 1500°F (816°C) temperature. When a voltage is applied across the contacts and monitored on an oscilloscope, a failure is indicated by a hash due to intermittent contact or voltage increase due to high resistance or an open circuit. Under these conditions, a standard production connector which has operated satisfactorily for over 150 hours in the field would fail in a matter of 2 1/2 hours test time at 1000°F (538°C).

The stud and nut type of thermocouple electrical connection was discarded early in the development. This type of junction has several draw-backs. The contact pressure relies on the care with which the nut is tightened and locked and the studs are subject to damage by cross-threading and galling. Its use also presents the constant risk that field personnel may use nuts of standard aircraft design to replace special thermocouple alloy parts which are required. Tests by the National Bureau of Standards have also indicated that considerable error can result from this type of connection.

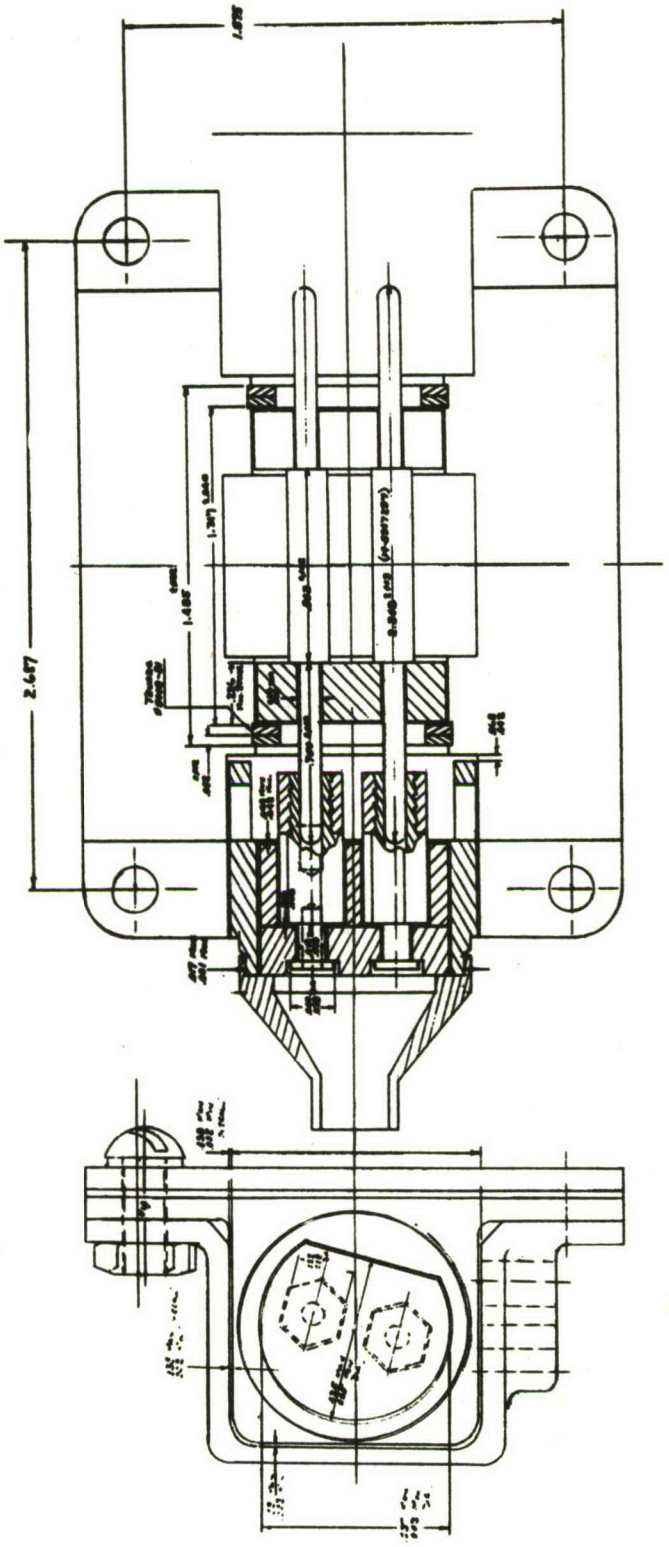
Three basic connector designs were evaluated; the Williamsgrip connector (Figure 53) which utilizes a tapered thread to obtain the contact pressure, the G-E 705 type connector (Figure 54) which is the improved version of the connector used on the B-47 and F-86 aircraft, and the Canadair type connector (Figure 55). Connectors were also requested of the Thermo Electric Co. of Saddle River Township, New Jersey, and Fenwal Incorporated of Ashland, Mass., however, were not received in time for evaluation under this contract.

All connector evaluation tests were made with chromel alumel lead wires as developmental lead wire material contacts had not been determined when testing was initiated. The results were deemed valid for the Canadair and G-E 705 types as the contact force was supplied by a spring of Inconel X in the test unit. It has also been recommended that the contacts be protected by platinum plate as are the present chromel alumel counterparts for comparable oxidation and wear resistance of the surface.

The Williamsgrip connectors (Figure 53) failed in 15 hours or less. The failures observed were; breakage of the lead wire where it entered the MgO insulation, breakage of the wire at the end of the socket, and loose interconnecting nuts. As a result, this connector was not recommended for use since-

1. The present design does not provide adequate space to tighten the socket nuts properly. It was recommended that a housing design change could pro-

Figure _____



2 CONTACT
WILLIAMSGRIP CONNECTOR
LAYOUT

Fig. 53

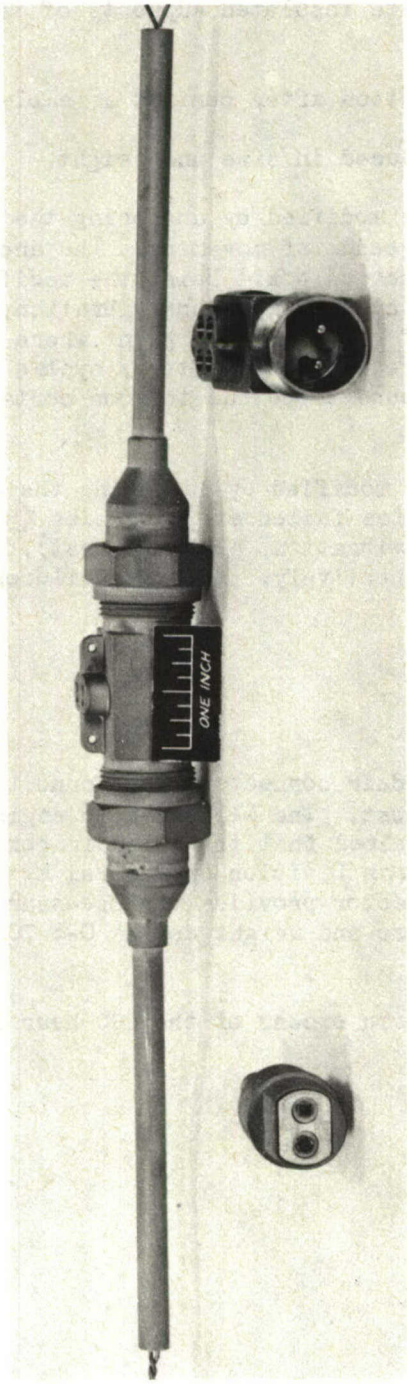


FIGURE 54. G. E. TYPE 705 CONNECTOR

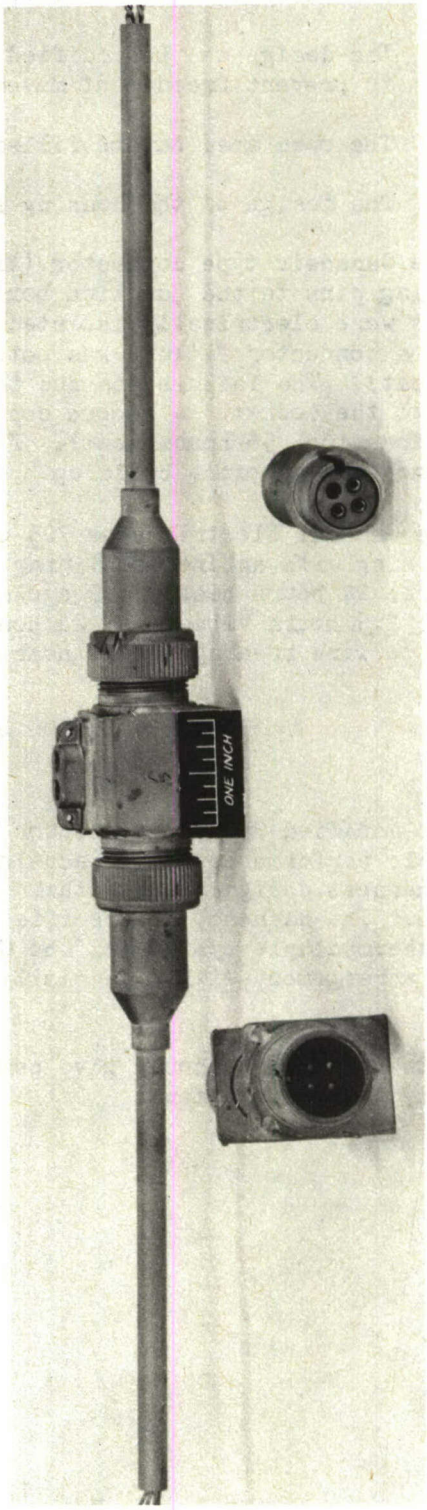


FIGURE 55. CANADAIR TYPE CONNECTOR

vide sufficient access space.

2. The sockets should be lengthened to effect a decrease in wire vibration.

3. The design can be modified to incorporate insulated supports of the pins to prevent freedom of movement.

4. The open area can be filled with insulation after contact assembly.

5. The design of the housing should be reduced in size and weight.

The Canadair type connector (Figure 55) was modified by anchoring the interconnecting pins to the junction box to reduce freedom of movement. The anchoring supports were electrically isolated from the junction box. Using the modified design, a connector failure was noted after 3.4 cycles (47 hours vibration, 24 hours heat). The failure was due to breakage of one lead at a point where it was welded to the socket. A second connector failure was noted after 7 cycles (98 hours vibration, 56 hours heat). Failure was found to be due to poor contact resistance due to oxide build up.

The General Electric type 705 connector was modified by replacing the SS420 locking ring with an Inconel X ring. Three samples failed at 3.7 cycles (51.5 hours vibration, 24 hours heat), 4.2 cycles (58 hours vibration, 32 hours heat), and 3.8 cycles (52.5 hours vibration, 24 hours heat) respectively. All the failures were related to wire breakage at or near the socket.

Conclusion

The modified G-E 705 connector and the Canadair connector were found to have comparable performance in the accelerated life test. The Allison T-56 engine thermocouple harness designed under this contract, required that the Canadair connector be selected. The harness, as specified by the Allison Division of General Motors, has a dual thermocouple system and the Canadair connector provides the necessary four-contact arrangement with essentially the same size and weight as the G-E 705 connector.

Both connectors should give performance far in excess of the 400 hour life required by this development.

Section VIII - Harness Design

The purpose of the harness is to permit the electrical joining of more than one thermocouple and to present at the end device an electro motive force which has a relation to the temperature in the engine. The most useful output would be an average of the thermocouple pattern throughout the engine cross-section.

The five basic circuit types presently used for thermocouple averaging are as follows:

1. Common junctions
2. Ladder harness
3. Equal resistance
4. Geometrically balanced harness
5. Compensated ladder harness

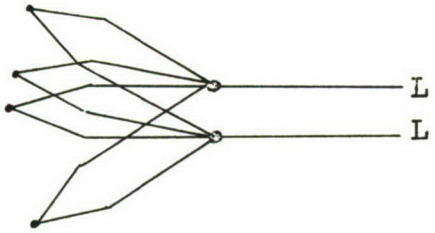
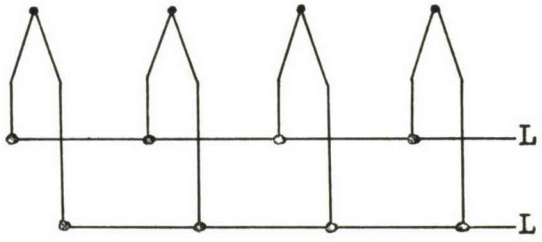
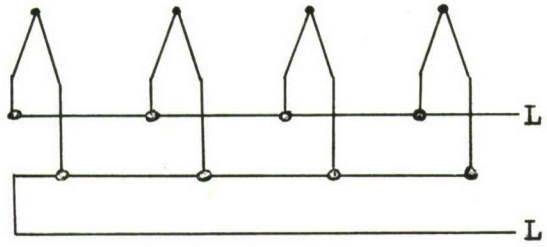
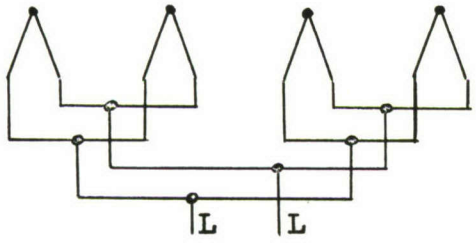
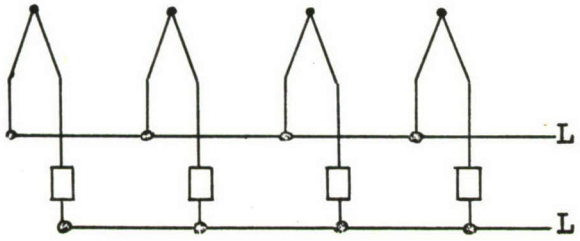
These are also illustrated in figure 56. Combinations of two or more of the above can be used in particular cases.

The simplest type of harnessing is the common junction harness. In this circuit, all thermocouples are connected at a common point and all branches have the same resistance. This design involves balancing wire sizes to yield equal resistance or the use of leads of equal length and wire size. The multiple leads running to the junction point, however, result in extra weight. The millivolt averaging characteristic is good and the upset in the resistance balance due to ambient temperature variations is small.

The ladder harness involves connecting the individual thermocouples between common leads or bus-bars. It is apparent that the thermocouple closest the end device has the least resistance in the circuit and would exert the greatest influence on the output voltage. The thermocouple farthest from the end device would contribute the least output. The averaging error depends on the ratio of the thermocouple branch to the bus segment. Since the branch wire size is determined by the mechanical strength required at the junction, the bus conductor would have to be large to obtain a high ratio. With a 10:1 ratio or higher the loss of a thermocouple branch circuit would introduce a small error which becomes a problem of size and weight balanced against acceptable error. These ratios and their errors are discussed in reference 36.

The equal resistance harness determines the lead wire resistance in such a manner that at the design ambient temperature the two lead wire elements have the same resistance per unit length. In this way, the effects of the lead wire are the same for all junctions. A change of ambient temperature from the design value will cause a large upset in the balance in the thermocouple circuit due to differences in temperature coefficient of resistance of the leads. Loss of a probe will not upset the averaging ability of the remaining circuit.

The geometrically balanced system is essentially a series of common junction harnesses combined into an entire system. In the normal form, pairs of thermocouples

DIAGRAM	TYPE	AVERAGE	ERROR
	COMMON JUNCTION HARNESS	1250°F	0 %
	LADDER HARNESS	1243°F	0.53%
	EQUAL RESISTANCE HARNESS	1280°F	2.46%
	GEOMET-RICALLY BALANCED HARNESS	1247°F	0.21%
	COMPEN-SATED LADDER HARNESS	1250°F	0%

HARNESSES AVERAGING THE SAME PATTERN. AMBIENT=800°F

PATTERN: 1200°F, 1100°F, 1300°F, 1400°F. AVERAGE: 1250°F

FIGURE 56. FIVE BASIC HARNESS DESIGNS

are joined, then sets of pairs joined. A variation of this basic type of system is one in which a proper choide of lead lengths, balances unequal numbers of probes. Another variation involves the use of compensating resistors to obtain the same electrical balance while maintaining a desirable mechanical design. This system gives a true millivolt average as long as the probes are all at an equal temperature and the harness is at a constant temperature. The harness in this case, does not have a design temperature for a true average as in the case of the equal resistance and compensated ladder harness. Variations of temperature between probes or in harness temperatures will introduce small errors. Loss of a branch in this circuit will introduce errors in averaging.

The compensated ladder harness is similar to the basic ladder except that each branch resistance is adjusted to give a circuit which balances the effective contribution of each thermocouple to the output. This system is affected by the changes in resistance due to ambient temperature. The effect of ambient temperature and loss of branch circuits can be reduced by increasing the thermocouple to bus resistance ratio. This type of harness is adaptable to any number of thermocouples.

A typical four thermocouple harness which has linear output characteristics can be used as an indication of the errors involved by loss of a probe. For a resistance ratio of 10:1, the error due to the loss of a probe is 4.1°F when occurring in a 200°F spread. For a ratio of 20:1, the error would only be 2°F.

The possibility of averaging error due to non-linearity of noble metal thermoelements was investigated by John Wood of the General Electric Company's Aircraft Gas Turbine Division. For this purpose, he used a 12 thermocouple common junction type circuit and the thermocouple elements of rhodium-palladium as being representative. For a spread of temperatures between 1650°F and 1950°F with a normal distribution around the average temperature of 1800°F, the error due to averaging was calculated as 1.7°F. This error is small when compared with the present day temperature amplifier and other components in the temperature system. For all the parallel circuit arrangements discussed above, the averaging error is found to be proportional to the temperature spread.

Consideration was also given to construction of a flexible type cable which would be suitable for high temperatures and vibration. This construction utilizes bellows type flexible conduit with ceramic beads. The design is such that the beads are not put under any undue strains as long as the flexible conduit is not bent in a sharper radius than that recommended by the manufacturer.

Figure 57 shows a construction of this type which would be suitable for a four wire harness which could be used with dual junction thermocouples.

This type of construction has been used successfully on a J-73 engine thermocouple system, however, the bead was redesigned and a stronger material substituted to give improved life. The flexible construction was found to be somewhat more expensive to fabricate. It is also more susceptable to damage due to mishandling and requires more support from the engine. Except for applications where the extra flexibility is essential, the rigid construction has been recommended.

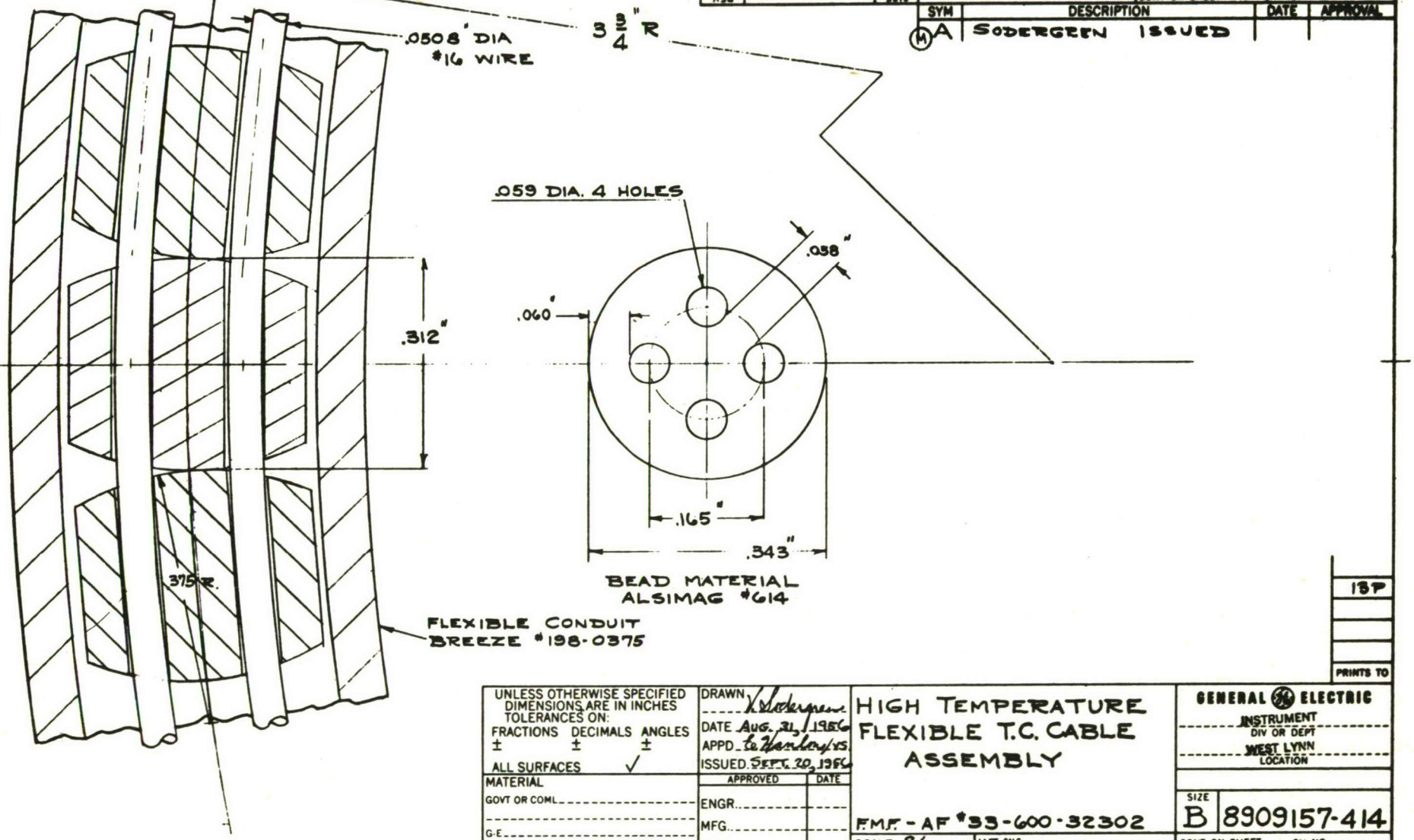
Conclusion

One of the harness types as required to be supplied under this contract, is for the Allison T-56 engine. The Allison T-56 engine has 18 dual thermocouple

WADC TR 57-744

94

REVISIONS				REV
SIZE	CONT ON SHEET	SH NO.		
SYM	DESCRIPTION		DATE	APPROVAL
(M) A	SODERGREEN ISSUED			



ISP

PRINTS TO

UNLESS OTHERWISE SPECIFIED DIMENSIONS ARE IN INCHES TOLERANCES ON: FRACTIONS ± DECIMALS ± ANGLES ± ALL SURFACES ✓	DRAWN K. Sodergreen	HIGH TEMPERATURE FLEXIBLE T.C. CABLE ASSEMBLY	GENERAL ELECTRIC
	DATE Aug. 31, 1956		INSTRUMENT DIV OR DEPT
	APPD L. Hanley/RS		WEST LYNN LOCATION
	ISSUED Sept. 20, 1956		
MATERIAL	APPROVED / DATE		
GOVT OR COML	ENGR		SIZE B 8909157-414
	MFG		
G-E	MATL	FMF - AF #33-600-32302	
		SCALE 8/1 WT CALC ACTUAL	CONT ON SHEET SH NO.

FP-5B2 15M (7-56) PRINTED IN U.S.A.

probes. The design selected utilizes six interchangeable elements of three probes each. The three branch circuits are balanced by the use of a compensating resistor to give an average output. The elements are interconnected by a harness which forms a six element compensated ladder circuit.

The three probe segment permits engine installation without introducing special problems. The harness is to be supported from the engine so that vibration of the harness junction box does not unduly load the thermocouple structure.

The connector is located at a point aft of the thermocouple probes. This places the connector in a zone of relatively uniform temperature rather than the large gradient due to conduction if located directly on the thermocouple mounting pad. This reduces any spurious emf due to temperature gradients.

Individually replaceable thermocouples have been considered and based on economic and reliability consideration; they have not been recommended. Fabrication and circuitry is simplified by the use of the three probe elements. This simplification reduces the resultant size and weight of the overall system. An individual thermocouple connector operating under conditions of high ambient temperatures and vibration has always been a point of hazard from improper assembly, poor locking of parts, and the introduction of foreign material. By reducing the number of connectors from 18 to 6, the probability of failure is reduced correspondingly. In addition, the reduced number of connections will involve less tedious repetition and, perhaps, result in greater care being exerted during installation and replacement operations.

Section IX - Conclusions

The thermocouple systems which will meet the requirements of this contract are recommended to be of the following materials and dimensions:

Fast Response System

Thermoelements - Palladium/Platinum 15% Iridium

Palladium-C.P. Grade as supplied by the Baker Co., Inc.
133 Astor Street, Newark 5, New Jersey
Platinum 15% Iridium - ISA Standard as supplied by the
Sigmund Cohn Co., Mount Vernon, New York
Wire Diameter - 0.051 inch, 16 AWG.
Junction form - Inert-arc butt welded type in machined loop configuration.

Insulation - Magnesium Oxide, however, more preferably Aluminum Oxide for its higher resistivity. Magnesium Oxide was recommended since it has been found to withstand vibration better than aluminum oxide when in the swaged form.

Lead Wires - An alloy of 4.31% Silicon balance Nickel/Nichrome*

Since the nickel-silicon alloy and the Nichrome are not supplied to particular thermocouple characteristics, these would require standardization. Standardization would require melt selection from a thermocouple manufacturer based on thermoelectric characteristics which are within the specifications required by this contract.
Wire diameter - 0.051 inches, 16 AWG.

Sheath Material - Inconel 702 as supplied by the International Nickel Company, New York. Material dimensions would be determined by the particular application.

Connector - Canadair type for Allison T-56 harness as required for delivery under this contract. Modified G.E. type 705 for the experimental harness also required for delivery.

Harness Design - Six-element compensated ladder harness for the Allison T-56 harness. The experimental harness should also be of this type designed to fit the application.

High Recovery System

All components of this system are identical to those listed under the fast response system. The only exception is the requirement of a stagnation cup. The stagnation cup should be of the same materials as the sheath, however, it is understood that Allison has requested that some be made of Inconel for the T-56 type harness.

National Bureau of Standards Informal Report

This report was received on December 18, 1957 and has been included as it was

*Driver Harris Company, Harrison, New Jersey

received since time did not permit its inclusion in the body of this report.

General Electric Palladium vs. Platinum + 15% Iridium Thermocouples

Thermocouple probes suitable for use in the temperature range of 2000°F to 2500°F are under development for the Air Force (WADC) by the General Electric Co. A group of eight experimental thermocouples were submitted for determination of their temperature-emf characteristics and rates of response.

All samples were of similar construction. The thermocouple junctions were made from 0.051 inch diameter palladium versus platinum 15% iridium thermoelements. The junctions were butt-welded and formed into a stirrup-type configuration. The junctions in most bases protrude 5/16 inches to 7/16 inches beyond their ceramic insulators. The thermocouple elements extended approximately 6 inches inside the insulator, where they are welded to matched extension leads. The extension leads were nickel + 4.31% silicon alloy versus Nichrome.

Probes 1 and 2 were heated in air in an electric tube furnace, and the temperature-emf relation of each was determined over the range of temperatures from 800°F to 2000°F. Measurements were made on samples 3, 4, 5, 6, 7, and 8 at temperatures of 800°F and 1600°F. A calibrated thermocouple of platinum versus platinum 10% rhodium was used to measure the actual temperatures of the furnace; all reference junctions were maintained at 32°F. The depth of immersion of all measuring junctions in the furnace was about 7 inches.

The temperature of the area where the lead wires joined the thermoelements was not measured. In all cases, these junctions were approximately one inch inside the furnace. Although temperature gradients exist along the furnace tube, especially at the ends, it is believed that the environment is fairly reproducible, and that effects due to the presence of the junctions between the thermocouple and leads are small. Further measurements will be made with the lead junctions completely outisde of the furnace tube to test the latter belief.

The results obtained from calibrating these thermocouples are summarized in Table I. The values of emf versus temperature were adjusted to correspond to even values of temperature to facilitate comparison of samples.

Table I

Thermocouple No.	Thermal emf in millivolts at temperatures, °F, of						
	800	1000	1200	1400	1600	1800	2000
1	9.750	12.934	16.452	20.290	24.352	28.666	33.374
2	9.684	12.800	16.300	20.169	24.178	28.474	33.036
3	9.738	------	------	------	24.099	------	------
4	9.814	------	-----	------	24.344	------	------
5	9.724	------	------	------	24.400	------	------
6	9.718	------	-----	------	24.223	-----	------
7	9.770	-----	-----	------	24.359	------	------
8	9.665	-----	------	------	24.218	------	------
Average	9.736	12.867	16.376	20.230	24.270	28.570	33.205

At a given temperature, the maximum deviation of any one thermocouple from an average value of thermal emf for all samples was not greater than 171 microvolts or approximately 8°F. However, this difference was about 3° to 5°F at most temperatures checked.

The thermocouples were checked a second time following a heating period in the exhaust gas stream. The largest change in thermal emf corresponds to 5°F at 2000°F, and at most temperatures checked was less than 2°F.

The rates of response of these thermocouples were determined in the exhaust gas stream. Measurements were made at a gas temperature of 1600°F, and at mass flow rates of 2, 4, 6 and 8 lbs/ft^{2}sec. for thermocouples 1, 2, 3, 4 and 8. Observations were made at 2 and 8 lbs/ft^2 sec on thermocouples 5, 6 and 7. All measurements were made with the thermocouples oriented in the gas stream so that a plane through the thermoelements was normal to the gas flow (0° orientation). In addition, the response rate of probe No. 3 was determined at 90° orientation.

The results of these tests are summarized in table II.

Table II

Thermocouple No.	Characteristic Time in Seconds at Mass Flow Rates (lbs/ft^2 sec) of			
	2	4	6	8
1	1.31	1.01	0.86	0.77
2	1.40	1.06	0.91	0.82
3 0°)	1.42	1.08	0.93	0.84
90°)	1.55	1.15	1.00	0.88
4	1.39	1.08	0.94	0.84
5	1.56	----	----	0.94
6	1.63	----	----	0.96
7	1.56	----	----	0.93
8	1.60	1.22	1.01	0.90

Except for one value at 2 lb/ft^2 sec, the maximum spread at any mass velocity is about 0.2 second. The fact that the results are divided into two sets in which the characteristic times of probes 5 through 8 are somewhat higher than those of 1 through 4 is unexplained. The observations were taken in a random order rather than the order in which the probes are listed in table II; changes in the exhaust gas system thus cannot be the cause. It seems reasonable, therefore, that these small differences may have been built into the probes, through design or otherwise, by different treatment of the elements at or near the junctions.

Combustion Controls Section
National Bureau of Standards
Washington, D.C.
December 12, 1957

Section X General Bibliography

General References

1. Hampel, C.A., Rare Metals Handbook, Reinhold Publishing Corp., New York, c 1954.

2. Campbell, F.E. High Temperature Technology. John Wiley & Sons, Inc., New York c 1956.

3. Wise, E.M. The Platinum Metals & Their Alloys. International Nickel Co., Inc. New York, c 1941.

4. Uhlig, H.H. The Corrosion Handbook. John Wiley & Sons, Inc., New York, c 1948.

5. Rhodes, T.J. Industrial Instruments for Measurement and Control. McGraw-Hill Book Co., Inc., New York, N.Y. c 1941.

6. Marks, L.S. Mechanical Engineers' Handbook. McGraw-Hill Book Co., Inc. New York c 1956.

7. McAdams, W.H. Heat Transmission. McGraw-Hill Book Co., Inc., New York C 1942.

8. Materials & Methods, Handbook of New Engineering Materials, Reinhold Publication New York. c 1956.

9. Ladenburg, R.W., Lewis, B., Pease, R.N., Taylor, H.S. Physical Measurements in Gas Dynamics and Combustion. Princeton University Press, New Jersey. c 1954.

10. Benesovsky, F. Plansee Procedings 1955, Sintered High Temperature and Corrosion-Resistant Materials. Metallwerk Plausee Ges. M.B.H., Reutte/Tyrol. c 1956.

11. American Society for Metals, Metals Handbook, New York. c 1948.

12. Troy, W.C., Gary, Stevens. Discussions. Transactions of ASME, 42, p 1131, 1950.

14. Moffat, R.J. How to Specify Thermocouple Response. I.S.A. Journal, June 1957.

15. Carbon, M.W., Kutsch, H.J., & Hawkins, G.A. The Response of Thermocouples to Rapid Gas-Temperature Changes. Trans. of ASME, 72, July, 1950.

16. Bailey, N.P. The Response of Thermocouples. Mechanical Engineering, 53, pp 797-804, 1931.

17. ASTM Publication #174, Symposium on Metallic Materials for Service at Temperatures Above 1600°F, Philadelphia, c 1956.

18. Scandron, M.D., Warshawsky, I., Gettleman, C.C. Thermocouples for Jet Engine Gas Temperature Measurement. ISA Proceedings, 7, 1952.

19. Troy, W.C. High Temperature Thermocouple, The Frontier, Armour Research Foundation, Dec. 12, 1949.

20. Hensler, J.F., Henry, E.C. Electrical Resistance of Some Refractory Oxides and Their Mixtures in the Temperature Range 600 to 1500°C. Journal of ACS, 36 (3), pp 76-83, 1953.

21. Goodwin, H.W., Wailey, R.D. On the Physical Properties of Fused Magnesium Oxide Phys. Rev., 23 pp 22, 1956.

22. Kinnison, C.S. The Electrical Conductivity of a Porcelain Mixture and a Shale Upon Heating. Trans. of ACS, 17, p 421.

23. Foex, W. Conductibilities electrique de la glucine et de la Magnesie aux temperatures elevees. Compt. rend. 214, pp 665-666, 1942.

24. Rochow, E.G. Electrical Conduction in Quartz, Periclase and Corundum at Low Field Strength, Jour. Appl. Phy. 9, 10, (1938).

25. Hottel, H.C., Kaltinsky, A. Temperature Measurements in High Velocity Air Streams Journal of Applied Mechanics. March, 1945.

26. Anon: Steels for Elevated Temperature Service. United States Steel Corporation, Pittsburgh, Pa. c 1952.

27. Anon: Stainless Steel Handbook. Allegheny Ludlum Steel Corporation, Pittsburgh, Pa. c 1951.

28. Cox, F.G. Welding & Brazing Refractory Metals, Murex Review, Rainham Essex, England, November, 1956.

29. Laud, T. Recent Developments in Temperature Measurement and Control. Metallurgical Reviews. Vol 1, Part 2, 1956.

30 Crooks, W. Proc. Roy. Soc. A 86 (1921) 461.

31. Droms, C.R. Dahl, A.I. Iridium versus Iridium-Rhodium Thermocouples for Gas Temperature Measurement Up to 3500°F. ASME Joint Conference on Combustion, Section 5, June, 1955.

32. Caldwell, F.R. Emf of Iridium Vs. Iridium Rhodium Alloys. Private Communication September 1956.

U.S. Government Publications

33. Anthony, M., Himelblan, H., Steven, G., Freeze, P., Fioch, E. Rapid Response with Tubular Hot Junctions. WADC TR56-213, April, 1956.

34. Battelle Memorial Inst., Investigations of Rhenium, WADC 54-371, June, 1954.

35. Battelle Memorial Inst., Investigations of Rhenium, WADC 54-371 (Supplement 1) September, 1956.

36. Dahl, A.I., Fiock, E.F. Circuitry Errors of Ladder-Type Thermocouple Harness Assemblies, WADC TR53-4, December, 1952.

37. Arbiter, W. New High-Temperature Intermetallic Materials. WADC TR53-190. May, 1953.

38. Ohio State Research Foundation, The Properties of Oxidation Resistant Scales Formed on Molybdenum - Base Alloys at Elevated Temperatures, WADC TR467-3, February, 1955.

39. Gowen, F.E., Perkins, E.W. Drag of Circular Cylinders for a Wide Range of Reynolds Numbers and Mach Numbers. NACA TN2960, June, 1953.

40. Havill, C.D., Rolls, L.S. A Sonic-Flow Orifice Probe for the In-Flight Measurement of Temperature Profiles of a Jet Engine Exhaust with Afterburning. NACA TN3714, May, 1956.

41. Stickney, T.M. Recovery and Time-Response Characteristics of Six Thermocouple Probes in Subsonic and Supersonic Flow. NACA TN 3455, July, 1955.

42. Simmons, F.S. Recovery Corrections for Butt-Welded, Straight Wire Thermocouples in High-Velocity, High Temperature Gas Streams. NACA RM E54G22a, September, 1954.

43. Glawe, G.E., Simmons, F.S. Stickney, T.M. Radiation and Recovery Corrections and Time Constants of Several Chromel-Alumel Thermocouple Probes in High Temperatures, High Velocity Gas Streams, NACA TN 3766, October, 1956.

44. Glawe, G.E., Shepard, C.E. Some Effects of Exposure to Exhaust-Gas Streams on Emittance and Thermoelectric Power of Base-Wire Platinum Rhodium-Platinum Thermocouples. NACA TN3253, August, 1954.

45. Scandron, M.D., Warshawsky, I. Experimental Determination of Time Constants and Nusselt Numbers for Bare-Wire Thermocouples in High Velocity Air Streams and Analytic Approximation of Conduction and Radiation Errors. NACA TN2599, Jan., 1952.

46. Goldstein, D.L., Scherrer, R. Design and Calibration of a Total-Temperature Probe for Use at Supersonic Speeds. NACA TN1885, May, 1949.

47. Lewis Flight Propulsion Laboratory, Correlation of Physical Properties of Ceramic Materials with Resistance to Fracture by Thermal Shock. NACA TN1918, Cleveland, Ohio

48. McQuillan, M.K. The Calibration and Use of the Molybdenum-Tungsten Thermocouple at High Temperatures. ASTIA Report No. ATI65926, July, 1949.

49. McQuillan, M.K. The Use of Precious Metal Thermocouples at High Temperatures, ASTIA Report ATI-51303, October, 1948.

50. Roberts, R.P. Thermocouples for Use in High Speed Gas Streams. ASTIA Report AD88868, May, 1943.

51. Dahl, A.I., Freeze, P.D. Tests of Total Temperature Probes. ASTIA Report #AD18753, June, 1953.

52. Technical Information Service, The Reactor Handbook-General Properties of Materials, AECD-3647, c 1955.

53. Anon: General Properties of Materials, The Reactor Handbook, AECD-3647, Vol. 3, Sect. 1, March, 1955.

54. California Research and Development Co., Ceramic Based Materials for High Temperature Service, AECD-3847, June 1951.

55. Wilhelm, H.A., Svec, H.J., Snow, A.I., Daune, A.H. High Temperature Thermocouples, AECD-3275, Ames Laboratory, June, 1948.

56. Bates, W.A. Ceramic-Based Materials for High Temperature Service AECD-3847, June, 1951.

57. Scheufleu, K. Wagner, C. Heat Transfer from Combustion Gases to Wall as Basis for the Construction of Uncooled Rocket Motors. PB-119371, March, 1948.

58. Cross, H.C. Metal and Ceramic Materials for Jet Propulsion Devices (AC-75) OSAD 6571-M-648, January, 1948.

59. U.S. Government Printing Office, "Properties of Metals and Alloys," Washington, D.C.

60. Dahl, A.I., Fiock, E.F. Use of Parallel Thermocouples in Turbojet Engines, TR6546, National Bureau of Standards, July, 1951.

61. Harper, D.H. Thermometric Lag. Bulletin of the Bureau of Standards 8, p 664, 1921.

62. Fiock, E.F. Development of Thermocouple Pyrometers for Gas Turbines. National Bureau of Standards, Ref III-2/I TPU (3225). Washington, D.C.

General Electric Company Publications

63. Ihnat, M.E., Clark, R.B. Supplementary Technical Proposal High Temperature Thermocouple System. G.E. DF56MI-354, Jan. 21, 1957.

64. Ihnat, M.E., Clark, R.B. Monthly Report #7, High Temperature Thermocouple Development, Feb. 18, 1957.

65. Ihnat, M.E., Clark, R.B. Monthly Report #8, High Temperature Thermocouple Development, March 14, 1957.

66. Clark, R.B., Ihnat, M.E. High Temperature Thermocouple Development, Monthly Report #9, June 11, 1957.

67. Clark, R.B., Ihnat, M.E. High Temperature Thermocouple Development, Monthly Report #10, June 11, 1957.

68. Carreker, R.P., Creep of Platinum RL-297 Research Laboratory, New York December, 1949.

69. Toensing, C.H. Preliminary Investigation on Flash Butt Welding of Tungsten Rod 56LWP-50 Lamp Wire Dept., Dleveland, Ohio

70. Swalin, R.A., Geisler, A.H. The Recrystallization Process in Tungsten as Influenced by Impurities. 56RL-1613, September, 1956.

71. Berry, J.M., Martin, D.L. Thermoelectric Stability of Thermocouple Materials at Elevated Temperatures, 55-RL-1234, March, 1955.

72. Hogue, L.J. Properties of High Temperature Insulation R56GL127, April, 1956.

73. Hogue, L.J. High Temperature Insulation for Thermistor Probe Leads, June, 1956.

74. Recupero, P.C. High Temperature Resistance Study. G.E. Technical Information Series DF57MI-30, Feb.1, 1957.

75. Anon: General Electric Design Data Handbook. Engineering Standards Dept., Schenectady, N.Y., June, 1955.

76. Pohlman, M.A. Properties of Inconel 702, V-36, and L-605. G.E. DF54AGT429, Jan. 27, 1955.

77. Pohlman, M.A. Oxidation Resistance of 30 Alloys. G.E. DF54AGT600, Jan. 27, 1955.

78. Beadle, R.G., Heising, C.R. Accuracy of Exhaust Gas Thermocouples. G.E. DF49 AGT90, September 28, 1950.

79. Fisher, J.C. Strength of Alloys at Elevated Temperatures. G.E. Report No. 56-RL-1605, August, 1956.

80. Anon: Tables of Thermocouple Characteristics General Electric Co. GE144592.

81. Barber & Pemberton Jour. of Sci. Inst. V. 32, Dec. 1955, p. 486.

82. Dahl, A.I., Fiock, E.F. Trans. ASME Feb. 1949, pp 153f.

83. Smith, C.G., Gas Turbines & Jet Propulsion, Philosophical Library, Inc. New York c 1955.

84. Hansche, G.E. and Rinehart, J.S. Air Drag On Cubes at Mach Numbers 0.5 to 3.5 Jour. Areo Society. February, 1952.

85. Margenan, Watson, Montgomery. Physics Principal and Application. D. Van Nostrand Co., Inc., Princeton, New Jersey.

Appendix I

THERMOELECTRIC PROPERTIES OF MATERIALS COMPILED FOR STUDY

ELEMENTS NEGATIVE RELATIVE TO PLATINUM

Element	Range of Thermo-Electric Measurement - °C	Microvolts/°C
Si	0 - 300	- 367
Co	0 - 800	- 17.5
Pd	0 - 1500	- 15.2
Ni	0 - 1100	- 12.4

ELEMENTS POSITIVE TO PLATINUM

Ti	0 - 900	+ 12.8
Fe	0 - 1000	+ 14.6
Ir	0 - 1500	+ 15.0
Zr	0 - 260	+ 16.2
Rh	0 - 1500	+ 16.9
Ta	0 - 1200	+ 17.8
Mo	0 - 1200	+ 30.8
W	0 - 1200	+ 31.5

ALLOY SYSTEMS RELATIVE TO PLATINUM

Au-Pd

(0 - 100°C exp. range)

Wgt. %	Microvolts/°C
0 Au 100 Pd	- 5.7
10 Au 90 Pd	- 8.5
20 Au 80 Pd	-12.5
30 Au 70 Pd	-14.2
40 Au 60 Pd	-16.9
50 Au 50 Pd	-24.4
60 Au 40 Pd	-29.7
70 Au 30 Pd	-26.3
80 Au 20 Pd	- 4.6
90 Au 10 Pd	- 0.5
100 Au 0 Pd	+ 7.8

Ni-Cr

(25-1000°C exp. range)

Wgt. %	Microvolts/°C
99.6 Ni, 0 Cr, 0.4 Mn	- 12.9
97.6 Ni, 2 Cr, 0.4 Mn	+ 15.6
94.6 Ni, 5 Cr, 0.4 Mn	+ 28.6
89.6 Ni,10 Cr, 0.4 Mn	+ 32.0
84.6 Ni,15 Cr, 0.4 Mn	+ 27.8
79.6 Ni,20 Cr, 0.4 Mn	+ 22.9
Chromel P (nominal 90 Ni 10 Cr)	+ 32.7
76.2 Ni, 19.1 Cr, 4.8 Al	+ 17.0
76.2 Ni, 19.1 Cr, 4.8 Si	+ 17.9

Ni-Mo-Cr

(25 - 1000°C exp. range)

Wgt. %	Microvolts/°C
Ni, 5 Mo, 9.4 Cr	+30.7
Ni, 10 Mo, 8.9 Cr	+30.2
Ni, 15 Mo, 8.4 Cr	+28.4
Ni, 18.8 Mo, 5 Cr	+30.0
Ni, 17.8 Mo, 10 Cr	+25.2
Ni, 13.8 Mo, 3.2 Cr	+35.0
Ni, 6.9 Mo, 6.6 Cr	+33.9

Ni-Mo

(25 - 1000°C exp. range)

Wgt. %	Microvolts/°C
Ni, 5 Mo, 1 Mn	+6.5
Ni, 10 Mo, 1 Mn	+29.0
Ni, 16 Mo, 1 Mn	+35.7
Ni, 20 Mo, 1 Mn	+41.0
Ni, 20 Mo, 3 Mn	+29.2
Ni, 20 Mo, 5 Mn	+30.4
Ni, 25 Mo, 1 Mn	+38.9
Ni, 30 Mo, 1 Mn	+38.4

Fe-Mo

(25 - 1000°C exp. range)

Wgt. %	Microvolts/°C
Fe, 1 Mo, 1 Mn	+14.6
Fe, 7 Mo, 1 Mn	+20.8

MISCELLANEOUS ALLOYS RELATIVE TO PLATINUM

Alloy	Approx. Melting Point °C	Thermo-electric Power
Constantan (45 Ni 55 Cu)	1290	-43.9 (0 - 900°C)
40 Pd 60 Au	1460	-42.8 (0 - 900°C)
50 Pd 50 Au	1485	-38.4 (0 - 900°C)
30 Pd 70 Au	1425	-31.7 (0 - 900°C)
60 Pd 40 Au	1500	-31.0 (0 - 900°C)
70 Pd 30 Au	1515	-25.6 (0 - 900°C)
80 Pd 20 Au	1535	-20.2 (0 - 900°C
90 Pd 10 Au	1550	-15.7 (0 - 900°C)
Driver Harris No. 99 Alloy (.02 C, .01 Mn, .01 Si, Bal Ni)	1450	-10.4 (0 - 900°C)
Alumel (94 Ni, 2Al, 3 Mn, 1 Si)	1400	-8.8 (0 - 900°C)
20 Pd 80 Au	1375	- 8.3 (0 - 900°C)
98 Pt 2 Pd	1552	-1.25 (0 - 1200°C)
10 Pd 90 Au	1265	+2.3 (0 - 900°C)

Alloy	Approx. Melting Point °C	Thermo-electric Power
94 Pt 6 Pd	1552	+3.25 (0 - 1200°C)
98 Pt 2 Rh	1790	+3.58 (0 - 1200°C)
88 Pt 12 Pd	1552	+5.1 (0 - 1200°C)
98 Pt 2 Ir	1780	+5.75 (0 - 1200°C)
94 Pt 6 Rh	1825	+7.75 (0 - 1200°C)
98 Pt 2 Ru	1774	+9.2 (0 - 1200°C)
90 Pt 10 Rh	1840	+9.9 (0 - 1200°C)
18-8 Stain. Steel	1420	+10.0 (0 - 900°C)
88 Pt 12 Rh	1865	+10.4 (0 - 1200°C)
87 Pt 13 Rh	1870	+11.0 (0 - 1200°C)
84 Pt 6 Ir	1790	+11.7 (0 - 1200°C)
80 Pt 20 Rh	1900	+12.3 (0 - 1200°C)
98 Pt 2 Os	1774	+12.9 (0 - 1200°C)
70 Pt 30 Rh	1930	+13.5 (0 - 1200°C)
60 Pt 40 Rh	1950	+14.2 (0 - 1200°C)

Alloy	Approx. Melting Point °C	Thermo-electric Power
Driver-Harris No. 525 Alloy (1.37 Mn, .14 Si, 16.02 Cr, 36.4 Ni, Bal Fe)	1525	+13.1 (0 - 900°C)
98 Pt 2 Fe	1745	+14.6 (0 - 1200°C)
99 Pt 1 Re	1774	+15.0 (0 - 1200°C)
98 Pt 2 Re	1774	+15.6 (0 - 1200°C)
10 Ir 90 Rh	1966	+16.2 (0 - 1200°C)
90 Ir 10 Rh	1966	+16.5 (0 - 1200°C)
90 Pt 10 Ir	1780	+15.4 (0 - 900°C)
96 Pt 4 Fe	1740	+16.7 (0 - 1200°C)
94 Pt 6 Ru	1774	+16.9 (0 - 1200°C)
88 Pt 12 Ir	1800	+17.7 (0 - 1200oC)
25 Ir 75 Rh	1966	+17.9 (0 - 1200°C)
85 Pt 15 Ir	1820	+16.2 (0 - 900°C)
75 Ir 25 Rh	1966	+18.5 (0 - 1200°C)
40 Ir 60 Rh	1966	+19.1 (0 - 1200°C)
60 Ni, 24 Fe, 16 Cr	1350	+17.2 (0 - 900°C)
60 Ir 40 Rh	1966	+19.2 (0 - 1200°C)

Alloy	Approx. Melting Point °C	Thermo-electric Power
Nichrome V (80 Ni 20 Cr)	1350	+20.4 (0 - 900°C)
94 Pt 6 Os	1774	+22.2 (0 - 1200°C)
88 Pt 12 Os	1774	+30.0 (0 - 1200°C)
Nirex (13 Cr, 6 Fe, Bal Ni)	1425	+25.1 (0 - 900°C)
Driver-Harris No. 105 Alloy (2.11 Mn, .11 Si, 3.85 Cr, Bal Ni)	1440	+25.4 (0 - 900°C)
Chromel P (90 Ni 10 Cr)	1430	+32.1 (0 - 1200°C)
82 Ni 18 Mo	1400	+36.8 (0 - 900°C)
79 Ni, 20 Mo, 1 Mn	1400	+41.0 (25 - 1000°C)

Appendix II

THERMOELECTRIC CHARACTERISTICS OF BASE METAL ALLOYS USED IN LEAD WIRE DEVELOPMENT

The following alloys were tested against a platinum reference and have been included for general information. Reference junction 0°C.

Alloy	500°F	1000°F	1500°F
Stainless Steels			
302	1.44	3.93	7.42
304	1.43	3.99	7.62
305	1.46	4.02	7.63
310	1.58	4.32	8.24
316	1.51	4.23	8.03
316	1.43	4.09	7.83
321	1.44	3.97	7.56
330	1.92	5.45	10.3
347	1.46	4.03	7.66
Almet C-2	1.75	5.07	9.61
Misc. Alloys			
Alloy 45	-9.56	-22.4	-34.5
Alloy 529	1.86	5.30	9.97
Beraloy	2.29	6.50	12.4
Hastelloy C	2.66	7.28	13.4
Nichrome	2.72	7.23	13.0
Nichrome	2.76	7.33	13.2
Nichrome V	3.78	9.50	16.4
Nichrome V	3.94	9.82	16.8

Figures (58) through (60) have also been included to designate those commercial material combination which were found to have the nearest characteristics for the indicated thermocouples.

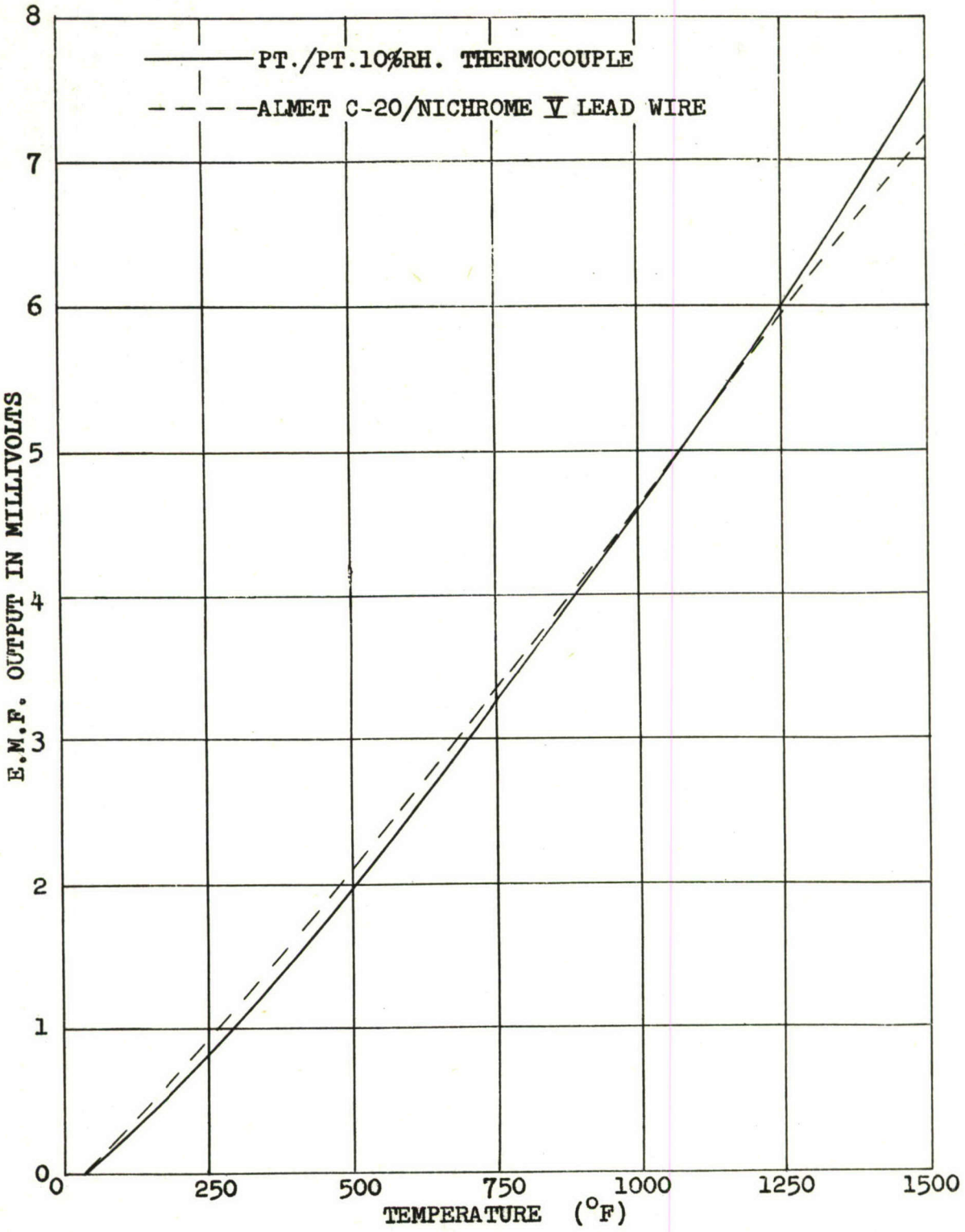


FIGURE 58. PROBABLE LEAD WIRES FOR NOBLE METAL THERMOELEMENTS

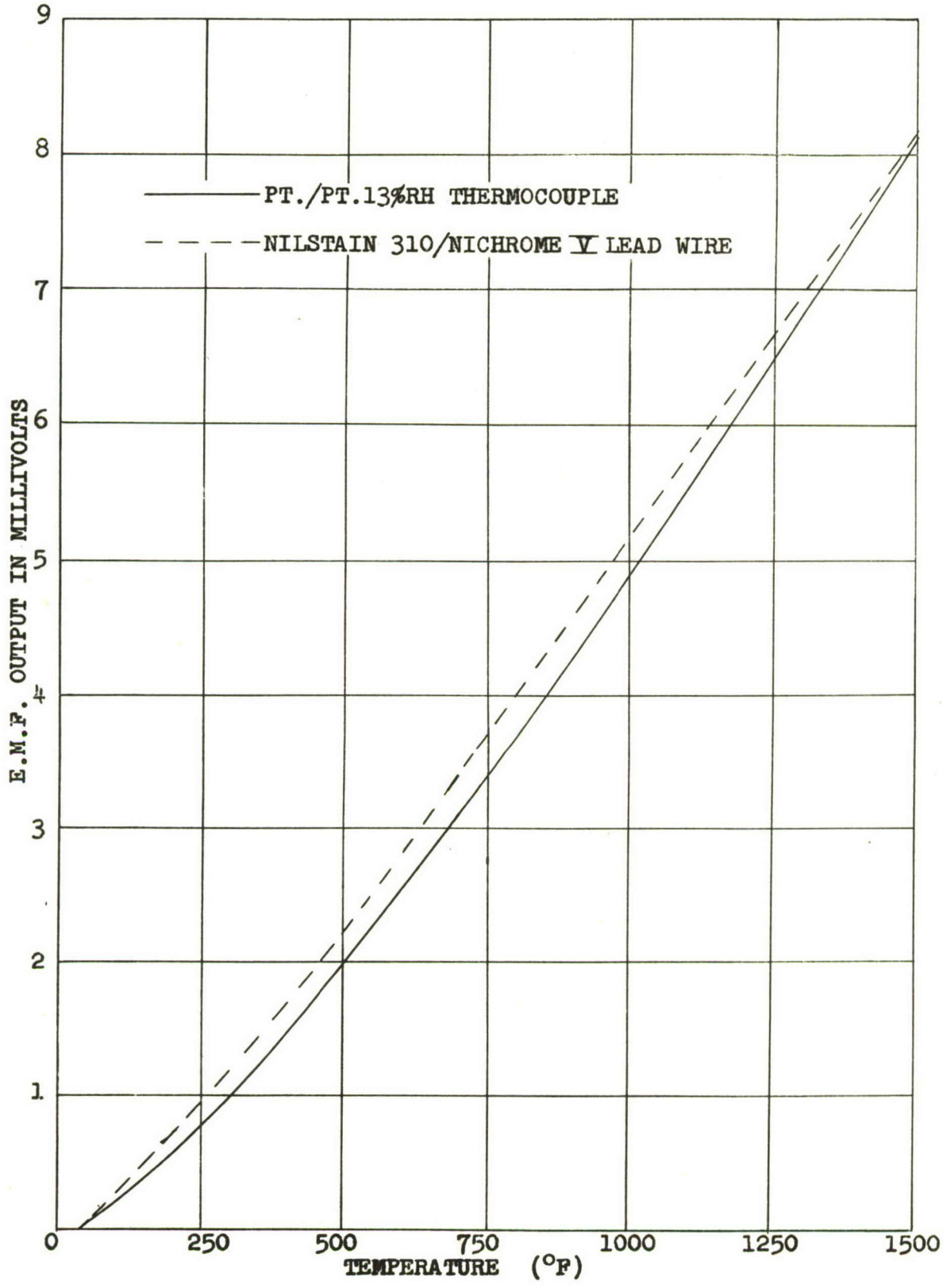


FIGURE 59. PROBABLE LEAD WIRES FOR NOBLE METAL THERMOELEMENTS

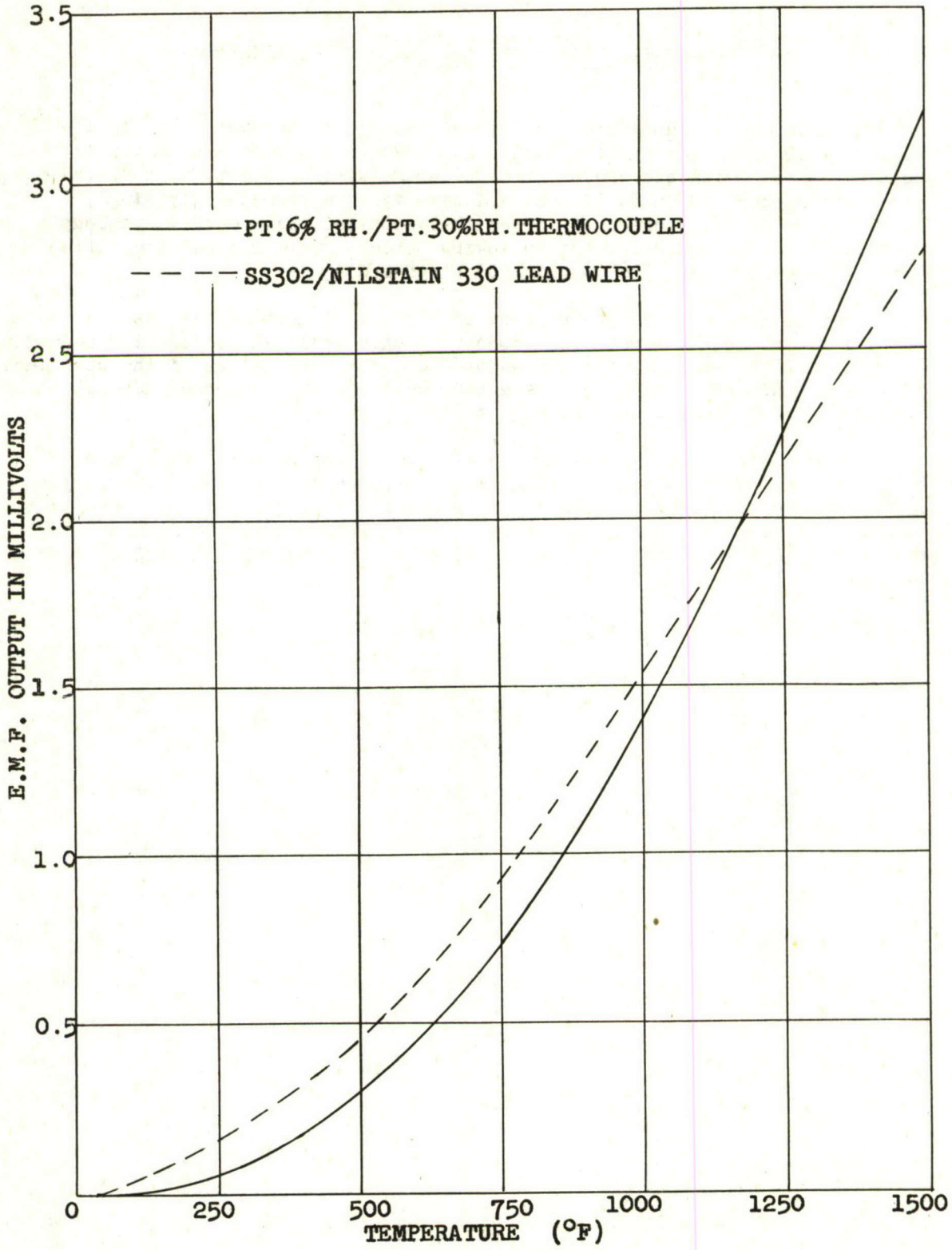


FIGURE 60. PROBABLE LEAD WIRES FOR NOBLE METAL THERMOELEMENTS

Appendix III

STATISTICAL ANALYSIS OF LEAD WIRE EXPERIMENT

The data of this analysis consists of voltage measurements on thermocouples, each type made up of a particular combination of one of sixteen stainless steel wires and one of three nichrome wires. Thirty-nine of these types were reproduced in duplicates and nine types were made only singly. Thus data was obtained on eighty-seven thermocouples. For each thermocouple the voltage was measured for the following three temperature differentials 500°F, (260°C) 1000°F, (538°C) and 1500°F, (816°C).

For each type of wire the percent of all constituent metals, as well as a random variable, was given. The object of this analysis was to find equations that will predict the output in terms of these characteristics of the stainless steel wire. Nine such equations have been derived, one for each combination of nichrome wire and temperature differential.

Besides iron, there were eleven constituent metals in the steel wire. The percentages of these were treated as the independent variables. The percent of iron was not considered in the regression equations since it was redundant in terms of the other eleven constituents. Its inclusion would lead into mathematical difficulties. X_{12} was included as the twelfth independent random variable.

The following notations were used in computations.

X_1	is	the	percent	of	carbon							
X_2	"	"	"	"	phosphorus							
X_3	"	"	"	"	nickel							
X_4	"	"	"	"	chromium							
X_5	"	"	"	"	manganese							
X_6	"	"	"	"	sulfur							
X_7	"	"	"	"	molybdenum							
X_8	"	"	"	"	columbium							
X_9	"	"	"	"	copper							
X_{10}	"	"	"	"	titanium							
X_{11}	"	"	"	"	silicon							
X_{12}	"	a	random	variable								

Y_1	is	the	emf	(in	mv)	obtained	with	a	nichrome	wire	at	500°F
Y_2	"	"	"	"	"	"	"	"	"	"	"	1000°F
Y_3	"	"	"	"	"	"	"	"	"	"	"	1500°F
Y_4	"	"	"	"	"	"	"	another	"	"	"	500°F
Y_5	"	"	"	"	"	"	"	"	"	"	"	1000°F
Y_6	"	"	"	"	"	"	"	"	"	"	"	1500°F
Y_7	"	"	"	"	"	"	"	a	nichrome V	"	"	500°F
Y_8	"	"	"	"	"	"	"	"	"	"	"	1000°F
Y_9	"	"	"	"	"	"	"	"	"	"	"	1500°F

For each y it was postulated that y can be approximated by an equation of the type

$$y = b_0 + b_1x_1 + b_2x_2 \cdot \cdot \cdot + b_{11}x_{11} + b_{12}x_{12}$$

The coefficients b_1 were estimated by least square methods. The results of this estimation and further analysis shows that within the range of the independent variables in this experiment the above equation gave a rather good approximation. The primary interest of this investigation was to detect differences between equations for different y's. If the b's pertaining to y's of different temperature levels are different, then one can make thermocouples with desirable characteristics by choosing the x's properly.

This experiment did not give all the information that might have been obtained with respect to the differences in the b's. The reason for this was that there existed small variations in most of the x's. It was difficult to assess the effect of a constituent if this constituent was observed only within a range of a fraction of a percent. The only constituent which was present with greatly differing amounts was nickel. In fact, the amount of nickel in the steel wire seems to dominate the data. The Nilstain 330 and Almet C-20 stainless steel wires which had the highest nickel content yielded the lowest output for all temperatures in combination with nichrome. On the other hand, the output of the 302 stainless steel wire with the lowest nickel content was among those having the highest output. However, from the regression analysis, it seemed very plausible that other constituents have a greater effect than nickel. Titanium, for example, was estimated to have an effect about 15 to 100 times larger than that of nickel. However, the estimate of b_{11} (pertaining to titanium) was not very precise because of the small variation in titanium. The maximum amount of titanium in any steel wire was only .03%. However, in spite of these experimental shortcomings, the results obtained are useful in constructing thermocouples with appropriate lead wires.

The experiment provided thirty-nine pairs of thermocouples which, for this analysis, were assumed to be identical. However, the output of identical thermocouples differed from each other. These observed differences may be considered as due to inherent random errors with which this investigation was not directly concerned. The standard deviations of these random errors were estimated to have the following values.

Sample X - Nichrome			Sample Y - Nichrome			Sample Z - Nichrome		
500°F	1000°F	1500°F	500°F	1000°F	1500°F	500°F	1000°F	1500°F
.00596	.00611	.00886	.00537	.00690	.00985	.00348	.00836	.00635

These standard deviations were taken as being within standard deviation (within pairs of identical thermocouples). Unless the methods of experimentation was made more precise, nothing could be done to reduce the variability that is measured by the within standard deviation.

Constructing a regression equation presumably gives the correct expected value of the observed dependent variable y. It was possible to estimate standard deviation of the differences between observed and the predicted values. This measure of variability was called the standard deviation from the regression equation. If the expected value of y can be precisely expressed by the type of the regression equation used in the analysis, then the standard deviations as estimated from regression should approximately equal the standard deviation as estimated from within pairs of identical thermocouples. If the former standard deviation is much larger than the latter, then there is a very strong indication that the proposed type of equation does not give an exact fit.

It was found that the standard deviations from regression were about three to four times as large as the within standard deviation.

Such large differences in the standard deviations are overwhelming evidence that something is "wrong". The lack of perfect fit may have been due to the possible fact that x's were not precisely measured. More than likely the lack of fit could be attributed to the postulated equations. Several theoretical considerations indicate that a linear equation would not fit this data perfectly.

The value of a regression equation does not necessarily depend on a perfect fit. Its value lies in its potential predicting ability. If no account were taken of the x's, a likely prediction of a y value would be the observed average of the y's, which may be considered as the most representative y value. The standard deviation of the differences of the observed y values from the mean of the y values is a measure of the variability of the y's without prediction. The comparison of this standard deviation with that from regression demonstrates the value of the regression equation. The standard deviations from the mean are about 10 to 30 as large as those from the prediction equations. The following table gives the values of the estimates of both these standard deviations.

	Nichrome			Nichrome			Nichrome V		
	500°F	1000°F	1500°F	500°F	1000°F	1500°F	500°F	1000°F	1500°F
R	.0154	.0252	.0346	.0175	.0200	.0417	.0417	.0198	.0244
M	.1595	.4297	.7517	.1526	.4312	.7511	.1468	.4272	.7554

This table clearly demonstrates predicting ability of the computed regression equations.

It is customary to run statistical analysis on the regression coeffients b. The validity of these analyses depend on various assumptions, among others is that the postulated equation fits perfectly. Since this is obviously not the case, these analyses were not made here. The following two tables give the values of the b's as estimated by least square procedures and the estimates of the standard deviation of the estimates of the b's. The standard deviation from regression was used in the estimation of the standard deviation of the b's. Since no rigorous analysis was possible as a rough guide it was considered that a regression coefficient was "significant" if it exceeded several times its standard deviation as given in the table. An estimate of a regression coefficient of the value of about one standard deviation or less may in fact be due solely to random fluctuations.

The tables of the regression coefficients and their standard deviations along with an interpretation of the coefficients are as follows:

REGRESSION COEFFICIENTS

	Nichrome			Nichrome			Nichrome V		
	500 F	1000 F	1500 F	500 F	1000 F	1500 F	500 F	1000 F	1500 F
	1	2	3	4	5	6	7	8	9
0	2.785	6.865	10.964	2.914	7.113	11.664	1.748	4.544	7.743
1	.644	.998	1.378	.497	.997	2.347	.421	.956	1.760
2	.591	-1.871	-2.816	.360	-2.378	-4.820	.242	-2.182	-4.282
3	-.022	-.064	-.111	-.022	-.064	-.111	-.021	-.063	-.111
4	-.029	-.058	-.085	-.025	-.056	-.093	-.026	-.056	-.088
5	.046	.021	-.017	.052	.014	-.042	.044	.033	-.040
6	.114	2.453	2.066	1.813	4.321	3.165	1.098	4.094	+3.837
7	-.050	-.093	-.152	-.050	-.093	-.134	-.048	-.102	-.154
8	-.120	-.133	-.143	-.097	-.118	-.157	-.086	-.144	-.138
9	.052	.063	.066	.057	.062	.058	.048	.068	.072
10	-2.171	-2.354	-3.149	-2.759	-2.715	-1.576	-2.685	-3.139	-3.261
11	.370	.672	.858	.433	.696	.626	.383	.641	.742
12	-.791	.592	1.217	-.826	.538	2.032	-.821	.283	1.580

STANDARD DEVIATIONS OF REGRESSION COEFFICIENTS

	1	2	3	4	5	6	7	8	9
0	.0979	.1602	.2203	.1118	.1273	.2651	.0936	.1257	.1550
1	.3474	.5686	.7820	.3967	.4518	.9410	.3322	.4462	.5501
2	.8169	1.3368	1.8386	.9327	1.0623	2.2124	.7810	1.0490	1.2934
3.	.0006	.0010	.0014	.0007	.0008	.0017	.0006	.0008	.0010
4	.0037	.0060	.0083	.0042	.0046	.0099	.0035	.0047	.0058
5	.0139	.0228	.0314	.0159	.0181	.0377	.0133	.0179	.0221
6	1.3514	2.2116	3.0417	1.5430	1.7574	3.6600	1.2920	1.7354	2.1397
7	.0065	.0107	.0147	.0074	.0085	.0176	.0062	.0084	.0103
8	.0199	.0326	.0448	.0227	.0259	.0539	.0190	.0256	.0315
9	.0094	.0153	.0211	.0107	.0122	.0253	.0089	.0120	.0148
10	.4598	.7525	1.0349	.5250	.5980	1.2453	.4396	.5905	.7280
11	.0512	.0838	.1153	.0585	.0666	.1388	.0490	.0658	.0811
12	.5096	.8339	1.1469	.5818	.6627	1.3801	.4872	.6544	.8069

The b's are obviously different for the different temperatures. The Nichrome V wire obviously has different b_0 values from those of nichrome wires. From this data it is difficult to determine whether the steel and nichrome wires interact. If there are interactions, they seem to be moderate. This means that the effects of the nichrome wire and of the steel wire are largely additive. (c.f. comment in Nickel).

Carbon (b_1) seems to raise the output; the increase seems to be roughly proportional to the output without any carbon.

Phosphorous (b_2) tends to lower the output for higher temperatures.

Nickel (b_3) lowers the output. The effect is more marked for the higher temperatures. Even though the coefficients have very small standard deviations, the b's for the different nichromes but the same temperatures differ very little from each other. This shows that the effects of nickel are not much influenced by the type of nichrome wire used.

Chromium (b_4) lowers the output; the lowering is more pronounced with the higher temperatures. The b_4 seems nearly proportional to the corresponding b_0.

Manganese (b_5) raises the output for the lower temperatures. At 1500°F (816°C) there is an indication of lowering the output.

Sulfur (b_6) is interesting because it yielded the largest coefficients and because those pertaining to 1000°F (538°C) do not lie between those of 500°F (260°C) and 1500°F (816°C). Unfortunately, the standard deviations of the coefficients are so large that not much could be asserted about these phenomena with great assurance. The only reasonable statement that could be made was that sulfur seems to raise the output and the increase seemed more pronounced at the higher temperatures.

Molybdenum (b_7) lowers the output. The decrease is more pronounced at higher temperatures.

Columbium (b_8). Columbium lowers the output. Even though there is suggestion of a temperature trend, the effect of columbium seems relatively independent of the temperature level.

Copper (b_9). Copper raises the output. Like columbium, the effect seems relatively constant with a slight indication of temperature trend.

Titanium (b_{10}) yields large coefficients; however, the standard deviations are large. Titanium lowers the output, apparently at a relatively constant rate.

Silicon (b_{11}) raises the output. The increase is less pronounced at 500°F (260°C).